Submitted to Chaos

A chaotic lattice field theory in two dimensions

Predrag Cvitanović and Han Liang
School of Physics, Georgia Institute of Technology, Atlanta, GA 30332-0430

(*Electronic mail: han_liang@gatech.edu.)

(*Electronic mail: predrag.cvitanovic@physics.gatech.edu.)

(Dated: August 20, 2025)

We describe spatiotemporally chaotic (or turbulent) field theories discretized over d-dimensional lattices in terms of sums over their multi-periodic orbits. 'Chaos theory' is here recast in the language of statistical mechanics, field theory, and solid state physics, with the traditional periodic orbits theory of low-dimensional, temporally chaotic dynamics a special, one-dimensional case.

In the field-theoretical formulation, there is no time evolution. Instead, treating the temporal and spatial directions on equal footing, one determines the spatiotemporally periodic orbits that contribute to the partition sum of the theory, each a solution of the system's defining deterministic equations, with sums over time-periodic orbits of dynamical systems theory replaced here by sums of d-periodic orbits over d-dimensional spacetime, the weight of each orbit given by the Jacobian of its spatiotemporal orbit Jacobian operator. The weights, evaluated by application of the Bloch theorem to the spectrum of periodic orbit's Jacobian operator, are multiplicative for spacetime orbit repeats, leading to a spatiotemporal zeta function formulation of the theory in terms of prime orbits.

PACS numbers: 02.20.-a, 05.45.-a, 05.45.Jn, 47.27.ed

A temporally chaotic system is exponentially unstable with time: double the time, and exponentially more orbits are required to cover its strange attractor to the same accuracy. For a system of large spatial extent, the complexity of the spatial shapes also needs to be taken into account; double the spatial extent, and exponentially as many distinct spatial patterns might be required to describe the repertoire of spatial shapes to the same accuracy.[1–3] Based on the insight that temporal and spatial instabilities can be treated on equal footing, the 'chronotopic' theory of 1990's offers an elegant description of such spatiotemporal chaos, with predictions of the theory encapsulated in an 'entropy density' function.[4–7] The first decade of 2000's saw rapid progress in description of transitional turbulence in fluids, in terms of 'exact coherent structures', numerically exact spatiotemporally periodic unstable solutions of Navier-Stokes equations.[8–14] This approach to turbulence aims to predict measurable observables from the defining (Navier-Stokes) equations, without any statistical assumptions. But how are these solutions to be pieced together?[15] As a single such solution requires highly unstable time integration over $10^4 - 10^6$ discretization ODEs, estimates of 'chronotopic' theory observables based on large spacetime volume limits of numerical simulations are out of question. In this paper we develop a new spatiotemporal theory of turbulence, which assigns a new kind of a global weight, an 'orbit Jacobian', to each exact coherent structure, with a new enumeration of global solutions as sums over all Bravais lattices. Our deterministic field theory replaces numerical extrapolations of finite spacetime simulations of the 1990's chronotopy by our main result, the exact spatiotemporal deterministic zeta function, with computable cycle expansion truncations errors, decreasing exponentially with the spatiotemporal volumes of periodic states included in its evaluation.

Our goal here is to make this 'spatiotemporal chaos' tangible and precise (see Sec. X A), in a series of papers that introduce its theory and its implementations. The companion paper I[16] focuses on the $1d$ chaotic lattice field theory, and a novel treatment of time-reversal invariance. In this paper, paper II, we develop the theory of $2d$ spatiotemporal chaotic systems; and in the companion paper III[17] we apply the theory to several nonlinear field theories. As our intended audience spans many disjoint specialties, from fluid dynamics to quantum field theory, the exposition entails much pedagogical detail, so let us start by stating succinctly what the key novelty of our theory is.

There are two ways of studying stabilities of translationally-invariant systems, illustrated by Fig. 8 (b) and (c):

(i) In the textbook 'QM-in-a-box' approach, one starts by confining a system to a *finite* box, then takes the box size to infinity. In dynamical systems this point of view leads to the Gutzwiller-Ruelle[18–20] periodic orbit formulation of chaotic dynamics, with stability of each periodic solution computed over a finite time interval.

This approach is hampered by one simple fact that

complicates everything: the periodic orbit weight is *not* multiplicative for orbit repeats,

$$\det(\mathbb{1}-\mathbb{J}_p^r) \neq [\det(\mathbb{1}-\mathbb{J}_p)]^r\,. \tag{1}$$

Much work follows,[20] with some details elaborated in Sec. VIII.

(ii) A crystallographer, or field theorist starts with an *infinite* lattice, or continuum spacetime. The approach –as we show here in Sec. IX B– yields weights that are multiplicative for repeats of spatiotemporally periodic solutions,

$$\mathrm{Det}\,\mathcal{J}_{rp} \text{ “}=\text{ ”} (\mathrm{Det}\,\mathcal{J}_p)^r \tag{2}$$

(quotation marks, as the precise statement is in terms of stability exponents rather than determinants). This fact simplifies everything, and yields the main result of this paper, the spatiotemporal zeta function (Sec. X D), expressed as a product of Euler functions $\phi(t_p)$, one for each prime spatiotemporal solution of weight t_p,

$$\zeta=\prod_p \zeta_p\,, \qquad 1/\zeta_p=\phi(t_p)\,. \tag{3}$$

Analysis of a temporally chaotic dynamical system typically starts with establishing that a temporal flow (perhaps reduced to discrete time maps by Poincaré sections) is locally stretching, globally folding. Its state space is partitioned, the partitions labeled by an alphabet, and the qualitatively distinct solutions classified by their temporal symbol sequences.[20]

We do not do this here: instead, we find that the natural language to describe 'spatiotemporal chaos' and 'turbulence' is the formalism of field theory. Our work is a continuation of the 1995 chronotopic program of Politi, Torcini & Lepri[5,6,21,22] who, in their studies of propagation of spatiotemporal disturbances in extended systems, showed that the spatial stability analysis can be combined with the temporal stability analysis. The Floquet-Bloch approach to stability that we deploy was introduced for temporal evolution in 1981-1983 by Bountis & Helleman[23] and MacKay & Meiss,[24] and, for spatially extended systems, in 1989 by Pikovsky,[25] who noted that for spatiotemporally chaotic systems space and time could be considered on the same footing in the sense that there are settings in which 'time' and 'space' coordinates could be interchanged.

In our formulation the 'chaos theory' is a Euclidean deterministic field theory. But, as developed here, this theory looks nothing like the textbook expositions[20,26–31] of temporally chaotic, few degrees-of-freedom dynamical systems. There one is given an initial state, which then *evolves in time*, much like in mechanics, where given an initial phase-space point, the integration of Hamilton's equations traces out a phase-space trajectory. For a reader versed in fluid dynamics or atomic physics the most disconcerting aspect of the field-theoretic perspective is that time is just one of the coordinates over which a field configuration is defined: each field-theoretic solution is a static solution over the infinite spacetime. There is *no* 'evolution in time', no stable / unstable manifolds, no 'hyperbolicity', no 'mixing'.

Furthermore –just as the discretization of time by Poincaré sections aids analysis of temporal chaos– we find it convenient to discretize both time and space. Spatiotemporally steady turbulent flows offer one physical motivation for considering such models: a rough approximation to such flows is obtained discretizing them into spatiotemporal cells, with each cell turbulent, and cells coupled to their neighbors. Lattices also arise naturally in many-body problems, such as many-body quantum chaos models studied in Refs. 32–35, see Sec. III B.

Outline. We start our formulation of chaotic field theory (Sec. I) by defining the field theory partition sums in terms of spatiotemporally periodic states (Sec. I A). A *deterministic field theory* has support on the set of all solutions of systems' defining equations. Its building blocks are *periodic states*, spatiotemporally periodic solutions of system's defining equations (Sec. II).

In Sec. III we introduce the field theories studied here. In particular, the simplest of chaotic field theories, the spatiotemporal cat[36,37] of Sec. III A, a discretization of the compact boson Klein-Gordon equation,

$$(-\Box+\mu^2)\,\Phi-\mathsf{M}=0\,, \tag{4}$$

recently applied to transport in chaotic chains[38] and to black holes physics,[39,40] captures the essence of spatiotemporal chaos. Spatiotemporal cat is a lattice of hyperbolic 'anti-' or 'inverted' oscillators,[41,42] with an unstable 'anti-harmonic cat' ϕ_z of mass μ at each lattice site z, a 'cat' which, when pushed, runs away rather than pushes back.

In Sec. III B we motivate of choice of nonlinear field theories studied here by the 1955 Fermi-Pasta-Ulam-Tsingou[43,44] model which illustrates how many-body 'chaos theory' morphs into a Euclidian strong-coupling, anti-integrable deterministic field theory.

Crucial to 'chaos' is the notion of stability: in Sec. IV we describe spatiotemporal stability of above field theories' periodic states in terms of their orbit Jacobian operators. Periodic orbit theory for a time-evolving dynamical system on a one-dimensional temporal lattice is organized by grouping orbits of the same time period together.[16,18–20,45] For systems characterized by several translational symmetries, one has to take care of multiple periodicities; in the language of crystallography, organize the periodic orbit sums by corresponding *Bravais lattices*, or, in the language of field theory, by the 'sum over *geometries*'. In Sec. V we enumerate and construct spacetime geometries, or $d=2$ Bravais lattices $[L\times T]_S$, of increasing spacetime periodicities. The classification of periodic states proceeds in two steps. On the coordinate level, periodicity is imposed by the hierarchy of Bravais lattices of increasing periodicities. On the field-configuration level, the key to the spatiotemporal periodic orbit theory is the enumeration and determination

of *prime orbits*, the basic building blocks of periodic orbit theory (Sec. VI).

The central idea of spatiotemporal theory developed here, global orbit stability, has its origins in the 1886 work of Hill[46] and Poincaré.[47] The likelihood of each solution is given by the orbit Jacobian, the determinant of its spatiotemporal orbit Jacobian matrix. Compared to the temporal-evolution chaos theory, the orbit Jacobian (more precisely, the stability exponent) is the central innovation of our field-theoretic formulation of chaotic field theory, so we return to it throughout the paper. The calculations are carried out on the reciprocal lattice (Sec. VII). We discuss primitive cell computations in Sec. VIII, as prequel to introducing the stability exponent of a periodic state over spatiotemporally infinite Bravais lattice, computed on the reciprocal lattice (Sec. IX). For spatiotemporal cat we evaluate and cross-check orbit Jacobians by two methods, either on the reciprocal lattice (Sec. VIII B), or by the 'fundamental fact' evaluation (Appendix B 3).

Having enumerated all Bravais lattices (Sec. V), determined periodic states over each (Sec. VI A), computed the weight of each periodic state (Sec. IX), we can now write down the deterministic field theory partition sum as a sum over all spatiotemporal solutions of the theory (Sec. X). In Sec. X C we reexpress the partition sum in terms of prime orbits, and in Sec. X D we construct the spatiotemporal zeta function. What makes these resummations possible is the multiplicative property of orbit Jacobians announced in Eq. (2), provided by their evaluation over the spatiotemporally infinite Bravais lattice (Sec. IX), the key property that is violated by finite-dimensional matrix approximations that are the basis of the traditional Gutzwiller-Ruelle temporal periodic orbits theory (Sec. VIII). In Sec. X F explain how one computes expectation values of observables in deterministic chaotic field theories.

How is this global, high-dimensional orbit stability related to the stability of the conventional low-dimensional, forward-in-time evolution? The two notions of stability are related by Hill's formulas, relations that rely on higher-order derivative equations being rewritten as sets of first order ODEs, formulas equally applicable to energy conserving systems, as to viscous, dissipative systems. We derive them in Refs. 16 and 48. From the field-theoretic perspective, orbit Jacobians are fundamental, while the forward-in-time evolution (a transfer matrix method) is merely one of the methods for computing them.

Finally, we know that time-evolution cycle-expansions' convergence is accelerated by shadowing of long orbits by shorter periodic orbits.[49] In Sec. XI we check numerically that spatiotemporal cat periodic states that share finite spatiotemporal mosaics shadow each other to exponential precision. We presume (but do not show) that this shadowing property ensures that the predictions of the theory are dominated by the shortest period prime orbits.

This completes our generalization[16,17,37,50] of the temporal-evolution deterministic chaos theory[20,45] to spatiotemporal chaos / turbulence, and recasts both in the formalism of conventional solid state physics, field theory, and statistical mechanics. Our results are summarized and open problems discussed in Sec. XII. Our calculations are reported in Appendices. Icon ▶ on the margin links a block of text to a supplementary online video. For additional material, online talks and related papers, see ChaosBook.org/overheads/spatiotemporal.

I. LATTICE FIELD THEORY

In a d-dimensional hypercubic discretization of a Euclidean space, the d continuous Euclidean coordinates $x \in \mathbb{R}^d$ are replaced by a hypercubic integer lattice[51,52]

$$\mathcal{L} = \left\{ \sum_{j=1}^{d} z_j \mathbf{e}_j \mid z \in \mathbb{Z}^d \right\} , \quad \mathbf{e}_j \in \{\mathbf{e}_1, \mathbf{e}_2, \cdots, \mathbf{e}_d\} , \tag{5}$$

spanned by a set of orthogonal vectors $\mathbf{e}_j$, with lattice spacing $a_j = |\mathbf{e}_j| = \Delta x_j$ along the direction of vector $\mathbf{e}_j$. We shall use lattice units, almost always setting $a_j = 1$ (for another, modular function parametrization choice, see Eq. (75)). A field $\phi(x)$ over d continuous coordinates x_j is represented by a discrete array of field values over lattice sites

$$\phi_z = \phi(x) , \quad x_j = a_j z_j = \text{lattice site}, \qquad z \in \mathbb{Z}^d . \tag{6}$$

A lattice *field configuration* is a d-dimensional infinite array of field values (in what follows, illustrative examples will be presented in one or two spatiotemporal dimensions)

$$\Phi = \begin{array}{ccccccc} \cdots & \cdots & \cdots & \cdots & \cdots & \cdots & \cdots \\ \cdots & \phi_{-2,1} & \phi_{-1,1} & \phi_{0,1} & \phi_{1,1} & \phi_{2,1} & \cdots \\ \cdots & \phi_{-2,0} & \phi_{-1,0} & \phi_{0,0} & \phi_{1,0} & \phi_{2,0} & \cdots \\ \cdots & \phi_{-2,-1} & \phi_{-1,-1} & \phi_{0,-1} & \phi_{1,-1} & \phi_{2,-1} & \cdots \\ \cdots & \cdots & \cdots & \cdots & \cdots & \cdots & \cdots \end{array} . \tag{7}$$

A field configuration Φ is a *point* in system's *state space*

$$\mathcal{M} = \left\{ \Phi \mid \phi_z \in \mathbb{R} , \ z \in \mathbb{Z}^d \right\} , \tag{8}$$

given by all possible values of site fields, where ϕ_z is a single scalar field, or a multitplet of real or complex fields.

While we refer here to such discretization as a lattice field theory, the lattice might arise naturally from a many-body setting with the nearest neighbors interactions, such as many-body quantum chaos models studied in Refs. 32–35, with a multiplet of fields at every site.[36]

A. Periodic field configurations

We shall demand that defining equations are the same everywhere in spatially translation-invariant directions,

for all times. The only way to obey that is by deterministic solutions Φ_c being periodic. We say that a lattice field configuration is $\mathcal{L}_{\mathbb{A}}$-*periodic* if

$$\phi_{z+\mathsf{r}} = \phi_z \tag{9}$$

for any discrete translation $\mathsf{r} = n_1\mathbf{a}_1 + n_2\mathbf{a}_2 + \cdots + n_d\mathbf{a}_d$ in the *Bravais lattice*

$$\mathcal{L}_{\mathbb{A}} = \Big\{ \sum_{j=1}^{d} n_j\mathbf{a}_j \mid n_j \in \mathbb{Z} \Big\}, \tag{10}$$

where the $[d\times d]$ basis matrix $\mathbb{A} = [\mathbf{a}_1, \mathbf{a}_2, \cdots, \mathbf{a}_d]$ formed from primitive integer lattice vectors $\{\mathbf{a}_j\}$ defines a d-dimensional *primitive cell*.[53,54] If the lattice spacing Eq. (6) is set to 1, the lattice *volume*, or the volume of primitive cell

$$N_{\mathbb{A}} = |\mathrm{Det}\,\mathbb{A}| \tag{11}$$

equals the number of lattice sites $z \in \mathbb{A}$ within the primitive cell, see Fig. 2.

Primitive cell $\mathbb{A}$ field configuration lattice-site fields Eq. (7) take values in the $N_{\mathbb{A}}$-dimensional state space

$$\mathcal{M}_{\mathbb{A}} = \{\Phi \mid \phi_z \in \mathbb{R}\,,\ z \in \mathbb{A}\}\ . \tag{12}$$

For example, repeats of the $N_{\mathbb{A}} = 15$-dimensional $[5\times 3]$ primitive cell field configuration

$$\Phi = \begin{bmatrix} \phi_{-2,1} & \phi_{-1,1} & \phi_{0,1} & \phi_{1,1} & \phi_{2,1} \\ \phi_{-2,0} & \phi_{-1,0} & \phi_{0,0} & \phi_{1,0} & \phi_{2,0} \\ \phi_{-2,-1} & \phi_{-1,-1} & \phi_{0,-1} & \phi_{1,-1} & \phi_{2,-1} \end{bmatrix} \tag{13}$$

tile periodically the doubly-infinite field configuration Eq. (7).

We focus on the one-dimensional case for now, postpone discussion of higher-dimensional Bravais lattices to Sec. V.

B. Orbits

Consider a one-dimensional lattice $\mathcal{L}_{\mathbb{A}}$, defined by a single primitive vector $\mathbf{a}_1 = n$ in Eq. (10). One-lattice-spacing shift operator $\mathsf{r}_{zz'} = \delta_{z+1,z'}$ acts on the primitive cell $\mathbb{A}$ as the shift matrix

$$\mathsf{r} = \begin{pmatrix} 0 & 1 & & & \\ & 0 & 1 & & \\ & & \ddots & \ddots & \\ & & & 0 & 1 \\ 1 & & & & 0 \end{pmatrix}, \tag{14}$$

a cyclic permutation matrix that translates a field configuration by one lattice site, $(\mathsf{r}\Phi)_z = \phi_{z+1}$,

$$\begin{aligned} \Phi &= [\phi_0\,\phi_1\,\phi_2\,\phi_3\,\cdots\,\phi_{n-1}]\,, \\ \mathsf{r}\Phi &= [\phi_1\,\phi_2\,\phi_3\,\cdots\,\phi_{n-1}\,\phi_0]\,, \\ &\cdots \\ \mathsf{r}^{n-1}\Phi &= [\phi_{n-1}\,\phi_0\,\phi_1\,\phi_2\,\cdots\,\phi_{n-2}]\,, \\ \mathsf{r}^{n}\Phi &= [\phi_0\,\phi_1\,\phi_2\,\phi_3\,\cdots\,\phi_{n-1}] = \Phi\,. \end{aligned} \tag{15}$$

While each field configuration $\mathsf{r}^j\Phi$ might be a distinct point in the primitive cell's state space Eq. (12), they are equivalent, in the sense that they all are the same set of lattice site fields $\{\phi_z\}$, up to a cyclic relabelling of lattice sites.

In this way actions of the translation group T on field configurations over a multi-periodic primitive cell $\mathbb{A}$ foliate its state space into a union

$$\mathcal{M}_{\mathbb{A}} = \{\Phi\} = \cup\,\mathcal{M}_p \tag{16}$$

of translational *orbits*,

$$\mathcal{M}_p = \{\mathsf{r}^j\Phi_p \mid \mathsf{r}^j \in T\} \tag{17}$$

each a set of equivalent field configurations, labelled perhaps by Φ_p, one of the configurations in the set. Each orbit is a fixed point of T, as for any translation $\mathsf{r}^j\mathcal{M}_p = \mathcal{M}_p$. The number of distinct field configurations in the orbit is n_p, the period of the orbit. (For orbits over two-dimensional lattices, see Sec. VI).

C. Prime orbits over one-dimensional primitive cells

Definition: Prime orbit.

> A primitive cell field configuration Eq. (9) is *prime* if it is not a repeat of a lattice field configuration of a shorter period.

The simplest example of a prime field configuration is a *steady state* $\phi_z = \phi$. Its primitive cell $\mathbb{A}$ is the unit hypercube Eq. (5) of period-1 along every hypercube direction. A field configuration obtained by tiling any primitive cell Eq. (10) by repeats of steady state ϕ is a periodic field configuration, but *not* a prime field configuration.

Consider next a period-6 field configuration Eq. (15) over a primitive cell $2\mathbb{A}$ obtained by a repeat of a primitive cell $\mathbb{A}$ period-3 field configuration,

$$\begin{aligned} \Phi_{2\mathbb{A}} &= [\phi_0\,\phi_1\,\phi_2\,\phi_0\,\phi_1\,\phi_2]\,, & \Phi_{\mathbb{A}} &= [\phi_0\,\phi_1\,\phi_2] \\ \mathsf{r}\Phi_{2\mathbb{A}} &= [\phi_1\,\phi_2\,\phi_0\,\phi_1\,\phi_2\,\phi_0]\,, & \mathsf{r}\Phi_{\mathbb{A}} &= [\phi_1\,\phi_2\,\phi_0] \\ \mathsf{r}^2\Phi_{2\mathbb{A}} &= [\phi_2\,\phi_0\,\phi_1\,\phi_2\,\phi_0\,\phi_1]\,, & \mathsf{r}^2\Phi_{\mathbb{A}} &= [\phi_2\,\phi_0\,\phi_1] \end{aligned} \tag{18}$$

On the infinite Bravais lattice Eq. (7), field configuration $\Phi_{\mathbb{A}}$ and its repeat $\Phi_{2\mathbb{A}}$ are the same field configuration, with the same period-3 orbit $\mathcal{M}_p = (\Phi_{\mathbb{A}}, \mathsf{r}\Phi_{\mathbb{A}}, \mathsf{r}^2\Phi_{\mathbb{A}})$: every Bravais lattice orbit is a 'prime' orbit.

The distinction arises in enumeration of field configurations over a primitive cell. The primitive cell state spaces Eq. (12) are here 6-, 3-dimensional, respectively. Both orbits depend on the same 3 distinct lattice site field values ϕ_z. On the primitive cell $2\mathbb{A}$, however, the 6 lattice sites field configuration $\Phi_{2\mathbb{A}}$ is not *prime*, it is a *repeat* of the field configuration $\Phi_{\mathbb{A}}$. We elaborate this distinction in Sec. IV B.

This is how 'prime periodic orbits' and their repeats work for the one-dimensional, temporal lattice. For a two-dimensional square lattice the notion of 'prime' is a bit trickier, so we postpone its discussion to Sec. VI.

The totality of field configurations Eq. (8) can now be constructed by (i) enumerating all Bravais lattices $\mathcal{L}_{\mathbb{A}}$, (ii) determining prime orbits for each primitive cell $\mathbb{A}$, and (iii) including their repeats into field configurations over primitive cells $\mathbb{AR}$. Our task is to identify, compute and weigh *the totality* of these prime orbits for a given field theory.

D. Observables

A goal of a physical theory is to make predictions, for example, enable us to evaluate the expectation value of an *observable*. An observable 'a' is a function or a set of field configuration functions $a_z = a_z[\Phi]$, let's say temperature, measured on a spatiotemporal lattice site z. For a given $\mathcal{L}_{\mathbb{A}}$-periodic field configuration Φ, the Birkhoff average of observable a is given by the Birkhoff sum A,

$$a[\Phi]_{\mathbb{A}} = \frac{1}{N_{\mathbb{A}}} A[\Phi]_{\mathbb{A}} \,, \qquad A[\Phi]_{\mathbb{A}} = \sum_{z\in\mathbb{A}} a_z \,. \tag{19}$$

For example, if the observable is the field itself, $a_z = \phi_z$, the Birkhoff average over the lattice field configuration Φ is the average 'height' of the field ϕ_z in Eq. (7).

In order to evaluate the *expectation value* of an observable,

$$\langle a\rangle_{\mathbb{A}} \;=\; \int d\Phi_{\mathbb{A}}\, p[\Phi]_{\mathbb{A}}\, a[\Phi]_{\mathbb{A}} \,, \quad d\Phi_{\mathbb{A}} = \prod_{z\in\mathbb{A}} d\phi_z \,, \tag{20}$$

we need to know the state space probability density $p[\Phi]$ of field configuration Φ.

To understand what this probability is, and motivate the formalism that follows, a bit of quantum-mechanical intuition might be helpful. The semiclassical quantum field theory (for a derivation, see ChaosBook Appendix A37 *WKB quantization*[55]) assigns a quantum probability amplitude to a *deterministic* solution Φ_c,[56–59] with the partition sum

$$Z_{\mathbb{A}}[\mathsf{J}] \;\approx\; \sum_c \frac{e^{\frac{i}{\hbar}S[\Phi_c]+im_c+i\Phi_c\cdot\mathsf{J}}}{\left|\mathrm{Det}\,(\mathcal{J}_c/\hbar)\right|^{1/2}} \tag{21}$$

having support on the set of deterministic solutions Φ_c. A deterministic solution Φ_c satisfies the stationary phase condition, i.e., system's Euler-Lagrange equations

$$F[\Phi_c]_z = \frac{\delta S[\Phi_c]}{\delta\phi_z} = 0 \tag{22}$$

at every lattice site z (see sketch of Fig. 1 (a)). In the WKB approximation, its weight is obtained by expanding the action near the state space point Φ_c to quadratic order,

$$S[\Phi] \approx S[\Phi_c] + \frac{1}{2}(\Phi-\Phi_c)^\top \mathcal{J}_c\,(\Phi-\Phi_c) \,, \tag{23}$$

where we refer to the matrix of second derivatives

$$(\mathcal{J}_c)_{z'z} = \left.\frac{\delta^2 S[\Phi]}{\delta\phi_{z'}\delta\phi_z}\right|_{\Phi=\Phi_c} \,, \tag{24}$$

as the *orbit Jacobian matrix*. We will not return to quantum theory in this paper, but $\mathcal{J}_c$ will play the central role in all that follows.

II. DETERMINISTIC FIELD THEORY

For chaotic (or 'turbulent') systems deterministic solutions form a set of state space points, sketched in Fig. 1. In this paper we focus on this set of deterministic solutions. As we show here, despite vastly different appearances, the 'chaos theory' of 1970's is a deterministic Euclidean field theory (see Appendix XII A).

For pedagogical reasons, we first restrict the theory to finite-dimensional state space Eq. (12) of a primitive cell $\mathbb{A}$. These finite volumes are not meant to serve as finite approximations to the infinite Bravais lattices $\mathcal{L}_{\mathbb{A}}$: as is standard in solid state physics, the actual calculations are always carried out over the infinite lattice, more precisely (not standard in solid state physics, but necessary to describe a chaotic field theory) over the set of all periodic lattice field configurations Eq. (9) over all Bravais lattices $\mathcal{L}_{\mathbb{A}}$ Eq. (10), or, in field theory,[60,61] as the 'sum over geometries'.

A. Euclidean field theory

In Euclidean field theory a field configuration Φ over primitive cell $\mathbb{A}$ occurs with state space probability density

$$p_{\mathbb{A}}[\Phi] \;=\; \frac{1}{Z_{\mathbb{A}}}\, e^{-S[\Phi]} \,, \qquad Z_{\mathbb{A}} = Z_{\mathbb{A}}[0] \,, \tag{25}$$

where $Z_{\mathbb{A}}$ is a normalization factor ensuring that probabilities add up to 1, given by the *primitive cell partition sum*, an integral over the primitive cell $\mathbb{A}$ state space Eq. (12),

$$Z_{\mathbb{A}}[\beta] = \int d\Phi_{\mathbb{A}}\, e^{-S[\Phi]+\beta\cdot A_{\mathbb{A}}[\Phi]}, \quad d\Phi_{\mathbb{A}} = \prod_{z\in\mathbb{A}} d\phi_z \,. \tag{26}$$

$A_{\mathbb{A}}[\Phi]$, the Birkhoff sum Eq. (19) of the observable, or a set of observables, is multiplied by a parameter, or a set of parameters β. $S[\Phi]$ is the log probability (in statistics), the Gibbs weight (in statistical physics), or the action (in field theory) of the system under consideration (for examples, see Sec. III).

What is this 'action'? If lattice site fields are not coupled, the spatiotemporal field configuration Φ probability density Eq. (25) is a product of lattice site probability densities, and the partition sum is an exponential in the primitive cell volume $N_{\mathbb{A}}$. If lattice site fields are weakly

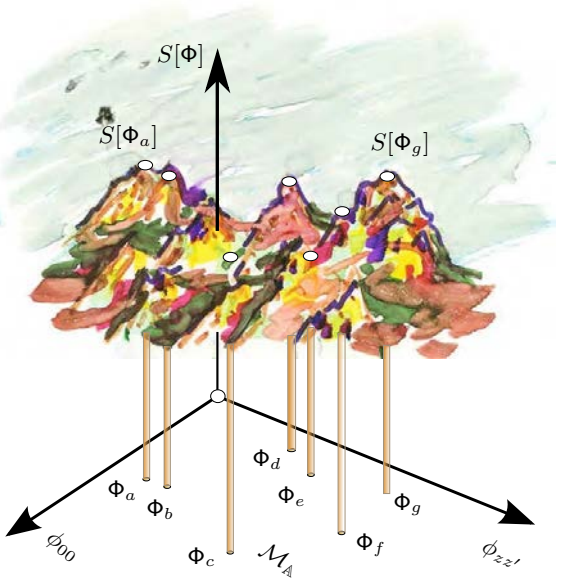

(a) quantum chaos : $\langle a\rangle \approx \sum_c a[\Phi_c] \frac{e^{\frac{i}{\hbar}S[\Phi_c]+im_c}}{|\mathrm{Det}\,(\mathcal{J}_c/\hbar)|^{1/2}}$

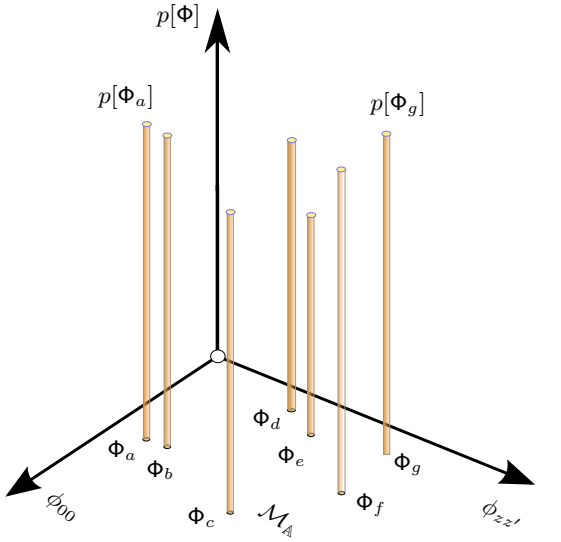

(b) deterministic chaos : $\langle a\rangle = \sum_c a[\Phi_c] \frac{1}{|\mathrm{Det}\,\mathcal{J}_c|}$

FIG. 1. A bird's eye view of the quantum action landscape over the primitive cell state space $\mathcal{M}_{\mathbb{A}}$, Eq. (12). White ellipses indicate the stationary points Eq. (22), i.e., the set of all deterministic solutions $\{\Phi_a, \Phi_b, \Phi_c, \cdots, \Phi_g\}$. They form the skeleton on which the partition sums of both quantum chaos and deterministic chaos / turbulence are evaluated, with the common deterministic backbone, but different weights. (a) For a quantum theory, the semiclassical partition sum Eq. (21) is an approximation, with quantum probability amplitude phases given by deterministic solutions' actions, and stability weights given by square roots of the deterministic ones. (b) For a deterministic field theory the probabilities that form the partition sum Eq. (33) are *exact*, a Dirac porcupine of delta function quills, a quill for each solution of defining equations.

coupled, this exponential depends on the shape of the primitive cell $\mathbb{A}$, $Z_{\mathbb{A}}[\beta] = \exp(N_{\mathbb{A}} W_{\mathbb{A}}[\beta])$. The expectation value Eq. (20) of observable a can be extracted from the log of the primitive cell partition sum $W_{\mathbb{A}}[\beta]$ by application of a $d/d\beta$ derivative:

$$\langle a\rangle_{\mathbb{A}} = \frac{d}{d\beta} W_{\mathbb{A}}[\beta]\Big|_{\beta=0} = \int d\Phi_{\mathbb{A}}\, a_{\mathbb{A}}[\Phi]\, p_{\mathbb{A}}[\Phi]\,. \tag{27}$$

In this series of papers we focus on spatiotemporal systems with bounded variation of $W_{\mathbb{A}}[\beta]$,

$$e^{N_{\mathbb{A}} W_{min}[\beta]} < Z_{\mathbb{A}}[\beta] < e^{N_{\mathbb{A}} W_{max}[\beta]}\,, \tag{28}$$

with field configuration independent bounds $W_{min}[\beta]$, $W_{max}[\beta]$, to be established in Sec. X A. This requirement is the spatiotemporal generalization of the *uniform hyperbolicity* of time-evolving dynamical systems, with Lyapunov exponents strictly bounded away from 0.

Consider a field theory over a large square primitive cell $\mathbb{A} = [L \times L]$. In the infinite volume $N_{\mathbb{A}} = L^2$ limit, exponential bounds of Eq. (28) guarantee convergence to the function

$$W[\beta] = \lim_{N_{\mathbb{A}}\to\infty} \frac{1}{N_{\mathbb{A}}} \ln Z_{\mathbb{A}}[\beta]\,, \tag{29}$$

whose derivative yields the *expectation value*

$$\langle a\rangle = \frac{d\,W[\beta]}{d\beta}\Big|_{\beta=0}\,. \tag{30}$$

In this limit the primitive cell contains the full hypercubic integer lattice $\mathcal{L} = \mathbb{Z}^d$, and the averaging integral $\int d\Phi\, a[\Phi]\, p[\Phi]$ is the integral Eq. (27) evaluated over the infinite d-dimensional hypercubic lattice state space Eq. (8), an integral which we do not know how to evaluate.

What we actually need to evaluate is not this integral, but the derivative W'. That we accomplish in Sec. X F.

B. Deterministic lattice field theory

What these field configuration probabilities Eq. (25) are depends on the theory. Here, motivated by the above semiclassical quantum field theory, we are led to a formulation of the *deterministic field theory*, where a field configuration Φ_c contributes only if it satisfies defining equations

$$F[\Phi_c]_z = 0 \tag{31}$$

on every lattice site z (for our examples of defining equations, see Eqs. Eq. (44) – Eq. (46) below). That is all we require, regardless of whether the system has a Lagrangian formulation, or not (for example, Navier-Stokes equations). Deterministic field theory, it turns out, is an elegant, to a novice perhaps impenetrable, definition of what we already know as deterministic chaos and/or turbulence (the precise relation is afforded by Hill's formulas, derived in Refs. 16 and 48).

Definition: Periodic state

> is a $\mathcal{L}_{\mathbb{A}}$-periodic set of field values $\Phi_c = \{\phi_z\}$ over the d-dimensional lattice $z \in \mathbb{Z}^d$ that satisfies defining equations on every lattice site.

As any field configuration Φ is a *point* in $N_{\mathbb{A}}$-dimensional state space Eq. (12), so is a periodic state Φ_c. Furthermore, just as a temporal evolution period n periodic point is a fixed point of the nth iterate (translation by n temporal lattice sites) of the dynamical time-forward map, every periodic state is a *fixed point* of a set of symmetries of the theory (Sec. VI A and Eq. (152)).

System's defining equations Eq. (31) are defining equations everyone must obey: look at your left neighbor, right neighbor, remember who you were, make sure you fit in just right. The set $\{\Phi_c\}$ of all possible periodic states is system's 'Book of Life' - a catalogue of all possible 'lives', spatiotemporal patterns that defining equations allow, each life a *point* in system's state space, each life's likelihood given by its orbit Jacobian.

A periodic state is a fixed spacetime pattern: the 'time' direction is just one of the coordinates. If you insist on visualizing solutions as evolving in time, a periodic state is a video, not a snapshot of the system at an instant in time (that these are merely different visualizations is proven in Ref. 48).

Definition: Deterministic probability density.

> For a deterministic field theory, the state space probability density is non-vanishing only at the exact solutions of defining equations,
>
> $$p[\Phi] \;=\; \frac{1}{Z}\,\delta(F[\Phi])\,, \tag{32}$$
>
> where the $N_{\mathbb{A}}$-dimensional Dirac delta function $\delta(\cdots)$ enforces defining equations on every lattice site.

In contrast to the quantum action landscape of Fig. 1 (a), for a chaotic (or 'turbulent') deterministic system the probability density Fig. 1 (b) is a Dirac porcupine, a set of delta function quills over the primitive cell state space $\mathcal{M}_{\mathbb{A}}$, Eq. (12), one for each solution of defining equations. The primitive cell $\mathbb{A}$ *deterministic partition sum* Eq. (26) is given by the sum over all periodic states, here labelled 'c',

$$\begin{aligned} Z_{\mathbb{A}}[\beta] &= \sum_c \int_{\mathcal{M}_c} d\Phi_{\mathbb{A}}\, \delta(F[\Phi])\, e^{\beta\cdot A_{\mathbb{A}}[\Phi]} \\ &= \sum_c \frac{1}{|\mathrm{Det}\mathcal{J}_{\mathbb{A},c}|}\, e^{\beta\cdot A_c}\,, \end{aligned} \tag{33}$$

where $\mathcal{M}_c$ is an open infinitesimal neighborhood of state space point Φ_c, and

$$A_c \;=\; \sum_{z\in\mathbb{A}} a_z[\Phi_c] \tag{34}$$

is the Birkhoff sum Eq. (19) of observable a over periodic state Φ_c, to be discussed in Sec. X F. Variants of deterministic partition sums had been computed, by different methods, in different contexts, by many,[60,62,63] but *always* on a given finite primitive cell (geometry), *never* on the totality of infinite Bravais lattices, as we do here.

We refer to

$$(\mathcal{J}_c)_{z'z} = \frac{\delta F[\Phi_c]_{z'}}{\delta\phi_z} \tag{35}$$

evaluated as the $[N_{\mathbb{A}}\times N_{\mathbb{A}}]$ matrix over the primitive cell $\mathbb{A}$, as the *orbit Jacobian matrix* $\mathcal{J}_{\mathbb{A},c}$, to the linear operator Eq. (35), evaluated over infinite Bravais lattice $\mathcal{L}_{\mathbb{A}}$, as the *orbit Jacobian operator* $\mathcal{J}_c$ (also called 'Hessian', a 'Jacobi matrix', or a discrete Schrödinger operator[23,64,65]), and to the determinant[46,47,56] $\mathrm{Det}\,\mathcal{J}_c$ in Eq. (33) as the *orbit Jacobian* (also called 'discriminant' or 'Hill discriminant'[66]). We add prefix 'orbit' to emphasize the distinction between the global *orbit* stability, and the stability of a forward-in-time evolved *state*. Our stability exponent λ_p, Eq. (111), is the temporal evolution sum of expanding Floquet exponents generalized to any spacetime dimension.

The orbit Jacobian is the central innovation of our formulation of spatiotemporal chaos, so we discuss at length in sections IV, VIII, IX, X and Appendix B.

C. Mosaics

The backbone of a *deterministic* chaotic system is thus the set of all spatiotemporal solutions of system's defining equations Eq. (31) that we here refer to as *periodic states*, or, on occasion, as (multi-)*periodic orbits*. Depending on the context, in literature they appear under many other names. For example, Gutkin & Osipov[36] refer to a two-dimensional periodic state Φ_c as a 'many-particle periodic orbit', with each lattice site field ϕ_{nt} 'doubly-periodic', or 'closed'.

Mosaics. For a d-dimensional spatiotemporal field theory, symbolic description is not a one-dimensional temporal "symbolic dynamics" itinerary, as, for example, a symbol sequence that describes a time-evolving N-particle system. The key insight –an insight that applies to coupled-map lattices, and field theories modeled by them,[36,37,67–70] not only systems considered here– is that a field configuration $\Phi = \{\phi_z\}$ over a d-dimensional spacetime lattice $z \in \mathbb{Z}^d$ is labelled by a finite alphabet symbol lattice $\mathsf{M} = \{m_z\}$ over the same d-dimensional spacetime lattice.

For field theories studied here, one can partition the values of a lattice site field ϕ_z into a set of $|\mathcal{A}|$ disjoint intervals, and label each interval by a letter $m_z \in \mathcal{A}$ drawn from an alphabet $\mathcal{A}$, let's say

$$\mathcal{A} = \{1, 2, \cdots, |\mathcal{A}|\}\,. \tag{36}$$

This associates a d-dimensional '*mosaic*' M_c to a field configuration Φ_c over d-dimensional lattice[71–74]

$$\mathsf{M}_c = \{m_z\}\ , \quad m_z \in \mathcal{A}\,, \tag{37}$$

elsewhere called 'symbolic representation';[67] 'spatiotemporal code';[75] 'symbol tensor';[76] 'symbol lattice';[37,77] 'symbol table';[78] 'local symbolic dynamics';[70] 'symbol block'.[16,37] A mosaic serves both as a proxy (a 'name') for the periodic state Φ_c, and its visualization as color-coded symbol array M_c (for examples, see Fig. 6, Fig. 12 and companion paper III[17]).

If there is only one, distinct mosaic M_c for each periodic state Φ_c, the alphabet is said to be *covering*. While each periodic state thus gets assigned a unique mosaic that paginates its location in the Book of Life, the converse is in general not true. If a given mosaic M corresponds to a periodic state, it is *admissible*, otherwise M has to be deleted from the list of mosaics. That's what we do in practice, see Appendix B 1.

In the temporal-evolution setting there is a variety of methods of finding grammar rules that eliminate inadmissible mosaics. While such rules for 2- or higher-dimensional lattice field theories remain, in general, not known to us, we are greatly helped by the observation that in the 'anti-integrable' limit[17,79–82] (also known as the 'anti-continuum limit' in solid state physics,[44] 'large dissipation limit' in nonlinear dynamics,[23], 'weak diffusive coupling' in stochastic field theory[82]) finite alphabets are known, and offer good starting approximations[17] to the corresponding numerically exact periodic states. For spatiotemporal cat, see Sec. XII B *Open questions*, question 6.

III. EXAMPLES OF SPATIOTEMPORAL LATTICE FIELD THEORIES

We shall construct the field theory's deterministic partition sum (Sec. X) by first enumerating all Bravais lattices (geometries) $\mathcal{L}_{\mathbb{A}}$ (Sec. V), determining prime orbits over each, computing the weight of each (Sec. IX), and then (Sec. X) adding together the contributions of periodic states for each. The potentials may be bounded (ϕ^4 theory) or unbounded (ϕ^3 theory), or the system may be energy conserving or dissipative, as long as the set of its periodic states Φ_c is bounded in system's state space Eq. (7). To get a feel for how all this works, we illustrate the theory by applying it to four lattice field theories that we now introduce.

A field theory is defined either by its action, for example a lattice sum over the Lagrangian density for a discretized scalar d-dimensional Euclidean ϕ^k theory,[83–89]

$$S[\Phi] = \sum_z \left\{ \frac{1}{2} \sum_{\mu=1}^{d} (\partial_\mu \phi)_z^2 + V(\phi_z) \right\}\,, \tag{38}$$

with a local potential $V(\phi)$ the same for every lattice site z, or, if lacking a variational formulation, by defining equations $F[\Phi]_z = 0$.

Defining equations Eq. (31) now take form of second-order difference equations

$$-\Box\,\phi_z + V'(\phi_z) = 0\,. \tag{39}$$

In lattice field theory 'locality' means that a field at site z interacts only with its neighbors. To keep the exposition as simple as possible, we treat here the spatial and temporal directions on equal footing, with the graph Laplace operator[90–93]

$$\Box\,\phi_z = \sum_{z'}^{||z'-z||=1} (\phi_{z'} - \phi_z) \quad \text{for all } z, z' \in \mathbb{Z}^d \tag{40}$$

comparing the field on lattice site z to its $2d$ nearest neighbors. For example, the two-dimensional square lattice Laplace operator is given by

$$\Box\ = \mathsf{r}_1 + \mathsf{r}_2 - 4\,\mathbb{1} + \mathsf{r}_2^{-1} + \mathsf{r}_1^{-1}\,, \tag{41}$$

where $\mathsf{r}_1, \mathsf{r}_2$ shift operators (see Eq. (70) for a group-theoretical perspective)

$$(\mathsf{r}_1)_{nt,n't'} = \delta_{n+1,n'}\,\delta_{tt'}\,, \quad (\mathsf{r}_2)_{nt,n't'} = \delta_{nn'}\,\delta_{t+1,t'} \tag{42}$$

translate a field configuration Φ,

$$(\mathsf{r}_1\phi)_{nt} = \phi_{n+1,t}\,, \quad (\mathsf{r}_2\phi)_{nt} = \phi_{n,t+1}\,,$$

by one lattice spacing Eq. (15) in the spatial, temporal direction, respectively.

Here, and in papers I and III[16,17] we investigate spatiotemporally chaotic lattice field theories using as illustrative examples the d-dimensional hypercubic lattice Eq. (6) discretized Klein-Gordon free-field theory, spatiotemporal cat, spatiotemporal ϕ^3 theory, and spatiotemporal ϕ^4 theory, defined respectively by defining equations Eq. (31)

$$-\Box\,\phi_z\ +\ \mu^2\phi_z = 0\,, \qquad \phi_z \in \mathbb{R}\,, \tag{43}$$
$$-\Box\,\phi_z\ +\ \mu^2\phi_z - m_z = 0\,, \qquad \phi_z \in [0,1) \tag{44}$$
$$-\Box\,\phi_z\ +\ \mu^2\,(1/4 - \phi_z^2) = 0\,, \tag{45}$$
$$-\Box\,\phi_z\ +\ \mu^2(\phi_z - \phi_z^3) = 0\,. \tag{46}$$

The anti-integrable form[79–81] of the spatiotemporal ϕ^3, Eq. (45), and spatiotemporal ϕ^4, Eq. (46), is explained in Sec. III B, and the companion paper III.[17]

The homogeneous, free-field case, Eq. (43) is known as the discretized *screened Poisson equation*,[94,95] with parameter μ the reciprocal screening length in the Debye-Hückel or Thomas-Fermi approximations. In statistical mechanics, the related lattice discretized Helmholtz equation is known as the 'Gaussian model',[96–99] and in field theory as the Yukawa or Klein–Gordon equation for a boson of Klein-Gordon (or Yukawa) mass μ. This free-field theory is studied by many, some recent examples are Refs. 63, 100, and 101.

While the free-field theory teaches us much about how a field theory works, it is not an example of a chaotic field theory: defining equations Eq. (43) are linear, with a single deterministic solution, the steady state $\phi_z = 0$.

A. Spatiotemporal cat

The spatiotemporal cat, Eq. (44), that we derive next, is arguably the simplest example of a chaotic (or 'turbulent') deterministic field theory, for which all local degrees of freedom are hyperbolic (anti-harmonic, 'inverted pendula') rather than oscillatory 'harmonic oscillators'. We will use it throughout this paper to illustrate our field-theoretic formulation of spatiotemporal chaos.

Definition: Spatiotemporal cat

defining equations are

$$\begin{aligned} &\left(-\Box + \mu^2\right) \phi_z \pmod 1 = 0\,, \\ &z \in \mathbb{Z}^d\,, \quad \phi_z \in [0,1)\,, \end{aligned} \tag{47}$$

or

$$\left(-\Box + \mu^2\right) \phi_z = m_z\,, \qquad z \in \mathbb{Z}^d\,, \quad \phi_z \in [0,1)\,, \tag{48}$$

with the circle ϕ_z (mod 1) condition enforced by integers m_z, called 'winding numbers',[102] or, as they shepherd stray points back into the state space unit hypercube, 'stabilising impulses'.[103]

For a primitive cell $\mathbb{A}$ we can write it in a matrix form,

$$F[\Phi_{\mathsf{M}}] = \mathcal{J}_{\mathbb{A}} \Phi_{\mathsf{M}} - \mathsf{M} = 0\,, \quad \Phi_{\mathsf{M}} \in [0,1)^{N_{\mathbb{A}}}\,, \tag{49}$$

where $\mathcal{J}_{\mathbb{A}} = -\Box + \mu^2\, \mathbb{1}$ is the orbit Jacobian matrix Eq. (35), and M a d-dimensional mosaic, Eq. (37).

Theories with lattice site field values compactifed to a circle are known as 'compact boson' or 'compact scalar' theories, see for example Refs. 104 and 105. The 'mod 1' in its definition makes the spatiotemporal cat a discontinuous piecewise-linear map, a theory that is *non*linear in the sense that it is not defined globally by a single linear relation, such as the free-field theory Eq. (43), but by a set of distinct piecewise linear conditions, one for each mosaic M.

The temporal cat,

$$-\phi_{t+1} + s\,\phi_t - \phi_{t-1} = m_t\,, \quad t \in \mathbb{Z}\,, \quad \phi_t \in [0,1)\,, \tag{50}$$

a one-dimensional case of spatiotemporal cat studied in companion paper I,[16] was introduced by Percival and Vivaldi[103] as a Lagrangian reformulation of the Hamiltonian Thom-Anosov-Arnol'd-Sinai 'cat map'[28,106,107] (for a historical overview, see Appendix A of companion paper I[16]).

To derive the spatiotemporal cat, add to the temporal cat a $(d-1)$-dimensional spatial lattice where each site field couples to its nearest spatial neighbors, in addition to its nearest past and future field values. Take the spatial coupling strength the same as the temporal coupling strength (just a lattice constant rescaling, as in the derivation of Eq. (54) below). The result is the Euclidean, space $\Leftrightarrow$ time-interchange symmetric difference equation Eq. (48).

In two spacetime dimensions, the spatiotemporal cat defining equations Eq. (48) are a five-term recurrence relation introduced by Gutkin & Osipov,[36,37]

$$-\phi_{j,t+1} - \phi_{j,t-1} + 2s\,\phi_{jt} - \phi_{j+1,t} - \phi_{j-1,t} \;=\; m_{jt}\,, \tag{51}$$

with $\mu^2 = 2(s-2)$. As in Eq. (41), the orbit Jacobian operator in Eq. (49) can be expressed in terms of shift operators,

$$\mathcal{J} = -\mathsf{r}_1 - \mathsf{r}_2 + 2s\,\mathbb{1} - \mathsf{r}_2^{-1} - \mathsf{r}_1^{-1}\,. \tag{52}$$

We study the one-dimensional temporal cat Eq. (50) in some depth in companion paper I.[16] In this paper we focus on the $d = 2$ spatiotemporal cat Eq. (51), with computational details relegated to Appendix B.

In the Hamiltonian, forward-in-time temporal evolution formulation, the dynamics is generated by iterations of a piecewise linear cat *map*. In the spatiotemporal formulation there is *no map*, only defining equations, in form of recurrence conditions, so we refer to the three-term recurrence Eq. (50) as the '*temporal cat*', and to the recurrence condition Eq. (48) in higher spatiotemporal dimensions as the '*spatiotemporal cat*'.

How is this kind of field theory related to more familiar field theories? Think of the discretized Helmholtz-type field theory as a spring mattress:[108] you push it, and it pushes back, it oscillates. Spatiotemporal cat, on the other hand, has a 'cat' (a 'rotor'[16]) at every lattice site: you push it, and the cat runs away, but, forced by the compact boson condition Eq. (48), it eventually has to come back. Chaos issues. Our task is to herd these cats over all of the spacetime.

B. A many-body example: deterministic ϕ^4 theory

The screened Poisson equation Eq. (43) is of the same form as the inhomogeneous Helmholtz equation, but for the sign of μ^2, with the oscillatory sin, cos solutions replaced by the hyperbolic sinh, cosh, and exponentials.[109] To understand how dynamical systems' 'chaos theory' morphs into a Euclidian strong-coupling, anti-integrable deterministic field theory, consider the 1955 Fermi-Pasta-Ulam-Tsingou[43,44] chain of molecules coupled with springs,

$$\frac{d^2\phi_n}{dt^2} - \frac{1}{(\Delta x)^2}(\phi_{n+1} - 2\,\phi_n + \phi_{n-1}) - \phi_n + \phi_n^3 \;=\; 0\,, \tag{53}$$

with spring constant $1/\Delta x$. In absence of nonlinear terms, the solutions are oscillatory eigenmodes. With nonlinearities they can also be breathers, intrinsic localized modes, etc., with perturbations that are oscillatory and bounded in magnitude.[44,110]

Next, consider equation Eq. (53) with a + sign,

$$\frac{d^2\phi_n}{dt^2} + \frac{1}{(\Delta x)^2}(\phi_{n+1} - 2\,\phi_n + \phi_{n-1}) - \phi_n + \phi_n^3 \;=\; 0$$

obtained by interpreting the *imaginary* spring constant as a Klein-Gordon mass $\mu^2 = -(\Delta x)^2$. Discretize time,

$$\frac{d^2\phi_n}{dt^2} \Rightarrow \frac{1}{(\Delta t)^2}(\phi_{n,t+1} - 2\,\phi_{nt} + \phi_{n,t-1})\,,$$

rescale by Δt, and combine the 2nd order derivatives into the $2d$ Laplacian of Eq. (41),

$$-\Box\,\phi_z \;+\; \mu^2(\phi_z - \phi_z^3) \;=\; 0\,. \tag{54}$$

This is the Euclidean massive scalar Klein-Gordon ϕ^4 field theory Eq. (46), an 'inverted potential' chaotic field theory that we study here, and in the companion paper III,[17] theory with hyperbolic instabilities and turbulence.

IV. SPATIOTEMPORAL STABILITY OF A PERIODIC STATE

For field theories Eq. (39) considered here, the orbit Jacobian operators Eq. (35) are of form

$$\mathcal{J}_{zz'} = -\Box_{zz'} + V''(\phi_z)\,\delta_{zz'}\,, \tag{55}$$

with the free field Eq. (43) and spatiotemporal cat Eq. (44), ϕ^3 Eq. (45), ϕ^4 Eq. (46) orbit Jacobian operators

$$\mathcal{J}_{zz'} = -\Box_{zz'} \;+\; \mu^2\delta_{zz'}\,, \tag{56}$$
$$\mathcal{J}_{zz'} = -\Box_{zz'} \;-\; 2\,\mu^2\phi_z\,\delta_{zz'}\,, \tag{57}$$
$$\mathcal{J}_{zz'} = -\Box_{zz'} \;+\; \mu^2(1 - 3\,\phi_z^2)\,\delta_{zz'}\,. \tag{58}$$

Sometimes it is convenient to lump the diagonal terms of the discrete Laplace operator Eq. (41) together with the site potential $V''(\phi_z)$. In that case, the orbit Jacobian operator takes the $2d+1$ banded form

$$\mathcal{J} = \sum_{j=1}^{d}(-\mathsf{r}_j + \mathcal{D} - \mathsf{r}_j^{-1})\,,$$
$$\mathcal{D}_{zz'} = d_z\delta_{zz'}\,,\;\; d_z = V''(\phi_z)/d + 2\,, \tag{59}$$

where r_j shift operators Eq. (42) translate the field configuration by one lattice spacing in the jth hypercubic lattice direction, and we refer to the diagonal entry d_z as the *stretching factor* at lattice site z. For the free field and spatiotemporal cat Eq. (56), ϕ^3 Eq. (57), ϕ^4 Eq. (58) theories the stretching factor d_z is, respectively,

$$s = \mu^2/d + 2\,, \tag{60}$$
$$d_z = -2\,\mu^2\phi_z/d + 2\,, \tag{61}$$
$$d_z = \mu^2(1 - 3\,\phi_z^2)/d + 2\,. \tag{62}$$

What can we say about the spectra of orbit Jacobian operators? In the anti-integrable limit[79–81] the diagonal, 'potential' term in Eq. (55) dominates, and one treats the off-diagonal Laplacian ('kinetic energy') terms as a perturbation. For field theories Eq. (56)-Eq. (58) considered here, in the anti-integrable limit, in any spacetime dimension, the eigenvalues of the orbit Jacobian operator are proportional to the Klein-Gordon mass-squared,

$$\mathcal{J}_{zz'} \;\to\; \mu^2 c_z\,\delta_{zz'}\,, \qquad \mu^2 \text{ large}, \tag{63}$$

where c_z is a theory-dependent constant. For details of ϕ^3 and ϕ^4 field theories, see the companion paper III.[17]

In what follows, it is crucial to distinguish the $[N_{\mathbb{A}}\times N_{\mathbb{A}}]$ orbit Jacobian matrix, evaluated over a finite volume primitive cell $\mathbb{A}$, from the infinite-dimensional orbit Jacobian operator Eq. (59) that acts on the infinite Bravais lattice $\mathcal{L}_{\mathbb{A}}$.

A. Primitive cell stability

The orbit Jacobian matrix Eq. (59) evaluated over a *finite volume* primitive cell $\mathbb{A}$ is an $[N_{\mathbb{A}}\times N_{\mathbb{A}}]$ *matrix*, with $N_{\mathbb{A}}$ discrete eigenvalues.

As an example, consider a periodic state c over the one-dimensional primitive cell of period n, Sec. I B. For a periodic state Φ_c of periodicity $\mathbb{A} = n$, the orbit Jacobian matrix is

$$\mathcal{J}_c = \begin{pmatrix} d_0 & -1 & 0 & \cdots & 0 & -1 \\ -1 & d_1 & -1 & \cdots & 0 & 0 \\ 0 & -1 & d_2 & \cdots & 0 & 0 \\ \vdots & \vdots & \vdots & \ddots & \vdots & \vdots \\ 0 & 0 & 0 & \cdots & d_{n-2} & -1 \\ -1 & 0 & 0 & \cdots & -1 & d_{n-1} \end{pmatrix}, \tag{64}$$

where the shift operators Eq. (14) in Eq. (59) are the off-diagonals.

For the free field, the spatiotemporal cat Eq. (56), and any steady state (constant) solution $\phi_z = \phi$ of a nonlinear field theory, this orbit Jacobian matrix is a tri-diagonal Toeplitz matrix (constant along each diagonal) of circulant form,

$$\mathcal{J}_{\mathbb{A}} = \begin{pmatrix} s & -1 & 0 & \dots & 0 & -1 \\ -1 & s & -1 & \dots & 0 & 0 \\ 0 & -1 & s & \dots & 0 & 0 \\ \vdots & \vdots & \vdots & \ddots & \vdots & \vdots \\ 0 & 0 & \dots & \dots & s & -1 \\ -1 & 0 & \dots & \dots & -1 & s \end{pmatrix}. \tag{65}$$

In what follows, we shall refer to this type of stability as the *steady state stability*.

The orbit Jacobian Eq. (33) of a finite-dimensional orbit Jacobian matrix over a primitive cell $\mathbb{A}$ is given by the product of its eigenvalues,

$$|\mathrm{Det}\,\mathcal{J}_c| = \prod_{j=1}^{N_{\mathbb{A}}} |\Lambda_{c,j}|\,. \tag{66}$$

Consider such determinant in the anti-integrable limit Eq. (63). For steady states, all $N_{\mathbb{A}}$ orbit Jacobian matrix eigenvalues tend to $\Lambda_{c,j} \simeq \mu^2$, so

$$\ln \mathrm{Det}\,\mathcal{J}_c = \mathrm{Tr}\,\ln\mathcal{J}_c \simeq N_{\mathbb{A}}\lambda\,, \quad \lambda = \ln\mu^2\,, \tag{67}$$

where λ is the stability exponent per unit-lattice-volume, with the exact steady state expression given below in Eq. (108).

This suggests that we assign to each periodic state c its average *stability exponent* λ_c per unit-lattice-volume,

$$\frac{1}{|\mathrm{Det}\,\mathcal{J}_c|} = e^{-N_{\mathbb{A}}\lambda_c}\,, \qquad \lambda_c = \frac{1}{N_{\mathbb{A}}}\sum_{j=1}^{N_{\mathbb{A}}} \ln|\Lambda_{c,j}|\,, \tag{68}$$

where λ_c is the Birkhoff average Eq. (19) of the logarithms of orbit Jacobian matrix's eigenvalues. This is a generalization of the temporal periodic orbit Floquet (or 'Lyapunov') stability exponent per unit time to any multi-periodic state, in any spatiotemporal dimension. (Continued in Sec. IX A.)

B. Bravais lattice stability

The linear orbit Jacobian *operator* acts on the *infinite* Bravais lattice $\mathcal{L}_{\mathbb{A}}$. For example, the orbit Jacobian operator a periodic state Φ_c over the one-dimensional Bravais lattice of a period n,

$$\mathcal{J}_c = \begin{pmatrix} \ddots & \ddots & \ddots & \ddots & \ddots & \ddots & \ddots & \ddots \\ \ddots & d_0 & -1 & 0 & 0 & 0 & 0 & \ddots \\ \ddots & -1 & d_1 & -1 & 0 & 0 & 0 & \ddots \\ \ddots & 0 & -1 & d_2 & -1 & 0 & 0 & \ddots \\ \vdots & \vdots & \vdots & \ddots & \ddots & \ddots & \vdots & \vdots \\ \ddots & 0 & 0 & 0 & -1 & d_{n-2} & -1 & \ddots \\ \ddots & 0 & 0 & 0 & 0 & -1 & d_{n-1} & \ddots \\ \ddots & \ddots & \ddots & \ddots & \ddots & \ddots & \ddots & \ddots \end{pmatrix}, \tag{69}$$

is an infinite matrix, with the diagonal block $d_0 d_1 \cdots d_{n-1}$ infinitely repeated along the diagonal.

Next, an elementary but essential observation. Consider a period-3 field configuration Eq. (18) obtained by a translation of another period-3 field configuration in its orbit. Or a period-6 field configuration obtained by a repeat of a period-3 field configuration. The orbit Jacobian operator Eq. (69) for all these field configurations is the *same*, of period 3. So, as announced in Eq. (2), and elaborated in Sec. IX, its spectrum is a property of its *orbit*, irrespective of whether it is computed over a prime periodic state primitive cell, or any lager primitive cell tiled by repeats of a prime periodic state.

But what is the 'orbit Jacobian' of an ∞-dimensional linear Bravais lattice operator? A textbook approach to calculation of spectra of such linear operators (for example, quantum-mechanical Hamiltonians) is to compute them in a large primitive cell $\mathbb{A}$, and then take the infinite box limit. It is crucial to understand that we *do not* do that here. Instead, as in solid state physics and quantum field theory, our calculations are always carried out over the *infinite* spatiotemporal Bravais lattice,[53,111,112] or *continuous* spacetime,[60] where one has to make sense of the orbit Jacobian[46] as a functional determinant.[47]

As we show in Sec. IX, for infinite lattices the appropriate notion of stability is the stability exponent Eq. (68) per unit-lattice-volume, averaged over the first Brillouin zone, which we evaluate by means of the Floquet-Bloch theorem.

V. BRAVAIS LATTICES

Periodic orbit theory of a time-evolving dynamical system on a one-dimensional temporal lattice is organized by grouping orbits of the same period together.[16,18–20,45] For systems characterized by several translational symmetries, one has to take care of multiple periodicities, or, in parlance of crystallography, organize the periodic orbit sums by corresponding *Bravais lattices*,[53] introduced here in Sec. I A.

The set of all transformations that overlay a lattice over itself is called the *space group* G. For the square lattice, the unit cell Eq. (5) tiles the hypercubic lattice under action of translations r_j Eq. (42) in d spatiotemporal directions, called 'shifts' for infinite Bravais lattices, 'rotations' for finite periods primitive cells. They form the abelian translation group

$$T = \{\mathsf{r}_1^{m_1}\mathsf{r}_2^{m_2}\cdots\mathsf{r}_d^{m_d} \,|\, m_j \in \mathbb{Z}\}\,. \tag{70}$$

The cosets of a space group G by its translation subgroup T form the group G/T, isomorphic to a point group g. For example, the square lattice space group $G = T \rtimes \mathrm{D}_4$ is the semi-direct product of translations Eq. (70), and the point group g of right angle rotations, time reversal, spatial reflection, and space-time interchanges. In addition, there might also be internal global symmetries, such as the invariance of spatiotemporal cat equations Eq. (44) under inversion of the field though the center of the $0 \le \phi_z < 1$ unit interval:

$$\phi_z \to 1 - \phi_z \text{ for all } z \in \mathbb{Z}^d\,. \tag{71}$$

Already in the case of chaotic lattice field theory over one-dimensional temporal integer lattice $\mathbb{Z}$ there is a sufficient amount of group-theoretical detail to merit the stand-alone companion paper I,[16] which treats in detail the time reversal invariance for $G = \mathrm{D}_\infty$ dihedral space group of translations and reflections. Here we focus only on the two-dimensional square lattice *translations* Eq. (70), as a full symmetry treatment would distract the reader from the main trust of the paper, the construction of the spatiotemporal zeta function (Sec. X).

A. Bravais lattices of the square lattice

In crystallography there are 5 Bravais lattices over a two-dimensional space. The square lattice Eq. (5) is one

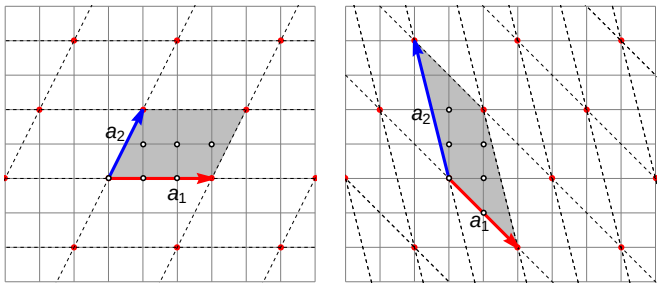

FIG. 2. (Color online) The intersections of the light grey lines -lattice sites $z \in \mathbb{Z}^2$- form the integer square lattice Eq. (6). (a) Translations of the primitive cell $\mathbb{A} = [3\times 2]_1$ spanned by primitive vectors $\mathbf{a}_1 = (3,0)$ and $\mathbf{a}_2 = (1,2)$ define the Bravais lattice $\mathcal{L}_\mathbb{A}$. (b) The primitive vectors $\mathbf{a}_1 = (2,-2)$ and $\mathbf{a}_2 = (-1,4)$ form a primitive cell $\mathbb{A}'$ equivalent to (a) by a unimodular transformation. The intersections (red points) of either set of dashed lines form the same Bravais lattice $\mathcal{L}_\mathbb{A} = \mathcal{L}_{\mathbb{A}'}$. The volume Eq. (11) of either primitive cell is $N_\mathcal{L} = 6$, the number of integer lattice sites within the cell, with the tips of primitive vectors and tiles' outer boundaries belonging to the neighboring tiles. Continued in Fig. 3.

of them. For brevity, whenever we refer here to a 'Bravais lattice', we mean one of the infinity of 'full rank sublattices of the square lattice'[113] that we now describe.

Consider a $[2\times 2]$ integer basis matrix Eq. (10)

$$\mathbb{A} = [\mathbf{a}_1, \mathbf{a}_2] = \begin{bmatrix} a_{1,1} & a_{2,1} \\ a_{1,2} & a_{2,2} \end{bmatrix}, \quad \mathbf{a}_j = \begin{bmatrix} a_{j,1} \\ a_{j,2} \end{bmatrix}, \tag{72}$$

formed from a pair of two-dimensional integer lattice primitive vectors $\mathbf{a}_1$, $\mathbf{a}_2$. A two-dimensional *Bravais lattice*, Fig. 2,

$$\mathcal{L}_\mathbb{A} = \{\mathbb{A}\mathbf{n} \,|\, \mathbf{n} \in \mathbb{Z}^2\} \tag{73}$$

generated by all discrete translations $\mathbb{A}\mathbf{n}$ is a sublattice of the integer lattice $\mathbb{Z}^2$.

As in a discretized field theory the fields are defined only on the hypercubic integer lattice, not on a continuum, we define the *primitive cell* Eq. (12) as the set of lattice sites within the parallelepiped Eq. (72) illustrated by Fig. 2. The tips of primitive vectors and parallelepiped's outer boundaries belong, by translation, to the neighboring tiles; this yields the correct lattice volume Eq. (11), the number of lattice sites $N_\mathbb{A}$ within the primitive cell $\mathbb{A}$.

A primitive cell is not unique:[114] the Bravais lattice $\mathcal{L}_{\mathbb{A}'}$ defined by basis $\mathbb{A}'$ is the same as the Bravais lattice $\mathcal{L}_\mathbb{A}$ defined by basis $\mathbb{A} = \mathbb{A}'\mathbb{U}$ if the two are related by a $[2\times 2]$ unimodular, volume preserving matrix $\mathbb{U} \in \mathrm{SL}(2,\mathbb{Z})$ transformation,[115–117] see Fig. 2 (b). This equivalence underlies many of the properties of elliptic functions and modular forms[118] (see Eq. (75)). Constructing *all* Bravais lattices, however, is straightforward, as each such infinite family of equivalent primitive cells contains a single, unique *Hermite normal form* primitive cell, with upper-triangular basis[119] primitive vectors $\mathbf{a}_1 = (L,0)$, $\mathbf{a}_2 = (S,T)$,

$$\mathbb{A} = \begin{bmatrix} L & S \\ 0 & T \end{bmatrix}, \qquad N_\mathbb{A} = LT, \tag{74}$$

where L, T are the spatial, temporal lattice periods, respectively, and $N_\mathbb{A}$ is the lattice volume Eq. (11). The tilt[120] $0 \le S < L$ imposes 'relative-periodic shift' boundary conditions.[20] In the literature these are also referred to as 'helical',[121] 'toroidal',[122] 'screw',[112] S-corkscrew,[71] 'twisted'[62] or 'twisting factor'[121] boundary conditions.

In the theory of elliptic functions[118] the primitive cell is represented by a complex modular parameter τ, with spatial period L taken as the lattice spacing constant Eq. (6), primitive vectors $\mathbf{a}_1 = (1,0)$, $\mathbf{a}_2 = (\tau_1,\tau_2)$, so $T \to \tau_2 = T/L$, $S \to \tau_1 = S/L$, and

$$\mathbb{A} = \begin{bmatrix} 1 & \tau_1 \\ 0 & \tau_2 \end{bmatrix}, \qquad |\mathrm{Det}\,\mathbb{A}| = \tau_2\,, \tag{75}$$

'Hermite normal form' corresponds to the modular parameter τ values in the fundamental domain. If the corresponding torus is visualised as a glueing of a unit square into a tube, τ_2 parameterizes how the tube is stretched, and τ_1 parameterizes how it is twisted before its edges are stitched together.

Here we refer to a particular Bravais lattice by its Hermite normal form Eq. (74), as

$$\mathcal{L}_\mathbb{A} = [L\times T]_S\,, \tag{76}$$

and to the set of lattice sites within the primitive parallelogram $\mathbb{A}$ as its primitive cell. Notation $[L\times T]_S$ refers to primitive cell being a rectangle of spatial width L, temporal height T, with the primitive cell above it shifted by S, see for example the $[3\times 2]_1$ primitive cell shown in Fig. 3 (b). In terms of lattice site fields, a field configuration $\phi_{z_1 z_2}$ Eq. (9), $z_1 z_2 \in \mathbb{Z}^2$, satisfies the S-corkscrew boundary condition[71],

$$\begin{aligned} \text{horizontally:} \quad & \phi_{z_1 z_2} = \phi_{z_1+L, z_2} \\ \text{vertically:} \quad & \phi_{z_1 z_2} = \phi_{z_1+S, z_2+T}\,, \end{aligned} \tag{77}$$

see Fig. 3.

VI. ORBITS OVER TWO-DIMENSIONAL LATTICES

For field theories studied here (Sec. III), the translation group T Eq. (70) is a symmetry, as their defining equations Eq. (31) retain their form (are 'equivariant') under lattice translations. For square lattice, these are 2-dimensional translations of form $g = \mathsf{r}_1^{m_1}\mathsf{r}_2^{m_2}$. (For symmetries other than translations, see remarks at the beginning of Sec. V.)

Typically a translation operation acting on periodic state Φ_p generates an equivalent (up to lattice sites relabelling) but state-space distinct periodic state $g\Phi_p$. The

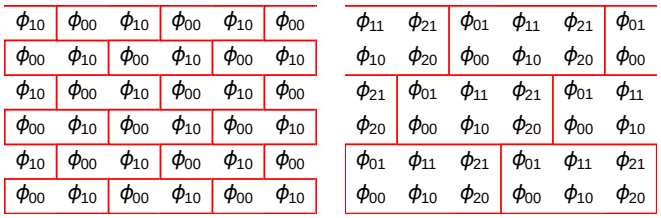

(a) (b)

FIG. 3. Examples of $[L\times T]_S$ field configurations Eq. (74) or 'bricks', together with their spatiotemporal Bravais lattice tilings, visualized as brick walls. (a) $[2\times 1]_1$, primitive vectors $\mathbf{a}_1 = (2,0)$, $\mathbf{a}_2 = (1,1)$; (b) $[3\times 2]_1$ of Fig. 2 (a), primitive vectors $\mathbf{a}_1 = (3,0)$, $\mathbf{a}_2 = (1,2)$. Rectangles enclose the primitive cell and its Bravais lattice translations. Continued in Fig. 5.

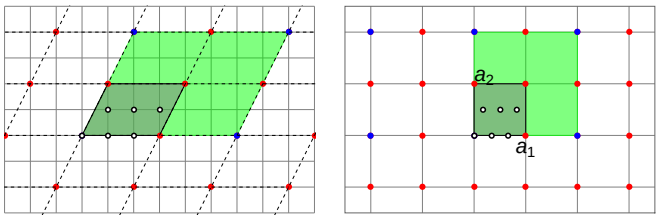

(a) (b)

FIG. 4. (Color online) (a) Bravais lattice $\mathbb{A} = [6\times 4]_2$, blue dots, is a sublattice of Bravais lattice $\mathbb{A}_p = [3\times 2]_1$, blue and red dots. Its primitive cell $\mathbb{A}$ (green parallelogram spanned by primitive vectors (6,0) and (2,4)) is tiled by repeats of the primitive cell $\mathbb{A}_p$ (gray parallelogram spanned by primitive vectors (3,0) and (1,2)). The primitive vectors of the 2 Bravais lattices are related by $\mathbb{A} = \mathbb{A}_p\mathbb{R}$ where $\mathbb{R} = [2\times 2]_0$. (b) Transform the primitive cell $\mathbb{A}_p$ to the unit square of a new square lattice, where each unit square supports a multiplet of 6 fields belonging to a prime $\mathcal{L}_{\mathbb{A}_p}$-periodic state. In this new square lattice, the prime periodic state is a steady state whose primitive cell is a $[1\times 1]_0$ unit square (gray square), while the repeat of the prime is a $\mathcal{L}_{\mathbb{R}}$-periodic state, whose primitive cell is $\mathbb{R} = [2\times 2]_0$ (green square).

totality of all actions of the translation group on periodic states foliates the state space into a union Eq. (16) of translational *orbits*

$$\mathcal{M}_p = \{g\,\Phi_p \mid g \in T\}\,. \tag{78}$$

Bravais lattices $\mathcal{L}_{\mathbb{A}}$ (Sec. I B) are infinite, and their translational symmetries Eq. (70) are infinite groups, but the orbit of a Bravais periodic state is finite, generated by the translations of the infinite lattice curled up into a $N_{\mathbb{A}}$-sites periodic primitive cell $\mathbb{A}$.

A. Prime orbits over two-dimensional primitive cells

A periodic state Φ_p may have all of system's symmetries, a subgroup of them, or have no symmetry at all. If Φ_p has no symmetry, its L_p horizontal translations, T_p vertical translations are all distinct periodic states, so its orbit consists of $N_{\mathbb{A}} = L_pT_p$ periodic states.

It is easy to check whether a one-dimensional periodic state Φ_p over a primitive cell $\mathbb{A}$ is prime, by comparing it to its translations, as in the period-6 example of Sec. I C. We use this test as an operational definition of a *prime* periodic state over a primitive cell $\mathbb{A}$ for a hypercubic lattice in two (or any) dimensions.

Definition: Prime orbit.

> A periodic state Φ_p over primitive cell $\mathbb{A}$ is *prime* if the number of distinct periodic states in its orbit equals $N_{\mathbb{A}}$, the number of lattice sites within its primitive cell $\mathbb{A}$ Eq. (11).

This notion of a 'prime' suffices to formulate our main result, the spatiotemporal zeta function (Sec. X D) for field theories in two spacetime dimensions. However, we have to emphasize the implementing this for a given theory requires determination of *all* of its prime orbits, and that is hard problem, in a sense all of 'chaos theory'. Here we use spatiotemporal cat to test the theory, but relegate details to Appendix B, and in the companion paper III[17] we apply the theory to several nonlinear field theories.

B. Repeats of a prime orbit over two-dimensional primitive cells

The simplest example of a prime periodic state is a *steady state* $\phi_z = \phi$, invariant under all of system's symmetries. Its primitive cell $[1\times 1]_0$ is the unit hypercube Eq. (5) of period-1 along every hypercube direction.

A periodic state obtained by tiling any larger primitive cell by repeats of steady state ϕ is *not a prime* periodic state. There is one such for each Bravais sublattice constructed in Sec. V A, with r_1 copies of lattice site field ϕ horizontally, r_2 copies vertically, and tilt $0 \le s < r_1$ Eq. (74),

$$\mathbb{R} = \begin{bmatrix} r_1 & s \\ 0 & r_2 \end{bmatrix}\,. \tag{79}$$

Next, note that every orbit is 'steady' in the sense that each orbit Eq. (78) is a fixed point of T, as any translation $g\,\mathcal{M}_p = \mathcal{M}_p$ only permutes the set of periodic states within the orbit, but leaves the set invariant. In particular (see Sec. IV B), the stability of an orbit is its intrinsic, translation invariant 'steady' property.

A way to visualize this is by multiplying the Bravais lattice $\mathcal{L}_{\mathbb{A}_p}$ by $\mathbb{A}_p^{-1}$, sending it into the unit integer lattice, as in Fig. 4 (b): in other words, every Bravais lattice is a hypercubic lattice, under an appropriate change of coordinates. In this new integer lattice, the primitive cell $\mathbb{A}_p$ is the *unit* square that supports a multiplet of $N_{\mathbb{A}}$ periodic states belonging to the $\mathcal{L}_{\mathbb{A}_p}$ orbit. Under lattice translations, this multiplet is an $N_{\mathbb{A}}$-dimensional steady state.

To find all repeats of a given prime periodic state, one only needs to find all Bravais lattices $\mathcal{L}_{\mathbb{R}}$, which can again be accomplished using the Hermite normal form repeat

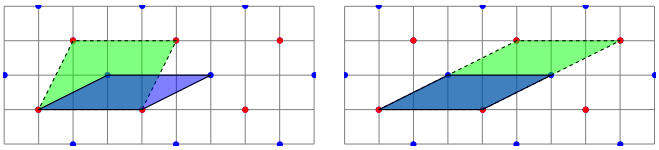

(a) (b)

FIG. 5. (Color online) (a) Bravais lattice $\mathbb{A} = [3\times 2]_1$ of Fig. 2, red dots, is a sublattice of Bravais lattice $\mathbb{A}' = [3\times 1]_2$, blue and red dots, even though the primitive cell $\mathbb{A}$ (green parallelogram spanned by primitive vectors (3,0) and (1,2)) does not appear to be tiled by a repeat of the primitive cell $\mathbb{A}'$ (blue parallelogram spanned by primitive vectors (3,0) and (2,1)). (b) If we shift the top edge of primitive cell $\mathbb{A}$ by 3 lattice units, to $[3\times 2]_4 = [3\times 2]_1$ (green parallelogram spanned by primitive vectors (3,0) and (4,2)), the tiling is clear.

matrix $\mathbb{R}$ Eq. (79). Each $\mathbb{R}$ gives a non-prime periodic state over a larger-periodicity Bravais sublattice $\mathcal{L}_{\mathbb{A}_p\mathbb{R}}$.

Example: A repeat of $[3\times 2]_1$ *prime periodic state.* Tiling of a $\mathcal{L}_{\mathbb{A}} = [6\times 4]_2$ periodic state by a repeat of the $\mathcal{L}_{\mathbb{A}_p} = [3\times 2]_1$ prime periodic state is shown in Fig. 4 (a). In Fig. 4 (b) the primitive cell of the prime $\mathcal{L}_{\mathbb{A}_p}$-periodic state is transformed into the unit square of the new integer lattice, where each unit square supports a multiplet of 6 fields. In this new integer lattice, the primitive cell of the repeat $\mathcal{L}_{\mathbb{A}}$-periodic state is given by $\mathcal{L}_{\mathbb{R}} = [2\times 2]_0$, where $\mathbb{A} = \mathbb{A}_p\mathbb{R}$.

Example: A repeat of $[3\times 1]_2$ *prime periodic state. A priori* is not obvious that $[3\times 1]_2$ primitive cell tiles the $[3\times 2]_1$ primitive cell, Fig. 5 (a). But if you stack $[3\times 1]_2$ primitive cell in the shifted temporal direction by 2 then the left edge of the tile is shifted by 4 in the spatial direction. With the spatial period being 3, shift by 4 in the spatial direction is same as shift by 1. So the boundary conditions of $[3\times 2]_1$ primitive cell are satisfied by the repeat of the $[3\times 1]_2$ primitive cell.

For further examples of prime orbits, see Appendix A.

In summary: to determine all periodic states, it suffices to enumerate all Bravais lattices, then compute their prime orbits on their finite-dimensional primitive cells. Their stabilities, however, will have to be evaluated on the infinite Bravais lattices, as we shall show in Sec. IX.

VII. RECIPROCAL LATTICE

If an operator, in case at hand the orbit Jacobian operator Eq. (55), is invariant under spacetime translations, its eigenvalue spectrum and orbit Jacobian can be efficiently computed using tools of crystallography, by going to the reciprocal lattice.

For a d-dimensional $\mathcal{L}_{\mathbb{A}}$-*periodic* Bravais lattice, discrete wave vectors k form a reciprocal lattice spanned by

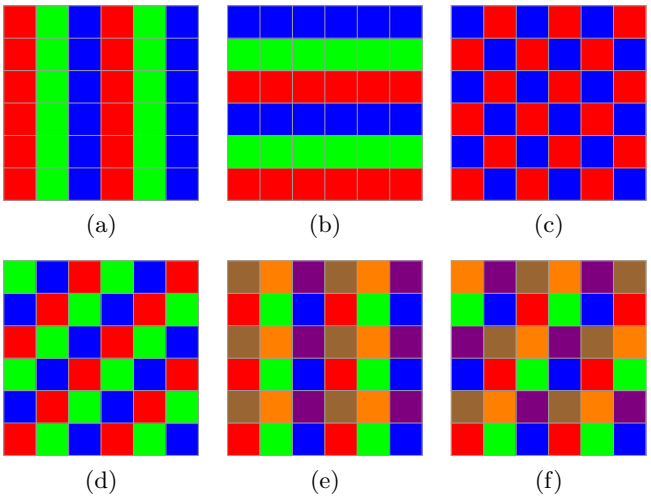

(a) (b) (c) (d) (e) (f)

FIG. 6. (Color online) Examples of spatiotemporal mosaic tilings Eq. (37) of $[6\times 6]_0$ primitive cell by repeats of smaller prime periodic states. (a) $[3\times 1]_0$ temporally steady state. (b) $[1\times 3]_0$ spatially steady state. (c) $[2\times 1]_1$ relative-periodic prime orbit, spatial period-2, temporal period-2; compare with Fig. 3 (a). (d) $[3\times 1]_1$ relative-periodic prime orbit, spatial period-3, temporal period-3. (e) $[3\times 2]_0$ spatial period-3, temporal period-2. (f) $[3\times 2]_1$ of figures 3 (b) and 5. It is a relative-periodic prime orbit, of spatial period-3, temporal period-6. See also Fig. 12 and Appendix A.

d reciprocal primitive vectors which satisfy

$$\mathcal{L}_{\tilde{\mathbb{A}}} = \left\{ \mathsf{k} = \sum_{j=1}^{d} m_j \tilde{\mathbf{a}}_j \mid m_j \in \mathbb{Z} \right\}, \quad \tilde{\mathbf{a}}_i \cdot \mathbf{a}_j = 2\pi\delta_{ij} \,. \tag{80}$$

Assembling the reciprocal primitive vectors $\{\tilde{\mathbf{a}}_j\}$ into columns of the $[d\times d]$ reciprocal primitive cell matrix $\tilde{\mathbb{A}} = [\tilde{\mathbf{a}}_1, \tilde{\mathbf{a}}_2, \cdots, \tilde{\mathbf{a}}_d]$, the reciprocity condition Eq. (80) takes form

$$\tilde{\mathbb{A}}^\top \mathbb{A} = 2\pi\, \mathbb{1} \,. \tag{81}$$

A. Reciprocal primitive cell in one and two dimensions

Translation invariance of a theory suggests its reformulation in a discrete Fourier basis, an approach that goes all the way back to Hill's 1886 paper.[46] The n consecutive shifts Eq. (15) return a period-n field configuration to itself, so acting on a one-dimensional periodic primitive cell, shift operator satisfies the characteristic equation

$$\mathsf{r}^n - \mathbb{1} = \prod_{m=0}^{n-1} (\mathsf{r} - e^{ik}\,\mathbb{1}) = 0 \,, \tag{82}$$

with eigenvalues $\{e^{ik}\}$ the n-th roots of unity, indexed by integers m,

$$k = \Delta k\, m \,, \qquad \Delta k = \frac{2\pi}{n} \,, \quad m = 0, 1, \cdots, n-1 \,, \tag{83}$$

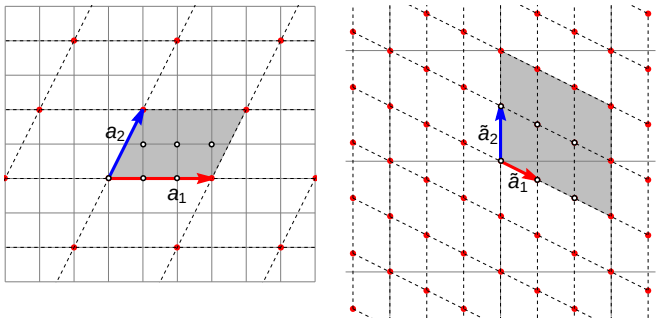

(a) (b)

FIG. 7. (Color online) (a) The intersection points z of the light grey lines form the integer square lattice Eq. (6). The primitive vectors $\mathbf{a}_1 = (3,0)$ and $\mathbf{a}_2 = (1,2)$ form the primitive cell $\mathbb{A} = [3\times 2]_1$ (see Eq. (76) and Fig. 2 (a)), whose translations tile the Bravais lattice $\mathcal{L}_{\mathbb{A}}$ (red points). (b) The intersection points k of the light grey lines form the reciprocal square lattice. Translations of reciprocal primitive vectors $\tilde{\mathbf{a}}_1$ and $\tilde{\mathbf{a}}_2$ (see Eq. (80), Eq. (89)) generate the reciprocal lattice $\mathcal{L}_{\tilde{\mathbb{A}}}$ (red points). (Shaded) The reciprocal primitive cell $\tilde{\mathbb{A}}$. A wave vector outside this region is equivalent to a wave vector within it by a reciprocal lattice translation. Note that the number of lattice sites within the reciprocal primitive cell $\tilde{\mathbb{A}}$ equals the number of sites within the spatiotemporal primitive cell $\mathbb{A}$.

and n eigenvectors $[\varphi(k)]_z = e^{\mathrm{i}\,kz}$,

$$[\mathsf{r}\varphi(k)]_z = [\varphi(k)]_{z+1} = e^{\mathrm{i}\,k(z+1)} = e^{\mathrm{i}k}[\varphi(k)]_z\,. \tag{84}$$

Wave numbers k form a one-dimensional reciprocal lattice Eq. (80),

$$\mathcal{L}_{\tilde{\mathbb{A}}} = \Big\{k = m\,\tilde{\mathbf{a}}_1 \mid m \in \mathbb{Z}\Big\}\,, \quad \tilde{\mathbf{a}}_1 \cdot \mathbf{a}_1 = 2\pi\,,$$

with the reciprocal lattice primitive vector $\tilde{\mathbf{a}}_1 = 2\pi/n$, and the reciprocal primitive cell –the interval $[0, 2\pi)$– that contains n discrete wave numbers Eq. (83).

In two spatiotemporal dimensions, the reciprocal lattice Eq. (80) of the Bravais lattice Eq. (74) is given by

$$\mathcal{L}_{\tilde{\mathbb{A}}} = \{\mathsf{k} = m_1\tilde{\mathbf{a}}_1 + m_2\tilde{\mathbf{a}}_2 \mid m_i \in \mathbb{Z}\}\,, \tag{85}$$

where the reciprocal lattice primitive vectors $\tilde{\mathbf{a}}_1 = \frac{2\pi}{N_{\mathbb{A}}}\,(T, -S)$ and $\tilde{\mathbf{a}}_2 = \frac{2\pi}{N_{\mathbb{A}}}\,(0, L)$ (see Fig. 7 (b)) satisfy the reciprocity condition Eq. (81). The reciprocal primitive cell matrix is also of Hermite normal (but lower-triangular) form,

$$\tilde{\mathbb{A}} = \frac{2\pi}{N_{\mathbb{A}}}\begin{bmatrix} T & 0 \\ -S & L \end{bmatrix}\,, \tag{86}$$

with the reciprocal basis condition Eq. (81) satisfied. The components of a reciprocal lattice wave vector k in Eq. (85) are

$$\mathsf{k} = \begin{bmatrix} k_1 \\ k_2 \end{bmatrix} = \frac{2\pi}{LT}\begin{bmatrix} m_1 T \\ -m_1 S + m_2 L \end{bmatrix}\,. \tag{87}$$

As in the one-dimensional case Eq. (83), the wave numbers along each direction of a two-dimensional square lattice can be restricted to $k_j \in [0, 2\pi)$ with $m_1 = 0, 1, \cdots, L-1$, $m_2 = 0, 1, \cdots, T-1$, $N_{\mathbb{A}} = LT$ distinct wave vectors. This set of reciprocal lattice sites, indexed by integer pairs $m = m_1 m_2$, forms the *reciprocal primitive cell* $\tilde{\mathbb{A}}$, which contains the same number of lattice sites $\mathsf{k} \in \tilde{\mathbb{A}}$ as the spatiotemporal Bravais lattice primitive cell $\mathbb{A}$ (see Fig. 7 (b)).

Example: A spatiotemporal primitive cell, reciprocal primitive cell. Primitive vectors $\mathbf{a}_1 = (3,0)$ and $\mathbf{a}_2 = (1,2)$ define the primitive cell $[3\times 2]_1$ drawn in Fig. 7 (a),

$$\mathbb{A} = \begin{bmatrix} 3 & 1 \\ 0 & 2 \end{bmatrix}\,, \qquad N_{\mathbb{A}} = 6\,. \tag{88}$$

The corresponding reciprocal primitive cell vectors (shaded region in Fig. 7 (b)),

$$\tilde{\mathbb{A}} = \frac{2\pi}{6}\begin{bmatrix} 2 & 0 \\ -1 & 3 \end{bmatrix}\,, \tag{89}$$

satisfy the reciprocal bases condition Eq. (81), and contain the same number of reciprocal lattice sites $\mathsf{k} \in \tilde{\mathbb{A}}$ as the Bravais lattice primitive cell $\mathbb{A}$ of Fig. 7 (a).

The next two sections are the conceptual core of the paper:

Sec. VIII Primitive cell stability. As noted in the introduction, the textbook Gutzwiller-Ruelle periodic orbit theory[18–20] is hampered by a simple fact: its periodic orbit weight Eq. (1) is *not* multiplicative for orbit repeats. This section recapitulates the conventional theory, in which all periodic orbit calculations are done in finite time 'cells', as in Fig. 8 (b), with the key non-multiplicativity fact illustrated by computation of Eq. (103). Our spatiotemporal theory illuminates the origin of this fact in several easy to grasp ways.

Sec. IX Bravais lattice stability. A crystallographer or a field theorist starts –*ab initio*– with an *infinite* lattice or continuous spacetime, as in Fig. 8 (c). This, we claim in the introduction, Eq. (2), is the correct approach which –as we show here, Eq. (111)– yields (multi)periodic state weights that are *multiplicative* for repeats of spatiotemporally periodic solutions. The stability exponent per unit spacetime volume is the spacetime generalization of the temporal periodic orbit Lyapunov exponent, the mean instability per unit time. No matter what repeat of a prime periodic state one starts with, its stability exponent is always given by the same integral over the prime orbit Brillouin zone. From this follows the main result of our paper, the spatiotemporal zeta function of Sec. X.

VIII. PRIMITIVE CELL STABILITY

As we now explain, it is crucial that we distinguish the *finite* primitive cell orbit Jacobian *matrix* (finite volume

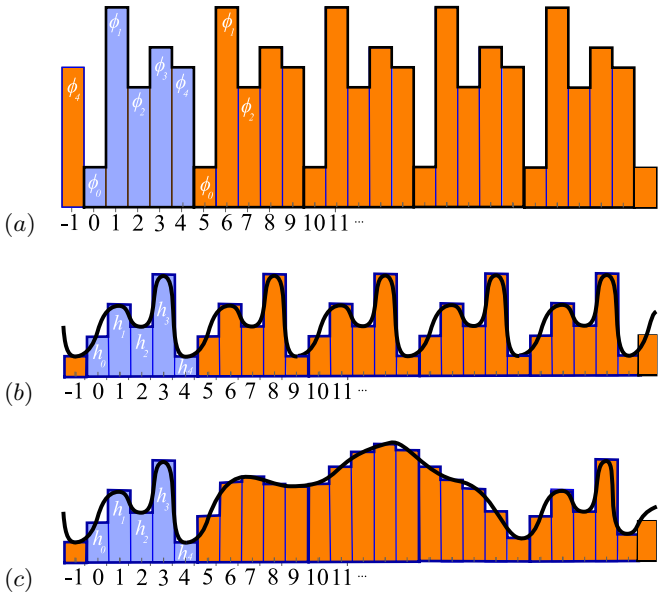

FIG. 8. (Color online) A one-dimensional temporal lattice period-5 periodic state $\Phi_c = [\phi_0\,\phi_1\,\phi_2\,\phi_3\,\phi_4]$ illustrated by (a) five repeats of the primitive cell periodic state. (b) An *internal* perturbation h_z has the same periodicity as the periodic state. Its spectrum, evaluated in Sec. VIII, is discrete. (c) A *transverse* perturbation h_z is an arbitrary, aperiodic function over the infinite lattice. Its spectrum, evaluated by the Floquet-Bloch theorem in Sec. IX, is a continuous function of wave number k. Horizontal: lattice sites labelled by $z \in \mathbb{Z}$. Vertical: (a) value of field ϕ_z, (b-c) perturbation h_z, plotted as a bar centred at lattice site z. Values of the field and perturbation are shown in blue within the primitive cell, and in orange outside the primitive cell.

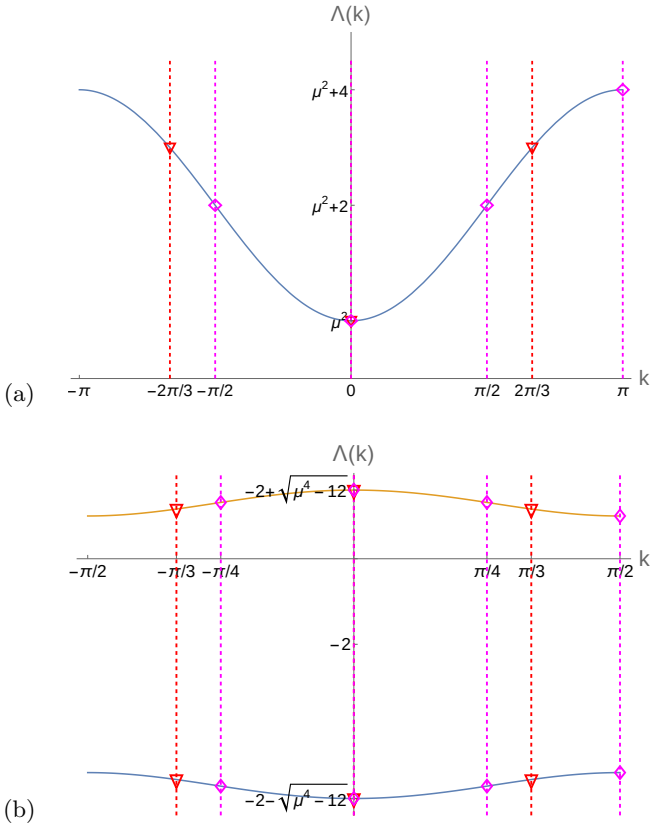

FIG. 9. (Color online) One-dimensional lattice orbit Jacobian operator spectra, as functions of the reciprocal lattice wave number k. For time-reversal invariant systems the spectra are $k \to -k$ symmetric. (a) The steady state $\Lambda(k)$ spectrum Eq. (90), as a function of the first Brillouin zone wave number $k \in (-\pi, \pi]$, plotted for $\mu^2 = 1$ value. Any period-n primitive cell Eq. (65) orbit Jacobian matrix spectrum consists of n discrete points embedded into $\Lambda(k)$, for example period-3 (red triangles) and period-4 (magenta diamonds) eigenvalues. (b) The nonlinear ϕ^3 theory $\Lambda_{01,\pm}(k)$ spectrum Eq. (115) of the Bravais lattice $\mathcal{L}_{01}$ tiled by the period-2 periodic state $\Phi_{01} = \{\phi_0, \phi_1\}$, together with the eigenvalues of 3rd repeat (red triangles) and 4th repeat (magenta diamonds) primitive cells. Plotted for $\mu^2 = 5$ value. See Appendix C 1. From companion paper I.[16]

primitive cell stability, discussed in this section) from the *infinite* orbit Jacobian *operator* (infinite Bravais lattice stability, discussed in Sec. IX) in stability calculations.

To the best of our knowledge, in all current implementations of the periodic orbit theory,[18–20,45,123] the calculations are always carried out on finite primitive cells, so a 'chaos' expert is free to skim over this section - it is a recapitulation of Hénon, Lorentz, etc., calculations in the spatiotemporal, field theoretic language. The radical departure takes place in Sec. IX.

We start by considering the steady state orbit Jacobian matrices, such as Eq. (65), with no lattice site dependence, $d_z = s$, which are fully diagonalized by going to the reciprocal lattice.

A. Primitive cell steady state stability in one dimension

For a one-dimensional primitive cell $\mathbb{A}$ of period n, the discrete Fourier transform Eq. (84) of Laplacian Eq. (40),

$$\mathcal{J}_{\mathbb{A}}\varphi_k = (-\Box + \mu^2\,\mathbb{1})\,\varphi_k = (p^2+\mu^2)\,\varphi_k \qquad (90)$$
$$p = 2\sin\frac{k}{2}\,, \quad k = \frac{2\pi}{n}m\,, \quad m = 0, 1, \cdots, n-1\,,$$

expresses the Fourier-diagonalized lattice Laplacian as the square of p_m, the 'lattice momentum', or the 'momentum measured in lattice units',

$$(\tilde{\mathcal{J}}_{\mathbb{A}})_{mm'} = (p_m^2+\mu^2)\,\delta_{mm'} \qquad (91)$$
$$p_m = 2\sin(\pi m/n)\,,$$

with n eigenvalues $\Lambda_m = p_m^2 + \mu^2$ indexed by integer m. The cord function $\mathrm{crd}(\theta) = 2\sin(\theta/2)$ was used already by Hipparchus cc. 130 BC in the same context, as a discretization of a circle by approximating n arcs by n cords.[124,125]

Example: The spectrum of orbit Jacobian matrix for a steady state of period-3. The wave numbers Eq. (90) take values $k = 0, 2\pi/3, 4\pi/3$, with lattice momentum

values $p(0) = 0\,,\ p(2\pi/3) = p(4\pi/3) = \sqrt{3}\,$. The lattice momentum square p_m^2 in Eq. (91) is a discrete field over the $N_{\mathbb{A}} = 3$ lattice sites of the reciprocal primitive cell $\tilde{\mathbb{A}}$, indexed by integer reciprocal lattice-site labels $m = 0, 1, 2$,

$$p_m^2 \;=\; \boxed{\begin{array}{|c|c|c|}\hline p_0^2 & p_1^2 & p_2^2 \\ \hline\end{array}} \;=\; \boxed{\begin{array}{|c|c|c|}\hline 0 & 3 & 3 \\ \hline\end{array}}\,, \tag{92}$$

The orbit Jacobian matrix $\mathcal{J}_{\mathbb{A}}$ eigenvalues are $\Lambda_m = p_m^2 + \mu^2$, and the corresponding orbit Jacobian is the product of the three $\mathcal{J}_{\mathbb{A}}$ eigenvalues. See Tables I and II for lists of such computations.

Why are eigenvalues in Eq. (92) placed in a box? That will be made clearer by example Eq. (97), when we compute $\mathsf{p}^2_{\tilde{\mathbb{A}}}$ for a two-dimensional lattice.

B. Primitive cell steady state stability in two dimensions

Discrete Fourier transforms diagonalize the hypercubic lattice steady state orbit Jacobian matrix over a periodic, 'rectangular' primitive cell $\mathbb{A}$ in any spatiotemporal dimension d,

$$(\tilde{\mathcal{J}}_{\mathbb{A}})_{mm'} = (\mathsf{p}_m^2 + \mu^2)\,\delta_{mm'} \tag{93}$$
$$\mathsf{p}_m^2 = \sum_{j=1}^{d} p_j^2\,, \quad p_j = 2\sin\frac{k_j}{2}\,, \quad k_j = \frac{2\pi}{L_j}\,m_j\,,$$

p_j is the lattice momentum in jth direction, and L_j is the period of the primitive cell $\mathbb{A}$ in jth direction, with $N_{\mathbb{A}}$ orbit Jacobian matrix eigenvalues $\Lambda_m = \mathsf{p}_m^2 + \mu^2$ taking values on the reciprocal lattice sites k, indexed by integer multiplets $m = m_1 m_2 \cdots m_d$. The inverse $1/(\mathsf{p}^2 + \mu^2)$ is known as the free-field propagator.

This is almost everything there is to a primitive cell stability, except that the 'rectangle' periodic boundary conditions Eq. (93) are only a special case of spacetime periodicity. Consider a steady state orbit Jacobian matrix over a two-dimensional integer lattice. For the general Eq. (74) case, as illustrated by Fig. 7 (b), the reciprocal primitive vector $\tilde{\mathbf{a}}_1 = \frac{2\pi}{L}\,(1, -S/T)$ has a $0 \le S < L$ tilt. Substituting wave vector Eq. (87) into the two-dimensional plane wave (as we did for the one-dimensional case, see Eq. (84)), we find that the kth eigenstate phase evaluated on the lattice site z is

$$[\varphi(\mathsf{k})]_z = e^{i(k_1 z_1 + k_2 z_2)} \tag{94}$$

where

$$\begin{aligned} &z = z_1 z_2 \in \mathbb{Z}^2\,, \quad \mathsf{k} = k_1 k_2 \in \mathcal{L}_{\tilde{\mathbb{A}}}\,, \quad m = m_1 m_2 \\ &m_1 = 0, 1, \cdots, L-1\,, \quad m_2 = 0, 1, \cdots, T-1 \\ &k_1 = \frac{2\pi}{L} m_1\,, \quad k_2 = \frac{2\pi}{T}(-\frac{S}{L} m_1 + m_2)\,. \end{aligned} \tag{95}$$

As illustrated by Fig. 7 (b), there are $N_{\mathbb{A}} = LT$ wave vectors in the reciprocal primitive cell $\tilde{\mathbb{A}}$. The spatiotemporal orbit Jacobian matrix Eq. (93) is diagonal on the reciprocal lattice, with eigenvalues

$$\Lambda_{m_1 m_2} = \mathsf{p}^2_{m_1 m_2} + \mu^2\,. \tag{96}$$

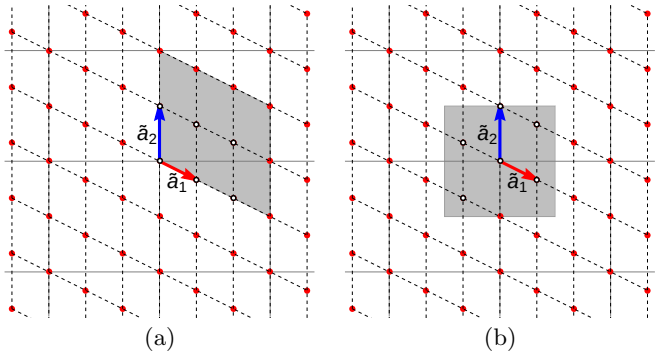

(a) (b)

FIG. 10. (Color online) (a) As in Fig. 7 (b): Translations of reciprocal primitive vectors $\tilde{\mathbf{a}}_1$ and $\tilde{\mathbf{a}}_2$ (see Eq. (80), Eq. (89)) generate the reciprocal lattice $\mathcal{L}_{\tilde{\mathbb{A}}}$ (red points), with (shaded) the reciprocal primitive cell $\tilde{\mathbb{A}}$. (b) By convention, one restricts the range of wave numbers to (shaded) the first Brillouin zone $\mathbb{B}$, with $k_1, k_2 \in (-\pi, \pi]$.

It is helpful to work out an example to illustrate how Eq. (96) gives us the orbit Jacobian matrix eigenvalues.

Example: The spectrum of steady state orbit Jacobian matrix, $[3 \times 2]_1$ primitive cell. Consider primitive cell $[3\times 2]_1$ of example Eq. (88), drawn in Fig. 7 (a). The screw boundary condition yields $S/T = 1/2$. The wave numbers k in Eq. (94) are indexed by integer pairs $m_1 = 0, 1, 2$ and $m_2 = 0, 1$. The $\mathsf{p}^2_{m_1 m_2}$ in the reciprocal lattice orbit Jacobian matrix Eq. (96) is

$$\mathsf{p}^2_{m_1 m_2} = p(k_1)^2 + p(k_2)^2\,,$$

where lattice momenta $p(k) = 2\sin(k/2)$ take values

$$p(0) = 0\,,\ p(\pi/3) = 1\,,\ p(2\pi/3) = \sqrt{3}\,,\ p(\pi) = 2\,.$$

A typical reciprocal lattice site $m_1 m_2$ evaluation: take $m_1 = 1$, $m_2 = 1$ in Eq. (95),

$$p_{11}^2 = p\Big(\frac{2\pi}{3}\Big)^2 + p\Big(\pi - \frac{2\pi}{3}\frac{1}{2}\Big)^2 = 3 + 3\,.$$

The values of p^2, indexed by integer pairs $m_1 m_2$, fill out the reciprocal lattice unit cell,

$$\mathsf{p}^2_{m_1 m_2} \;=\; \boxed{\begin{array}{|c|c|c|}\hline p_{01}^2 & p_{11}^2 & p_{21}^2 \\ \hline p_{00}^2 & p_{10}^2 & p_{20}^2 \\ \hline\end{array}} \;=\; \boxed{\begin{array}{|c|c|c|}\hline 4 & 6 & 4 \\ \hline 0 & 4 & 6 \\ \hline\end{array}}\,, \tag{97}$$

with, for example, the $(\tilde{\mathcal{J}}_{\mathbb{A}})_{21}$ eigenvalue $\Lambda_{21} = 4 + \mu^2$, and so on. Figure 11 (a) offers a perspective visualization of stability eigenvalues over such reciprocal cell, in that case $\mathcal{L}_{[8\times 8]_0}$ periodic state. The corresponding orbit Jacobians are products of the $\mathcal{J}_{\mathbb{A}}$ eigenvalues, some of which are tabulated in Tables I and II.

Note that all spatiotemporal cat orbit Jacobians have a μ^2 prefactor. This is due to the fact that for $\mu^2 = 0$ one is looking at a Laplacian, and Laplacian operator Eq. (40), which compares a site field to its neighbors, always has a zero mode for the constant eigenvector φ_{00}.

The values of the lattice momentum square happen to be integers only for the few smallest primitive cells: in general their values are expressed in terms of Hipparchus cord functions $\mathrm{crd}(2\pi\, m_j/L_j)$, or what we here call 'lattice momenta' Eq. (91). However, for integer values of spatiotemporal cat Klein-Gordon mass-square μ^2, the orbit Jacobians take integer values, so if we are not interested in details of the spectrum, their direct evaluation might be preferable. That we do in Appendix B 3.

The orbit Jacobian of any steady state $\phi_z = \phi$ of any field theory can be evaluated analytically by discrete Fourier diagonalization. Its orbit Jacobian matrix is constant along the diagonal, with eigenvalues evaluated in the same way as for the free-field theory and spatiotemporal cat Eqs. (94–96),

$$(\tilde{\mathcal{J}}_{\mathbb{A}})_{m_1 m_2} = \mathsf{p}^2_{m_1 m_2} + \tilde{\mu}^2\,, \tag{98}$$

where the steady state Klein-Gordon mass is, as explained in the companion paper III Ref. 17, $\tilde{\mu}^2 = -2\,\mu^2\phi$ for the spatiotemporal ϕ^3 Eq. (57), and $\tilde{\mu}^2 = \mu^2(1-3\,\phi^2)$ for the spatiotemporal ϕ^4 Eq. (58).

C. Primitive cell periodic state stability

Except for the steady state solutions discussed so far, the orbit Jacobian operators of field theories such as the ϕ^3 Eq. (57) and ϕ^4 Eq. (58) depend on the corresponding periodic states. The orbit Jacobian matrices evaluated over the primitive cells, such as Eq. (64), are generally not invariant under the spacetime unit-lattice spacing shift operator Eq. (42) translations, so they are only block-diagonalized by Fourier transforms.

In general, periodic state's orbit Jacobians are computed numerically, but -and that is basically the only exception- some period-2 periodic states can be worked out analytically.

Example: One-dimensional ϕ^3 field theory period-2 periodic state. The one spatiotemporal dimension ϕ^3 theory Eq. (45) has one period-2 prime orbit $\{\Phi_{01}, \Phi_{10}\}$ (for details, see Appendix C 1) with 2 orbit Jacobian matrix Eq. (57) eigenvalues

$$\Lambda_{01,\pm} = -2 \pm \sqrt{\mu^4 - 12}\,, \tag{99}$$

and orbit Jacobian

$$\mathrm{Det}\,\mathcal{J}_{01} = 16 - \mu^4\,. \tag{100}$$

Consider next a period-6 periodic state over a primitive cell $3\mathbb{A}$ obtained by three repeats of the period-2 prime periodic state (see Eq. (18) for another such example). The orbit Jacobian matrix Eq. (64) is a $[6\times 6]$ matrix, with 6 eigenvalues

$$\begin{aligned}
\Lambda_{-1,\pm} &= -2 \pm \sqrt{\mu^4 - 15} \\
\Lambda_{0,\pm} &= -2 \pm \sqrt{\mu^4 - 12} \\
\Lambda_{1,\pm} &= -2 \pm \sqrt{\mu^4 - 15}\,,
\end{aligned} \tag{101}$$

and orbit Jacobian

$$\mathrm{Det}\,\mathcal{J}_{3*01} = (16-\mu^4)(19-\mu^4)^2\,. \tag{102}$$

The eigenvalues of orbit Jacobian matrices for the prime periodic state Φ_{01} and its repetitions are plotted in Fig. 9 (b). The bands, denoted by k in Fig. 9 (b), and the subscript of the eigenvalues Eq. (101) will be explained in Sec. IX B. Two of the eigenvalues correspond to 'internal' eigenstates (of the same periodicity as the prime periodic state), so they coincide with the prime orbit eigenvalues Eq. (99), while the remaining four correspond to 'transverse' eigenstates,[25,126] of periodicity of the repeat primitive cell $3\mathbb{A}$. As a result, the orbit Jacobian of the third repeat is not the third power of the prime periodic state orbit Jacobian,

$$\mathrm{Det}\,\mathcal{J}_{3*01} \neq (\mathrm{Det}\,\mathcal{J}_{01})^3\,. \tag{103}$$

This confirms the assertion we had made in the introduction, Eq. (1): orbit Jacobians of primitive cell periodic states are *not multiplicative* for their repeats. (Continued in Sec. IX B.)

Example: Two-dimensional ϕ^4 field theory $[2\times 1]_0$ periodic state. In Appendix C 2 we work out as a further example the primitive cell stability of two-dimensional ϕ^4 theory Eq. (46) $[2\times 1]_0$ periodic state. The eigenvalues of the primitive cell prime periodic state and its repetition are plotted in Fig. 11 (b). Next, note that the primitive cell of Bravais lattice $[6\times 4]_0$ can be tiled by twelve repeats of a prime $[2\times 1]_0$ periodic state. The eigenvalues of its orbit Jacobian matrix, plotted in Fig. 11 (b), lie on the two orbit Jacobian operator Bloch bands, located at twelve wave vectors in the first Brillouin zone of $[6\times 4]_0$: $k_1 = -\pi/3, 0, \pi/3$ and $k_2 = -\pi/2, 0, \pi/2, \pi$. (Continued in Sec. IX B.)

Reciprocal lattice computations of orbit Jacobian matrix spectra can be automated, and we have carried them out for thousands of Bravais lattices. Further explicit, but not particularly illuminating spatiotemporal cat calculations are relegated to Appendix B.

IX. BRAVAIS LATTICE STABILITY

In Sec. IV A we have defined the stability exponent of a periodic state over a finite volume primitive cell, and in Sec. VIII we have explained how to compute them, setting the stage for the main result of section, the reciprocal lattice evaluation of the stability exponent for the *orbit Jacobian operator*.

An orbit Jacobian operator Eq. (69) acts on an infinite Bravais lattice periodic state $\Phi_{\mathbb{A}}$ Eq. (7), so it has infinitely many eigenvalues. What that means in context of dynamical systems theory was first explained by Pikovsky:[25] while a given periodic state $\Phi_{\mathbb{A}}$ is $\mathcal{L}_{\mathbb{A}}$-periodic on its infinite Bravais lattice, its perturbations can have periodicity of the periodic state, periodicity of

any Bravais sublattice $\mathcal{L}_{\mathbb{AR}}$, or no periodicity at all, as in Fig. 8 (c). By the Floquet-Bloch theorem Eq. (110), the stability exponent λ_p then depends on continuum wave numbers $\mathsf{k} \in \mathbb{B}$ within the first Brillouin zone,

$$k_j \in (-\pi/L_j, \pi/L_j] \,, \qquad j = 1, 2, \cdots, d \,. \tag{104}$$

Continuing on the discussion of Sec. VIII C: $k_j = 0$ eigenvalues correspond to 'internal' eigenstates, states of the same periodicity as the periodic state $\Phi_{\mathbb{A}}$, evaluated here in Sec. VIII for the primitive cell $\mathbb{A}$. The $k_j \neq 0$ continuum corresponds to 'transverse' eigenstates, perturbations that exit the $\mathbb{A}$-symmetric subspace, as in primitive cell example Eq. (102).

In textbook arguments leading to the Bloch theorem, one notes that larger and larger spatiotemporal primitive cells correspond to denser and denser reciprocal primitive cells (see, for example, Fig. 11 (b), and the arguments of the next section), leading in the infinite primitive cell limit to a parametrization by continuum values of wave vectors. Here we always evaluate stability exponents on infinite Bravais lattices, as integrals over the first Brillouin zone.

A. Steady state stability

Consider the stability exponent Eq. (68) of a steady state Φ_p, all lattice site fields equal, $\phi_z = \phi$, averaged over a primitive cell $\mathbb{A}$:

$$\lambda_{\mathbb{A}} = \frac{1}{N_{\mathbb{A}}} \ln \mathrm{Det}\, \mathcal{J}_{\mathbb{A}} \;=\; \frac{1}{N_{\mathbb{A}}} \mathrm{Tr}_{\,\mathbb{A}} \ln(\mathsf{p}^2 + \mu^2) \,.$$

The steady state orbit Jacobian matrix Eq. (65) is translation invariant along each lattice direction, and thus diagonalized by discrete Fourier transform Eq. (84).

For one-dimensional case Eq. (91)

$$\lambda_{\mathbb{A}} = \frac{1}{n} \sum_{m=0}^{n-1} \ln(p_m^2 + \mu^2) = \frac{1}{2\pi} \sum_{k_m} \Delta k \, \ln(p_m^2 + \mu^2) \,,$$

where

$$p_m = 2 \sin \frac{k_m}{2} \,, \quad k_m = \Delta k \, m \,, \; \Delta k = \frac{2\pi}{n} \,.$$

With the period n of the primitive cell $\mathbb{A}$ taken to infinity, the stability exponent is given by the integral over the first Brillouin zone,

$$\lambda = \frac{1}{2\pi} \int_{-\pi}^{\pi} dk \ln(p^2 + \mu^2) \,, \qquad p = 2 \sin \frac{k}{2} \,. \tag{105}$$

By same reasoning, for a d-dimensional hypercubic lattice, the steady state stability exponent is given by a d-dimensional integral over the first Brillouin zone $\mathbb{B}$,

$$\lambda \;=\; \frac{1}{(2\pi)^d} \int_{\mathbb{B}} dk^d \ln(\mathsf{p}^2 + \mu^2) \,,$$
$$\mathsf{p}^2 = \sum_{j=1}^{d} p_j^2 \,, \qquad p_j = 2 \sin \frac{k_j}{2} \,, \tag{106}$$

with continuous wave numbers restricted to 2π intervals, conventionally to the centered hypercubic first Brillouin zone

$$\mathbb{B} = \{\mathsf{k} \mid k_1, k_2, \cdots, k_d \in (-\pi, \pi]\} \,. \tag{107}$$

The one-dimensional steady state integral Eq. (105) is frequently encountered in solid state physics, statistical physics and field theory, and there are many ways of evaluating it (see, for example, Gradshteyn and Ryzhik[109] Eq. 4.226 2):

$$\begin{aligned} \lambda \;&=\; \frac{1}{2\pi} \int_{-\pi}^{\pi} dk \ln \left[4 \sin^2 \frac{k}{2} + \mu^2 \right] \\ &=\; \ln \mu^2 + 2 \ln \frac{1 + \sqrt{1 + 4/\mu^2}}{2} \,. \end{aligned} \tag{108}$$

In this, one-dimensional temporal lattice example, the stability exponent λ is the cat map Lyapunov exponent,[16,37] presented here in a form that makes the anti-integrable limit Eq. (67) explicit.

The one-dimensional steady state *orbit Jacobian operator* eigenspectrum is plotted in Fig. 9 (a). The discrete eigenvalues of finite-dimensional primitive cell *orbit Jacobian matrices* are points on this curve. For any finite period primitive cell they only approximate the exact stability exponent Eq. (108).

The two-dimensional steady state stability exponent Eq. (106) is given by the integral over the square lattice two-dimensional first Brillouin zone (conventionally a centered square, see shaded domain in Fig. 10 (b)),

$$\begin{aligned} \lambda &= \frac{1}{4\pi^2} \int_{-\pi}^{\pi} \int_{-\pi}^{\pi} d\mathsf{k} \, \ln \left[\mathsf{p}(\mathsf{k})^2 + \mu^2 \right] \,, \\ d\mathsf{k} &= dk_1 dk_2 \,, \quad \mathsf{p}^2(\mathsf{k}) = p(k_1)^2 + p(k_2)^2 \,. \end{aligned} \tag{109}$$

Spectra of the two-dimensional steady state orbit Jacobian operators are plotted in Fig. 11 (a). The discrete eigenvalues of primitive cell $\mathbb{A}$ orbit Jacobian matrices embedded in these spectra yield only finite volume primitive cell approximations to the exact steady state stability exponent Eq. (109).

While it is possible to evaluate such steady state integrals analytically (see, for example, partition functions with twisted boundary conditions of Ivashkevich *et al.*,[62] and papers[127–129] on Green's function of a discrete Laplacian on a square lattice), there are no analytic formulas for general periodic states, so we evaluate all such integrals numerically. An example is the $\mu^2 = 1$ spatiotemporal cat stability exponent λ evaluated below in Eq. (149).

The steady state calculations are so simple, as their orbit Jacobians are fully diagonalized by discrete Fourier transforms. For a steady state the unit hypercube primitive cell state is *prime*, all other periodic states over larger primitive cells are non-prime repeats of the unit hypercube periodic state (see Sec. I C).

B. Periodic state stability

As discussed in Sec. VIII C, the nonlinear field theory orbit Jacobian operators typically depend on the periodic state and cannot be diagonalized by discrete Fourier transforms. The eigenvalues of the orbit Jacobian matrices in the primitive cells of prime periodic states can only be computed numerically.

For an arbitrary periodic state, in arbitrary dimension, the stability exponent λ calculation is carried out with the help of the Bloch (or Floquet) theorem:[53,130,131] A linear operator acting on field configurations with periodicity of Bravais lattice $\mathcal{L}_{\mathbb{A}}$ has continuous spectrum, with the lattice sites z eigenstates of form

$$[\varphi^{(\alpha)}(\mathsf{k})]_z = e^{i\mathsf{k}\cdot z}[u^{(\alpha)}(\mathsf{k})]_z\,, \quad \mathsf{k}\in\mathbb{B}\,, \tag{110}$$

where $u^{(\alpha)}(\mathsf{k})$ are band-index $\alpha = 1, 2, \cdots, N_{\mathbb{A}}$ labelled distinct $\mathcal{L}_{\mathbb{A}}$-periodic functions, and the continuous wave numbers k are restricted to a Brillouin zone $\mathbb{B}$. In solid-state physics, eigenstates Eq. (110) are known as Bloch states.[111] In mechanics they are called Floquet modes.[132]

For each primitive cell periodic state there is a corresponding prime periodic state over the infinite Bravais lattice, acted upon by periodic state's infinite-dimensional orbit Jacobian operator Eq. (69). We solve for the eigenvalue bands of the orbit Jacobian operators as functions of the wave vectors k, using Bloch eigenstates Eq. (110),

$$\begin{aligned}\lambda_p &= \frac{1}{(2\pi)^d}\int_{\mathbb{B}} d\mathbf{k}\,\ln|\mathrm{Det}\,\mathcal{J}_p(\mathbf{k})| \\ &= \frac{1}{(2\pi)^d}\sum_{\alpha}^{N_{\mathbb{A}}}\int_{\mathbb{B}} d\mathbf{k}\,\ln|\Lambda_{p,\alpha}(\mathbf{k})|\,,\end{aligned} \tag{111}$$

where $\Lambda_{p,\alpha}(\mathbf{k})$ is the eigenvalue of the prime orbit p orbit Jacobian operator on the α-th eigenvalue band, corresponding to the eigenstate $\varphi^{(\alpha)}(\mathsf{k})$ in Eq. (110). This prime orbit stability exponent formula is, in the spirit of Sec. VI B, the generalization of the steady state stability exponent Eq. (106) to all periodic states.

It suffices to compute the stability exponent λ_p for a prime periodic state, as stability exponent is the same for a prime periodic state $\Phi_p = \Phi_{\mathbb{A}}$ and any of its repeats Eq. (79),

$$\lambda_p = \lambda[\Phi_{\mathbb{A}}] = \lambda[\Phi_{\mathbb{A}\mathbb{R}}] \quad \text{for all } \mathbb{R}\,, \tag{112}$$

as explained in Secs. IV B and VI B.

The Birkhoff average Eq. (19) of an observable a over periodic state Φ_p and any of its repeats is also the same, hence the weight of a non-prime periodic state $\Phi_{\mathbb{A}\mathbb{R}}$ contribution to primitive cell deterministic partition sum Eq. (33) factorizes

$$\frac{1}{|\mathrm{Det}\mathcal{J}_{\mathbb{A}\mathbb{R}}|}\,e^{N_{\mathbb{A}\mathbb{R}}\beta\cdot a_{\mathbb{A}\mathbb{R}}} = \left(e^{-\lambda_p+\beta\cdot a_p}\right)^{N_p r_1 r_2}\,, \tag{113}$$

with stability exponent λ_p -and this is the central point- evaluated over the reciprocal lattice first Brillouin zone

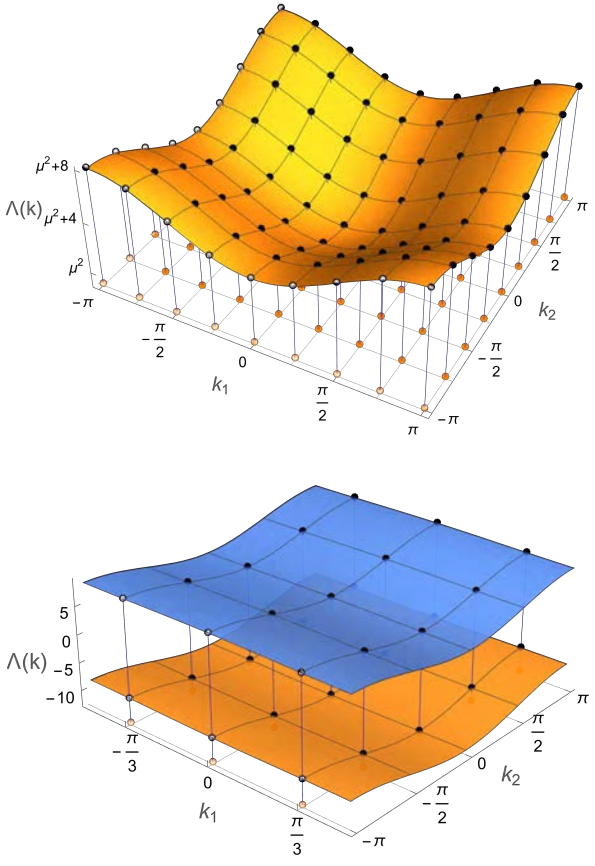

FIG. 11. (Color online) Square spatiotemporal lattice orbit Jacobian operator spectra, as functions of the wave vectors (k_1, k_2). For time and space-reflection and interchange invariant periodic states the spectra are $k_1 \to -k_1$, $k_2 \to -k_2$ and $k_1 \leftrightarrow k_2$ symmetric. (a) The steady state $\Lambda(\mathsf{k})$ Bloch band Eq. (106) as a function of the wave vector k, plotted for $\mu^2 = 1$ value. Black dots are eigenvalues of the orbit Jacobian matrix of periodic states over primitive cell with periodicity $[8\times8]_0$. (b) The two-dimensional ϕ^4 lattice field theory spectra of the Bravais lattice $\mathcal{L}_{[2\times1]_0}$ periodic state Eq. (C3), plotted for $\mu^2 = 5$ value. Black dots are eigenvalues of the orbit Jacobian matrix of a $[6\times4]_0$ primitive cell tiled by 12 repeats of a prime $[2\times1]_0$ periodic state, with $\Lambda_{\pm}(\mathsf{k})$ Bloch bands computed in Appendix C 2.

Eq. (111),

$$\frac{1}{|\mathrm{Det}\,\mathcal{J}_p|} \equiv e^{-N_p\lambda_p}\,.$$

Primitive cell label $\mathbb{A}$ is redundant here, as it is implicit in the periodic state p label: every periodic state has its Bravais lattice $\mathcal{L}_{\mathbb{A}}$ periodicity.

In particular, in contrast to the *primitive cell* orbit Jacobian Eq. (103), the Bravais lattice stability exponent of the third repeat Φ_{3*01} is thrice the prime orbit Φ_{01} stability exponent,

$$|\mathrm{Det}\,\mathcal{J}_{3*01}| = \left(e^{-\lambda_{01}+\beta\cdot a_{01}}\right)^{3N_{01}} = |\mathrm{Det}\,\mathcal{J}_{01}|^3\,. \tag{114}$$

This is the precise statement of the multiplicativity claim Eq. (2) we had made in the introduction: Bravais lattice orbit Jacobians are *multiplicative* for their repeats.

Example: One-dimensional ϕ^3 field theory period-2 periodic state. (Continued from Sec. VIII C.) Consider the simplest not-steady solution of ϕ^3 theory Eq. (45), its period-2 periodic state. The orbit Jacobian operator Eq. (69) of the period-2 prime orbit Eq. (C1) is invariant under translations of period $L = 2$, so its first Brillouin zone Eq. (104) is $(-\pi/2, \pi/2]$. This orbit Jacobian operator has two bands (for details, see Appendix C 1):

$$\Lambda_{01,\pm}(k) = -2 \pm \sqrt{\mu^4 - 12 - p(2k)^2}\,,$$
$$p(2k) = 2\sin(k)\,, \tag{115}$$

plotted in the first Brillouin zone in Fig. 9 (b).

Have a look back at the period-6 primitive cell of Sec. VIII C, with the prime periodic state Φ_{01} repeated three times. The wave numbers k are constrained to the period-6 reciprocal lattice of, taking values $\mathsf{k} = -\pi/3, 0, \pi/3$ within the first Brillouin zone. They are embedded into the two continuous eigenvalue bands Eq. (115), corresponding to the Eq. (101) eigenvalues $\Lambda_{-1,\pm}$, $\Lambda_{0,\pm}$ and $\Lambda_{1,\pm}$ respectively, as illustrated in Fig. 9 (b).

Example: Two-dimensional ϕ^4 field theory $[2\times1]_0$ periodic state. (Continued from Sec. VIII C.) Figure 11 (b) shows the two eigenvalue bands of a two-dimensional ϕ^4 $[2\times1]_0$ periodic state, plotted over the two-dimensional first Brillouin zone Eq. (104) $k_1 \in (-\pi/2, \pi/2]$, $k_2 \in (-\pi, \pi]$. For details, see Appendix C 2.

In summary, while a prime periodic state and its repeats have different *orbit Jacobian matrices* spectra, they share the same *orbit Jacobian operator* stability exponent, determined by integration over continuous Bloch bands. Inspection of Figs. 9 and 11 makes it clear what these different spectra are: orbit Jacobian matrix spectra are discrete approximations to orbit Jacobian operator continuous Bloch bands, with 'cords' approximation errors decreasing as the primitive cell volume increases. (For the convergence rate of such approximations, see shadowing Sec. XI). The wonderful property of the stability exponent λ_p computed over the infinite spacetime (as opposed to the stability exponent computed over a finite primitive cell) is that it is additive for prime periodic states repeated over larger primitive cells.

X. PERIODIC ORBIT THEORY

Now that we know how to enumerate all Bravais lattices $\mathcal{L}_\mathbb{A}$ (Sec. V), determine all periodic states over each (Sec. VI), and compute the weight of each periodic state (Sec. IX), we can combine all of that into one generating function sum of a very simple form, for any deterministic field theory, in any spacetime dimension:

Definition: Deterministic partition sum.

For integer lattices, the deterministic partition sum is the sum over all periodic states Φ_c, each of weight t_c,

$$Z[\beta, z] = \sum_c t_c\,, \quad t_c = \left(e^{\beta\cdot a_c - \lambda_c}\, z\right)^{N_c}\,, \tag{116}$$

where λ_c is the stability exponent Eq. (111), a_c the observable a averaged over periodic state Φ_c, Eq. (34), N_c is the Bravais lattice $\mathcal{L}_c$ volume Eq. (11), and z is a generating function variable.

Notation 't_c' is a vestige of referring to this weight in the time-evolution periodic orbit theory as the 'local trace' (see ChaosBook sect. 18.2).[133] Indeed, much of the time-evolution periodic orbit theory developed in ChaosBook generalizes to the multi-periodic, spatiotemporal deterministic field theory, with time period T_c replaced by the spatiotemporal volume N_c. Square brackets $[\cdots]$ in quantities such as $Z[\beta, z]$ are a here to remind us that we are dealing with spatiotemporal field theories,[134] not with a few degrees-of-freedom evolving forward in time (Sec. II).

A. Chaotic field theory

Ergodic theory of time-evolving dynamical systems is a rich subject. In this series of papers we stay within its most robust corner that we refer to as the 'chaotic field theory'. We say that a deterministic field theory is *chaotic* if (1) all of its periodic states are unstable, i.e., the stability exponent, Eq. (111), is strictly positive, $\lambda_c > 0$, for every deterministic solution Φ_c, and (2) the number of periodic states $|c|_\mathbb{A}$ grows exponentially with the primitive cell volume $N_\mathbb{A}$, with (3) periodic states are 'shadowed' by lower volume periodic states (Sec. XI).

To understand where the 'generating function variable' z in Eq. (116) comes from, consider $Z_\mathbb{A}[\beta]$, the primitive cell $\mathbb{A}$ partition sum Eq. (33) over all periodic states Φ_c of periodicity $\mathcal{L}_\mathbb{A}$. Their number $|c|_\mathbb{A}$ is the number of admissible mosaics (Sec. II C), with the mean of the log of the number of periodic states per lattice site given by $h_\mathbb{A} = \frac{1}{N_\mathbb{A}} \ln |c|_\mathbb{A}$.

If $|\mathcal{A}|$, the number of letters in the alphabet Eq. (37), is bounded, there are at most $|\mathcal{A}|^{N_\mathbb{A}}$ distinct mosaics over primitive cell $\mathbb{A}$, so $|c|_\mathbb{A}$, the number of spatiotemporal solutions $\{\Phi_c\}$ of system's defining equations Eq. (31) is bounded from above by $\exp(N_\mathbb{A} h_{max})$, where h_{max} is any upper bound on $h_\mathbb{A}$, for example

$$|c|_\mathbb{A} \leq e^{N_\mathbb{A} h_{max}}\,, \qquad h_{max} = \ln|\mathcal{A}|\,. \tag{117}$$

Now consider a system with a 2-letter alphabet (think of Ising 'spins'), with primitive cells $\mathbb{A}$ accommodating very few periodic states Φ_c, each with almost all

spins 'up' or 'down' (frozen phases in statistical mechanics, Pomeau–Manneville intermittency[135] in temporal evolution systems). For such long correlations systems $h_{\mathbb{A}} \to 0$.

To guarantee chaos, we consider here only field theories for which the number of solutions also has a strictly positive lower exponential bound $h_{\mathbb{A}} \geq h_{min} > 0$, with the $h_{\mathbb{A}}$ of large volume Bravais lattice bounded between h_{min} and h_{max}.

$$e^{N_{\mathbb{A}} h_{min}} \leq e^{N_{\mathbb{A}} h_{\mathbb{A}}} \leq e^{N_{\mathbb{A}} h_{max}} \,. \tag{118}$$

The exact value of $h_{\mathbb{A}}$ might require a calculation, and evaluation of the expectation value of system's entropy h will require the full machinery of the periodic orbit theory developed here in Sec. X F, but all we need to ensure that the theory is spatiotemporally chaotic is that all $h_{\mathbb{A}}$ are strictly positive.

Next: a typical observable is bounded in magnitude, so its contribution to the partition sum Eq. (116) weight is bounded by $\exp(N_{\mathbb{A}} \beta \cdot a_{max})$. And, crucially, throughout this series of papers we focus only on purely 'chaotic' systems, defined as systems for which every periodic state is unstable in the sense that its stability exponent Eq. (111) is strictly positive,

$$0 < \lambda_{min} \leq \lambda_c \,, \tag{119}$$

as illustrated by Figs. 9 and 11 and the anti-integrable limit calculations Eq. (67) and Eq. (108), so:

The primitive cell partition sum Eq. (33) is bounded exponentially in lattice volume $N_{\mathbb{A}}$,

$$Z_{\mathbb{A}}[\beta] \leq e^{N_{\mathbb{A}}(\beta \cdot a_{max} - \lambda_{min} + h_{max})} \,. \tag{120}$$

No Bravais lattice $\mathcal{L}_{\mathbb{A}}$ is special, all of them contribute, so we combine them into a generating function

$$\sum_{\mathbb{A}} Z_{\mathbb{A}}[\beta]\, z^{N_{\mathbb{A}}} \,, \tag{121}$$

a sum over all 'geometries'. Exponential bound Eq. (120) ensures that the sum is convergent for sufficiently small generating function variable z. With the stability exponent evaluated over the reciprocal lattice, as in Sec. IX, this is just the deterministic partition sum Eq. (116) arranged as a series in z^N. Our first task will be to determine the largest z for which the deterministic partition sum is convergent, Sec. X E.

In this paper we utilize only the translation group T symmetries, Eq. (70) (see Sec. V), and focus on the case of a two-dimensional square lattice. Translations stratify the deterministic field theory, Eq. (116), into *prime orbits*,[20,136,137] periodic states that are not repeats of a shorter period state (Secs. I C and VI A). To assemble the deterministic partition sum over all periodic states, we reorganize it by first determining all prime orbits Φ_p, and summing over their repeats (Sec. VI B). Then the deterministic partition sum Eq. (116) takes form

$$Z[\beta, z] \,=\, \sum_p Z_p \,, \tag{122}$$

with (β, z) dependent periodic states weights t_c, Eq. (116). The form of the prime partition sum Z_p depends on the spacetime dimensionality. To explain how, it suffices to consider the simplest case: the partition sum for a theory with a single prime orbit, a steady state.

B. Steady state partition sum

A steady state $\phi_z = \phi$ is a prime periodic state whose primitive cell $[1 \times 1]_0$ is the unit hypercube Eq. (5) (Sec. VI B). A periodic state is then obtained by tiling any larger primitive cell by repeats of steady state ϕ, one such periodic state for every Bravais sublattice.

For a one-dimensional, temporal Bravais lattice, the deterministic partition sum Eq. (116) is very simple. There is a non-prime periodic state for every repeat primitive cell $\mathbb{A}$ of period r, all of them with orbits of period 1 (Sec. I C), so thanks to repeat weights multiplicativity Eq. (113), the contribution of rth repeat to the partition sum Eq. (116) is $t_p^r = \left(e^{\beta \cdot a_p - \lambda_p} z\right)^r$, where r is the volume of the period r primitive cell. So, in *one dimension* the steady state partition sum is a geometric series,

$$Z_p = \sum_{r=1}^{\infty} t_p^r \,=\, \frac{t_p}{1 - t_p} \,, \qquad t_p = e^{\beta \cdot a_p - \lambda_p} z \,, \tag{123}$$

with steady state stability exponent λ_p Eq. (108), and the observable evaluated on the steady state ϕ, $a_p = a(\phi)$.

Thanks to repeat weights multiplicativity Eq. (113), the contribution of a $[r_1 \times r_2]_s$ steady state repeat to the partition sum Eq. (116) in two dimensions is

$$t_p^{r_1 r_2} \,=\, \left(e^{\beta \cdot a_p - \lambda_p} z\right)^{r_1 r_2} \,, \tag{124}$$

So for a two-dimensional, spatiotemporal steady state (see Sec. VI) there is a non-prime periodic state for every two-dimensional repeat primitive cell $[r_1 \times r_2]_s$ constructed in Sec. V A, with r_1 copies of lattice site field ϕ horizontally, r_2 copies vertically, with weights, as stated in Eq. (112), independent of the tilt $0 \leq s < r_1$ Eq. (79),

$$Z_p \,=\, \sum_{r_1=1}^{\infty} \sum_{r_2=1}^{\infty} r_1\, t_p^{r_1 r_2} \,,$$

where tilts s are summed over:

$$\sum_{s=0}^{r_1 - 1} 1 = r_1 \,.$$

Summing over heights r_2, the deterministic steady state partition sum Eq. (116) in *two dimensions* is thus

$$Z_p \,=\, \sum_{n=1}^{\infty} \frac{n\, t_p^n}{1 - t_p^n} \,. \tag{125}$$

Its expansion in powers of variable t_p

$$Z_p = \sum_{n=1}^{\infty} \sigma(n) t_p^n = t_p + 3t_p^2 + 4t_p^3 + 7t_p^4 + 6t_p^5 + 12t_p^6 + 8t_p^7 + \cdots , \quad (126)$$

was first studied by Euler, with $\sigma(n)$ known as the Euler sum-of-divisors function.

C. Prime orbit partition sum

As explained in Sec. VI B, every prime periodic state is morally a steady state, except that now the number of periodic states in the prime orbit is its primitive cell volume N_p. Hence in *one dimension* the prime orbit p deterministic partition sum, including steady states Eq. (123) as the $N_p = 1$ cases, is simply

$$Z_p = N_p \frac{t_p}{1 - t_p} , \qquad t_p = \left(e^{\beta \cdot a_p - \lambda_p} z\right)^{N_p} , \quad (127)$$

with prime orbit stability exponent λ_p Eq. (111), and a_p the Birkhoff average, Eq. (19), of an observable a over prime periodic state p_p.

The formula has form of the 'deterministic trace formula' (see ChaosBook Eq. (21.24)),[138] with a crucial difference: here the weight t_p is the *exact*, infinite Bravais lattice weight, while the Ruelle dynamical zeta function weight t_p is an *approximate* weight.

The contribution of a *two-dimensional* spatiotemporal prime periodic state p and its repeats to the deterministic partition sum, Eq. (122), is

$$Z_p = N_p \sum_{n=1}^{\infty} \frac{n\, t_p^n}{1 - t_p^n} , \quad (128)$$
$$t_p = \left(e^{\beta \cdot a_p - \lambda_p} z\right)^{N_p} , \quad N_p = L_p T_p .$$

D. Spatiotemporal zeta functions

We have a deterministic partition sum Eq. (116) of stunning simplicity. Still, we can do better, by taking into account symmetries (Sec. V) of the theory.

Definition: Deterministic zeta function.

For two-dimensional integer lattices, the deterministic zeta function is the product over all prime orbits, of form

$$1/\zeta = \prod_p 1/\zeta_p , \qquad 1/\zeta_p = \prod_{n=1}^{\infty} (1 - t_p^n) . \quad (129)$$

Who ordered this 'zeta'? Euler. Euler replaced the partition sum (in Euler's case, a weighted sum over natural numbers) by a zeta function (in Euler's case, the product over primes formula for the Riemann zeta function), by the logarithmic derivative relation between the partition sum and the zeta function

$$Z[\beta, z] = -z \frac{\partial}{\partial z} \ln 1/\zeta[\beta, z] \quad (130)$$

(see, for example, ChaosBook sect. 22.3).[139]

Why? (1) The deterministic partition sum Eq. (116) is a redundant sum over all *periodic states*, redundant as their weights depend only on *prime orbits*, which a zeta function counts only once per orbit. (2) Every periodic state weight contributes to the deterministic partition sum with a positive weight. Zeta functions are smarter, they exploit the key property of ergodic trajectories that they are *shadowed* by shorter trajectories (Sec. XI), with convergence of periodic states averaging formulas improved by shadowing cancellations. (3) Zeta functions have better analyticity properties, with divergence of deterministic partition sum Eq. (121) corresponding to the leading zero of deterministic zeta function.

In *one spatiotemporal dimension*, the deterministic zeta function is a product over all prime orbits, of form

$$1/\zeta = \prod_p (1 - t_p) , \quad (131)$$

as is easily checked by substitution into relation Eq. (130). The pseudo-cycle expansion of $1/\zeta$ then leads to averaging formulas with better convergence than the deterministic partition sum Eq. (116) (see ChaosBook sect. 23.5).[140]

In *two spatiotemporal dimensions*, the deterministic zeta function is again a product over all prime orbits, Eq. (129). Its correspondence to the deterministic partition sum, Eq. (128), is easily checked by substitution into the relation Eq. (130).

E. Evaluation of zeta functions

For large lattice volume N primitive cells, the exponential bounds of Eq. (28), (29) and (120) ensure convergence of high order z^N terms in deterministic partition sum, Eq. (121), to $(e^{W[\beta]} z)^N$, with sum convergent for sufficiently small z.

Definition: Function W.

The largest value of $z(\beta)$ for fixed β,

$$z(\beta) = e^{-W[\beta]} , \quad (132)$$

for which the deterministic partition sum Eq. (116) converges, or, equivalently, the value of $z(\beta)$ which is the first root of the inverse of deterministic zeta function, Eq. (129),

$$Z[\beta, z(\beta)] \to \infty ; \qquad 1/\zeta[\beta, z(\beta)] = 0 , \quad (133)$$

defines system's 'reject rate' $-W[0]$.

In dynamical systems theory, the rate at which trajectories leave an open system per unit time is called *escape rate* (see Ref. 141 and ChaosBook Eq. (1.3)). We put 'reject rate' into quotations here, as in spatiotemporal theory there is no escape in time - the exponent is a characterization of the non–wandering set, the state space set formed by the deterministic solutions. We evaluate it for the temporal cat in Appendix B 5, and for deterministic ϕ^3 and ϕ^4 theories in companion paper III.[17]

Much is known about the two-spatiotemporal dimensions zeta function, Eq. (129), as for each prime orbit $1/\zeta_p$ is the Euler function $\phi(t_p)$,

$$1/\zeta_p = \phi(t_p) = \prod_{n=1}^{\infty}(1-t_p^n)\,, \qquad |t_p|<1\,, \quad (134)$$

whose power series in terms of pentagonal number powers of z was given by Euler[142] in 1741

$$\begin{aligned}\phi(z) =& 1 - z - z^2 + z^5 + z^7 - z^{12} - z^{15} \\ &+ z^{22} + z^{26} - z^{35} - z^{40} + z^{51} + z^{57} \\ &- z^{70} - z^{77} + z^{92} + z^{100} + \dots \end{aligned} \quad (135)$$

In 1996 Lind[143] introduced topological zeta function of this form for two-dimensional, as well as higher-dimensional shifts. So, while for a one-dimensional lattice, the contribution Eq. (131) of a prime orbit Φ_p is simply $1/\zeta_p = 1 - t_p$, in two spatiotemporal dimensions the prime orbit weight is a yet another 'Euler function' with an infinite power series expansion. Presumably because of that, in our numerical work the z power series expansions of two-dimensional $1/\zeta$ do not appear to converge as smoothly as they do in the one-dimensional, temporal settings.

F. Periodic states averaging formula

While each primitive cell probability density Eq. (25) is easily correctly normalized, there is no natural 'overall' probability normalization for the generating function sum over all periodic states, the deterministic partition sum Eq. (116). For one-dimensional, temporally evolving systems, ChaosBook sect. 23.5 solves this problem by the method of 'cycle averaging'.[140] We now generalize this method to the higher-dimensional, spatiotemporal field theories.

The smallest value of the generating function variable $z(\beta)$ for which the deterministic zeta function equals zero, Eq. (133), is an implicit equation for the root $z = z(\beta)$ satisfied on the curve $0 = 1/\zeta[\beta, z(\beta)]$ in the (β, z) parameters plane. Take the derivative of this implicit equation (for brevity, we take $1/\zeta = 1/\zeta[\beta, z(\beta)]$):

$$0 = \frac{d}{d\beta}1/\zeta = \frac{\partial}{\partial\beta}1/\zeta + \frac{dz}{d\beta}\frac{\partial}{\partial z}1/\zeta\,.$$

Eq. (132) relates $dz/d\beta$ to the log of partition function evaluated on the infinite lattice, Eq. (29),

$$-\frac{1}{z}\frac{dz}{d\beta} = \frac{dW}{d\beta} = \frac{\frac{\partial}{\partial\beta}1/\zeta}{z\frac{\partial}{\partial z}1/\zeta}\,. \quad (136)$$

The *expectation value* of observable a, Eq. (30),

$$\langle a\rangle = \frac{d}{d\beta}W[\beta]\Big|_{\beta=0}$$

is now given by the *periodic states averaging formula*

$$\langle a\rangle = \frac{\langle A\rangle_\zeta}{\langle N\rangle_\zeta}\,. \quad (137)$$

Here the weighted Birkhoff sum of the observable $\langle A\rangle_\zeta$, Eq. (19), and the weighted multi-period lattice volume $\langle N\rangle_\zeta$, Eq. (11), are defined as

$$\begin{aligned}\langle A\rangle_\zeta &= -\frac{\partial}{\partial\beta}1/\zeta[\beta, z(\beta)]\Big|_{\beta=0,z=z(0)}\,, \\ \langle N\rangle_\zeta &= -z\frac{\partial}{\partial z}1/\zeta[\beta, z(\beta)]\Big|_{\beta=0,z=z(0)}\,. \end{aligned} \quad (138)$$

where the subscript in $\langle\cdots\rangle_\zeta$ stands for the deterministic zeta function evaluation of such weighted sum over prime orbits.

Expectation values $\langle\cdots\rangle_\zeta$ are evaluated by noting that all (β, z) dependence of the deterministic zeta function, Eq. (129), is contained in the prime orbits weights t_p, whose partial derivatives are simply

$$z\frac{\partial}{\partial z}t_p = N_p t_p\,, \qquad \frac{\partial}{\partial\beta}t_p = A_p t_p\,. \quad (139)$$

As an example, we compute the expectation value of stability exponent of temporal cat in Appendix B 6.

While power series expansions in z of functions such as the Euler function, Eq. (135), do not converge very well, the theory of doubly-periodic elliptic functions suggests other, more powerful methods to evaluate such functions. The Euler function can be expressed as the Dedekind eta function $\eta(\tau)$,

$$\phi(t_p) = t_p^{-\frac{1}{24}}\eta(\tau_p)\,, \qquad \mathrm{Im}(\tau_p) > 0\,, \quad (140)$$

where τ_p is the complex phase of the Euler function argument, $t_p = e^{i2\pi\tau_p}$. Our prime zeta function, Eq. (129), complex phases of prime periodic states follow from Eq. (128),

$$\tau_p = i\frac{N_p}{2\pi}(-\beta\cdot a_p + \lambda_p - S)\,, \qquad z = e^{-S}\,, \quad (141)$$

with the periodic state Φ_p probability weight having a pure positive imaginary phase

$$\tau_p = \frac{i}{2\pi}N_p\lambda_p\,.$$

The derivatives required for the evaluation of expectation values, Eq. (138), have their own elliptic functions representations. For example, the logarithmic derivative of Dedekind eta is known as the Weierstrass zeta function,

$$\eta'/\eta = \zeta_W \,. \tag{142}$$

The problem in evaluation of the deterministic zeta function, Eq. (129), is that it is an *infinite* product of Dedekind eta functions, and we currently know of no good method to systematically truncate and evaluate such products.

The spatiotemporal zeta function Eq. (129) is the main result of this paper. However, there are still a couple of questions of general nature that alert reader is likely to ask.

(i) How is this global, high-dimensional orbit stability related to the stability of the conventional low-dimensional, forward-in-time evolution? The two notions of stability are related by Hill's formulas (also known as the Gel'fand-Yaglom theorem,[144,145] for continuous spacetime), relations that are in our formulation equally applicable to energy conserving systems, as to viscous, dissipative systems. We derive them in Refs. 16 and 48. From the field-theoretic perspective, orbit Jacobians are fundamental, forward-in-time evolution is merely one of the methods for computing them.

(ii) One might wonder why do we focus so much on computing periodic states over every *small* primitive cell, omitting none? You never see that anywhere in the literature. But that's what the theory of (temporal) chaos and (spatiotemporal) turbulence demands: the support of a deterministic field theory is on *all* deterministic solutions, as sketched in Fig. 1.

Next –the beauty of the periodic orbit theory of chaos– due to the shadowing of longer periods unstable periodic states by shorter periods ones, the smallest periodicites periodic states dominate, the longer ones come in only as corrections. The convergence periodic states-expansions is accelerated by shadowing of long orbits by shorter periodic orbits.[49] Are d-dimensional tori (primitive cells) periodic states also shadowed by smaller tori periodic states? In Sec. XI we check numerically that spatiotemporal cat periodic states that share finite spatiotemporal mosaics indeed shadow each other to exponential precision.

XI. SHADOWING

In ergodic theory 'shadowing lemma': "a true time-trajectory is said to shadow a numerical solution if it stays close to it for a time interval[146,147]" is often invoked to justify collecting statistics from numerical trajectories for integration times much longer than system's Lyapunov time.[148] In periodic orbit theory, the issue is neither the Lyapunov time, nor numerical accuracy: all periodic orbits are 'true' in the sense that in principle they can be computed to arbitrary accuracy.[149] In present context 'shadowing' refers to the shortest distance between two orbits decreasing exponentially with the length of the shadowing time interval. Long orbits being shadowed by shorter ones leads to controllable truncations of cycle expansions,[49] and computation of expectation values of observables of dynamical systems to exponential accuracy.[20]

Field configurations are points in state space Eq. (7), with the separation of two periodic states Φ, Φ' given by the state space vector $\Phi - \Phi'$, so we define 'distance' as the average site-wise state space Euclidean distance-squared between field configurations Φ, Φ', i.e., by the Birkhoff average Eq. (19)

$$|\Phi - \Phi'|^2 = \frac{1}{N_{\mathbb{A}}} \sum_{z\in\mathbb{A}} (\phi'_z - \phi_z)^2 \,. \tag{143}$$

This notion of distance is intrinsically spatiotemporal, it does not refer to time-evolving unstable trajectories separating in time. For spatiotemporal cat we have an explicit formula for pairwise separations: If two spatiotemporal cat periodic states Φ, Φ' share a common sub-mosaic M, they are site-fields separated by

$$\phi_z - \phi'_z = \sum_{z'\notin\mathsf{M}} g_{zz'}(m - m')_{z'} \mod 1 \,, \tag{144}$$

where matrix $g_{zz'}$ is the spatiotemporal cat Green's function Eq. (B1).

It was shown numerically by Gutkin *et al.*[36,37] that pairs of interior alphabet Eq. (B5) spatiotemporal cat periodic states of a fixed spatial width L that share sets of sub-mosaics, shadow each other when evolved forward-in-time. Here, in Sec. XI B, we check numerically spatiotemporal cat shadowing for arbitrary periodic states, without alphabet restrictions, and without any time evolution. Intuitively, if two unstable periodic states Φ, Φ' share a common sub-mosaic M of volume N_{M}, they shadow each other with exponential accuracy of order of $\propto \exp(-\lambda N_{\mathsf{M}})$. In time-evolution formulation, λ is the leading Lyapunov exponent. What is it for spatiotemporal systems?

We first explain how the exponentially small distances follow for the one-dimensional case.

A. Shadowing, one-dimensional temporal cat

As the relation between the mosaics M and the corresponding periodic states Φ_{M} is linear, for M an admissible mosaic, the corresponding periodic state Φ_{M} is given by the Green's function

$$\Phi_{\mathsf{M}} = \mathsf{g}\,\mathsf{M} \,, \qquad \mathsf{g} = \frac{1}{-\mathsf{r} + s\,\mathbb{1} - \mathsf{r}^{-1}} \,. \tag{145}$$

For an infinite one-dimensional lattice $t \in \mathbb{Z}$, the lattice field at site t is determined by the sources $m_{t'}$ at all

sites t', by the Green's function $g_{tt'}$ for one-dimensional discretized heat equation,[103,150]

$$\phi_t = \sum_{t'=-\infty}^{\infty} g_{tt'} m_{t'} \,, \quad g_{tt'} = \frac{1}{\Lambda - \Lambda^{-1}} \frac{1}{\Lambda^{|t-t'|}} \,, \tag{146}$$

with Λ the expanding cat map stability multiplier Eq. (B22). While the orbit Jacobian operator $\mathcal{J}$ is sparse, it is not diagonal, and its inverse is the full matrix g, whose key feature is the matrix element $g_{tt'}$ factor $\Lambda^{-|t'-t|}$, which says that the magnitude of a matrix element falls off exponentially with its distance from the diagonal. This fact is essential in establishing the 'shadowing' between periodic states sharing a common sub-mosaic M. Suppose there is a non-vanishing point source $m_0 \neq 0$ only at the present, $t' = 0$ temporal lattice site. Its contribution to $\phi_t \sim \Lambda^{-|t|}$ decays exponentially with the distance from the origin. If two periodic states Φ, Φ' share a common sub-mosaic M of length n, they shadow each other with accuracy of order of $O(1/\Lambda^n)$.

B. Shadowing, two-dimensional spatiotemporal cat

Following Refs. 36 and 37, consider families of spatiotemporal orbits that share a sub-mosaic region. The periodic states used in numerical examples of Ref. 37 were restricted to those whose mosaics used only the interior, always admissible, alphabet Eq. (B5). Here we check numerically spatiotemporal cat shadowing for generic periodic states, with no alphabet restrictions.

The two-dimensional $\mu^2 = 1$ spatiotemporal cat Eq. (49) periodic states are labelled by two-dimensional mosaics, 8-letter alphabet Eq. (B3), as in Fig. 12.

To investigate the spatiotemporal cat shadowing properties, we considered spatiotemporal cat periodic states with periodicity $[18\times18]_0$, all sharing the same $[12\times12]$ sub-mosaic, see Fig. 12. We generated 500 such periodic states by randomly changing the lattice site symbols outside the sub-mosaic, finding the corresponding periodic state by solving the spatiotemporal cat defining equation Eq. (48), and keeping only those admissible solutions that still contained the same $[12\times12]$ sub-mosaic.

The spatiotemporal shadowing suggests that for periodic states with identical sub-mosaics, the distances between the corresponding field values decrease exponentially with the size of the shared sub-mosaics.

To find the rate of decrease of distances between shadowing periodic states, we compute the mean point-wise distances of field values of the 250 pairs of periodic states over each lattice site in their primitive cells. The exponential shadowing of periodic states is shown in Fig. 13. The distances between field values of two periodic states $|\phi_z - \phi'_z|$ decrease exponentially as z approaches the center of the common sub-mosaic. Figure 13 (a) is the log plot of the mean distances. The logarithm of the mean distances across the center of the primitive cell is plotted

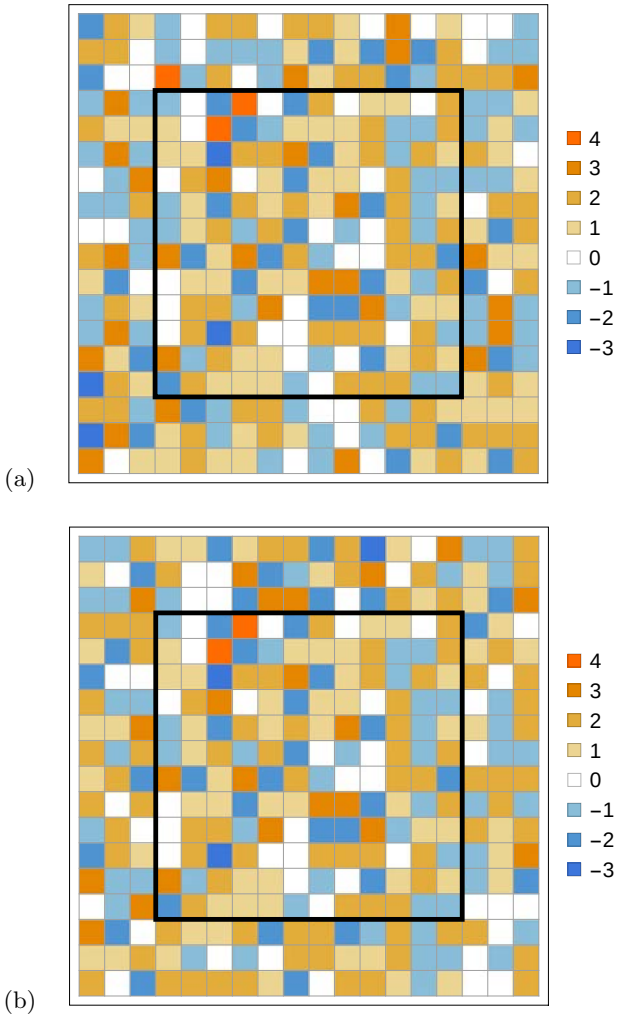

FIG. 12. (Color online) Mosaics Eq. (37) of two $[18\times18]_0$ spatiotemporal cat periodic states which share the sub-mosaic within the $[12\times12]$ region enclosed by the black square, and have different symbols outside the sub-mosaic. Color coded 8-letter alphabet Eq. (B3), $\mu^2 = 1$. Continued in Fig. 13.

in Fig. 13 (b), where the decrease is approximately linear, with a slope of -1.079. What determines this slope?

C. Green's function of two-dimensional spatiotemporal cat

Mosaic M is admissible (see Sec. II C) if field configuration Φ_{M} is a periodic state, i.e., all lattice site fields are confined to Eq. (B2), the compact boson hypercube state space $\phi_z \in [0, 1)$.

The Green's function measures the correlation between two lattice sites in the spacetime. In our problem the distances between the shadowing periodic states can be interpreted using the Green's function, which gives variations of field values ϕ_t induced by a 'source', in this example by change of a letter $m_{t'}$ at lattice site z'. The decrease of the differences between field values of shadowing periodic states is a result of the decay of cor-

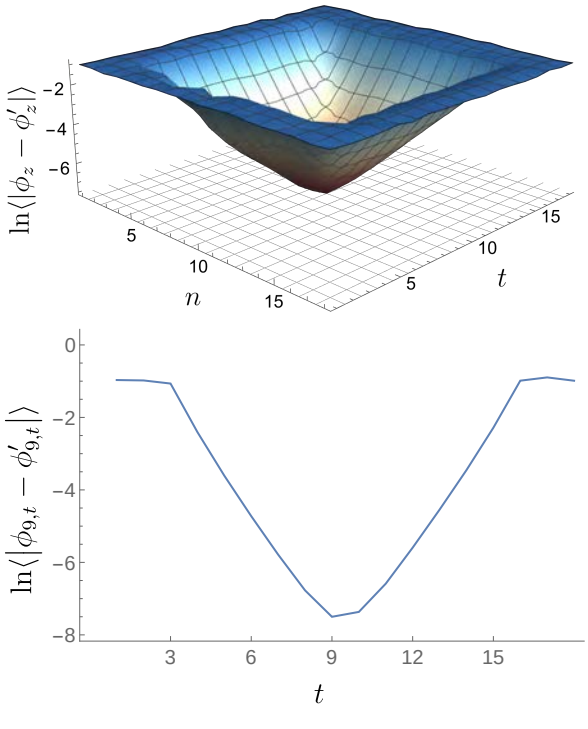

FIG. 13. (Color online) $\mu^2 = 1$ spatiotemporal cat. (a) The log of mean of point-wise field value distances $|\phi_z - \phi'_z|$ over all lattice sites of $z \in [18{\times}18]$ primitive cell, averaged over the 250 pairs of periodic states, like the pair of Fig. 12. (b) The log of mean point-wise distances $|\phi_{9,t} - \phi'_{9,t}|$ evaluated across the strip $z = (9, t)$, $t = 1, 2, \ldots, 18$, going through the center of the primitive cell. The decrease from edge to the center is approximately linear, with slope ≈ -1.079.

relations. The Green's function for massive free-boson on integer lattices Eq. (B1) has been extensively studied.[37,63,100,101,103,127–129,150–168] But to understand qualitatively the exponential falloff of spacetime correlations, it suffices to consider the large spacetime primitive cell (small lattice spacing) continuum limit:

$$(-\Box + \mu^2)\,\phi(x) = m(x)\,, \qquad x \in \mathbb{R}^2$$

whose Green's function is the radially symmetric

$$G(x, x') = \frac{1}{2\pi} K_0\left(\mu|x - x'|\right)\,, \tag{147}$$

where K_0 is the modified Bessel function of the second kind. For large spacetime separations, $|x - x'| \to \infty$, the asymptotic form of the Green's function is

$$G(x, x') \sim \sqrt{\frac{1}{8\pi\mu r}}\, e^{-\mu r}\,, \qquad r = |x - x'|\,. \tag{148}$$

In the numerical example of Sec. XI B, we have set Klein-Gordon mass $\mu = 1$, so the Green's function of the continuum screened Poisson equation is a good approximation to the discrete spatiotemporal cat Green's function, where the rate of decrease of correlations computed

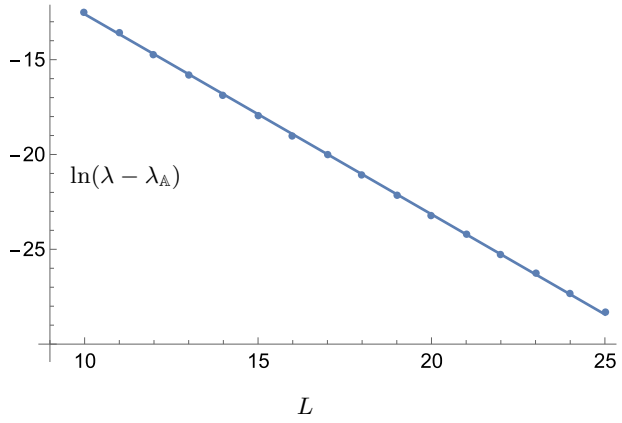

FIG. 14. The convergence of primitive cells stability exponents $\lambda_{\mathbb{A}}$ to λ, the exact Bravais lattice value Eq. (149), for square primitive cells $[L \times L]_0$ sequence Eq. (150), $\mu^2 = 1$. A linear fit of the logarithm of the distance as a function of the side length $L = 10, 11, \cdots, 25$, with slope -1.05538.

from the Fig. 13 (b) is approximately $\exp(-\mu' r)$, with $\mu' = -1.079$ the slope computed from the log plot of the mean distances of field values between shadowing periodic states.

D. Convergence of evaluations of observables

Computed on primitive cells $\mathbb{A}$ of increasing volume $N_{\mathbb{A}}$, the expectation value of an observable (Sec. I D) converges towards the exact, infinite Bravais lattice value (Sec. IX). As the simplest case of such sequence of primitive cell approximations, take a rectangular primitive cell $[L \times T]_0$, and evaluate stability exponents $\langle\lambda\rangle_{[rL\times rT]}$ (Sec. VIII B) for the sequence of primitive cell repeats $[rL \times rT]_0$ of increasing r.

That the convergence of such series of primitive cell approximations is a shadowing calculation can be seen by inspection of Fig. 11. The exact stability exponent λ is obtained by integration over the bands (smooth surfaces in the figures). A shadowing approximation $\lambda_{[L\times T]_S}$ is a finite sum over primitive cells $[L \times T]_S$, black dots in the figures, that shadows the curved surface, with increasing accuracy as the primitive cell volume $N_{\mathbb{A}}$ increases. Here shadowing errors are Hipparchus' errors Eq. (91) of replacing arcs by cords, as in approximating 2π by the perimeter of a regular n-gon. The sense in which such shadowing or 'curvature' errors are exponentially small for one-dimensional, temporal lattice chaotic systems is explained in Refs. 49, 169, and 170. We have not extended such error estimates to the spatiotemporal case, so here we only present numerical evidence that they are exponentially small.

As a concrete example, we evaluate numerically the exact $\mu^2 = 1$ spatiotemporal cat stability exponent λ for the infinite Bravais lattice orbit Jacobian operator

Eq. (109),

$$\lambda = 1.507983\cdots , \tag{149}$$

and investigate the convergence of its finite primitive cell estimates $\lambda_{[rL\times rT]_0}$. For the unit cell $[1\times 1]_0$ sequence, plotted in Fig. 14, $\lambda - \lambda_{[L\times L]_0}$ decreases linearly as the side length L increases, with a linear fit has slope

$$\ln(\lambda - \lambda_{[L\times L]_0}) = -2.04611 - 1.05538\, L\,. \tag{150}$$

For various primitive cell sequences of rectangular shapes $[L\times T]_0$, the stability exponents of repeat primitive cells $[rL\times rT]_0$ also converge to λ exponentially, with the same convergence rate $\approx 1.055\cdots$. We have no theoretical estimate of this rate, but it appears to be close to the Klein-Gordon mass $\mu = 1$, within the shadowing error estimates of Sec. XI B.

XII. SUMMARY AND OPEN QUESTIONS

Gutzwiller's 1971 semiclassical quantization[18,171] yields deep insights into the quantum behavior of low-dimensional deterministically chaotic systems (ODEs). In dynamical systems theory this point of view leads to the 1976 Ruelle periodic orbit formulation of chaotic dynamics.[19,20,136] In this series of papers[16,17,48,50] we generalize the Ruelle temporal ODEs / iterated maps dynamical zeta functions theory to our field-theoretic, PDEs spatiotemporal zeta functions formulation of spatiotemporal chaos and turbulence.

Flows described by partial differential equations are in principle infinite dimensional, and, at first glance, turbulent dynamics that they exhibit might appear hopelessly complex. However, what is actually observed in experiments and simulations is that turbulence is dominated by repertoires of identifiable recurrent vortices, rolls, streaks and the like.[11] Dynamics on a low-dimensional chaotic attractor can be visualized as a succession of near visitations to exact unstable periodic solutions, interspersed by transient interludes.[20] In the same spirit, the long-term turbulent dynamics of spatially extended systems can be thought of as a sequence of visitations through the repertoire of admissible spatiotemporal patterns ('exact coherent structures',[8,9] 'recurrent flows'[172]), each framed by a finite spatiotemporal window. The question we address here is: can states of a strongly nonlinear field theory be described by such repertoires of admissible patterns, explored by turbulence? And if yes, what is the likelihood of observing any such pattern?

These questions have been studied extensively for systems of small spatial extent, whose inertial manifold dimension is relatively small.[173–177] Recent experimental and theoretical advances[11,14,15,178,179] support such forward-in-time dynamical vision also for spatially extended, turbulent systems (see Ref. 180 for a gentle introduction). By now thousands of such 'exact coherent structures' have been computed, always confined to small spatial domains, while the flows of interest (pipe, channel, plane flows) are flows on infinite spatial domains. Going from spatially small to spatially infinite systems requires a radical shift in the point of view. To describe those, we have to recast equations such as the Navier-Stokes as a spacetime theory, with all infinite translational symmetry directions treated on equal footing. It is a bold leap, a theory of turbulence that does away with dynamics. But we have no choice. For spatially extended systems evolution forward in time is insanely unstable.[13,181] Not only have time-evolution numerical codes[182,183] not worked on large domains, in retrospect it is clear that they never could have worked.

Conventional numerical computations confine spatial directions to a finite domain, then integrate forward in time, treating only time as inherently infinite. In contrast, our deterministic field theory formulation is global, in the sense that its building blocks are *orbits*, global field configurations that satisfy system's defining equations everywhere, over the infinite spacetime. We treat all translationally invariant directions democratically, each an infinite 'time'. Here there are no sketches of diverging trajectories, because in the deterministic spatiotemporal field theory formulation of turbulence, there is *no evolution* in time.

The first problem that we face is *global*: determining and organizing infinities of unstable multi-periodic states over ∞-dimensional state spaces, orbits that are presumed to form the skeleton of turbulence. We characterize and classify them by their shapes, captured by corresponding 'mosaics' (Sec. II C). The feel is of statistical-mechanics, like enumeration of Ising configurations. For *temporal* evolution, in the *large volume* $T\to\infty$ limit our partition sum Z, Eq. (116), is Ruelle's 'partition function',[19] our functional W, Eq. (29), is Ruelle's 'pressure',[184] and our deterministic zeta function ζ, Eq. (131), is Ruelle's 'dynamical zeta function'[136] (for nomenclature, see ChaosBook remark 20.2 *'Pressure'*). In the *spatiotemporal* theory, in the *large volume* $LT\to\infty$ limit our functional W is Grassberger's 'density of metric entropy'[4] and Politi, Torcini & Lepri's chronotopic 'entropy potential function'.[5–7] Furthermore, as had previously been done implicitly in cycle expansion calculations of observables,[185–187] see Sec. X F, Politi *et al.* relate expectation values of observables by Legendre transforms of W to appropriate 'effective actions' or 'Gibbs free energies'.

As we always follow Ruelle, who says this about 'pressure': "frankly the proper term ... should be free energy",[188,189] we provisorily settle for calling our function W, Eq. (132), the 'function W'.

A. What is new

In determining the totality of unstable multi-periodic states we are helped by working 'beyond perturbation theory', in the anti-integrable, strong coupling regime, in

contrast to much of the literature that focuses on weak coupling expansions around 'ground states'. Our calculations utilize standard optimization methods,[181,190–198] some of which precede spatiotemporal theory by decades. They are memory costly, but as there is no evolution, neither in time nor in space, there are no instabilities, and it suffices to determine a solution to a modest accuracy.

The next problem is: how important is a given spacetime configuration? Intuitively, more unstable solutions have smaller state space neighborhoods, are less likely. Here the orbit Jacobian operator Eq. (35) of a periodic state, its primitive cell determinant Eq. (66), and especially its infinite Bravais lattice stability exponent Eq. (111) are the most important innovations in our theory of spatiotemporal chaos.

The essential innovation of our approach is the computation of spatiotemporal stability exponents over infinite Bravais lattices, see Fig. 8, 9 and 11, rather than forward-in-time Floquet/Lyapunov stability of finite time solutions over rectangular spacetime primitive cells. We work in infinite spacetime, not a mix of modest or large spatial extent with either long time ergodic estimates, or compact periodic time solutions. The orbit Jacobian operator Eq. (69), Eq. (55), the orbit stability exponent λ_p Eq. (111), and the surprisingly simple exact deterministic spatiotemporal zeta function Eq. (129) are defined democratically over spacetime lattice momenta (Pikovsky's Bloch quasi-momenta *and* Bountis' Floquet quasi-energies).

Historically, in all of the previous work on spatially extended systems, the time and space instabilities were treated asymmetrically. While the spatial stability was parametrized by spatial Bloch wave number k_1, the time (in)stability was either estimated by forward evolution-in-time numerical Lyapunov-Bloch exponents[25] $\lambda(k_1)$ (the Oseledets multiplicative ergodic theorem), or by means of compact, finite primitive cell (Sec. VIII) periodic time solutions. Examples of the latter are spacetime periodic solutions of Kuramoto-Sivashinsky and Navier-Stokes PDEs studied in Ref. 12, 174, 181, 199–201.

In all previous spatiotemporal studies the large volume $LT \to \infty$ 'thermodynamic' limits were estimated by simulations of finite volume lattices. Our deterministic field theory is *ab initio* over infinite spacetime, there are no large volume limits to estimate. Our partition function Z sum over all Bravais lattices, our functional W, and our deterministic zeta function ζ are exact expansions in terms of exact prime orbit weights t_p.

That follows from the main advance of our Euclidean field theory of spatiotemporal chaos/turbulence, the functional determinant evaluations of infinite Bravais lattice stability exponent λ_c, Eq. (111), and multiplicative weight t_c, which, to best of our knowledge, do not appear in the earlier literature.

And, finally: now that we have a hierarchy of multiperiodic states, what is the expectation value of any observable of the theory? The answer is given by deterministic partition sums and zeta functions of Sec. X. All chaoticity is due to the intrinsic instability of *deterministic* solutions, and our spatiotemporal deterministic partition sums Eq. (116) and zeta functions Eq. (129) are *exact*, not merely saddle points approximations to a theory. The issues in their applications are numerical: how many periodic states, evaluated to what accuracy have to be included into a truncated zeta function, to attain a desired accuracy?

Our deterministic field theory replaces numerical extrapolations of finite spacetime simulations of the 1990's chronotopy by the *exact* deterministic zeta function, with computable cycle expansion truncations errors, decreasing exponentially with the spatiotemporal volumes of periodic states included in its evaluation. Our spatiotemporal deterministic zeta function, as far as we know, is new.

B. Open questions

At the present stage of development, our spatiotemporal theory of chaos leaves a number of open problems that we plan to address in future publications:

1. Can the 2- and higher- spatiotemporal dimension zeta function Eq. (129) and expectation value Eq. (137) computations be organized into 'cycle expansions', dominated by the small spacetime volume periodic states, as is the case for the one-dimensional, temporal theory?[20]

2. For pedagogical reasons –in order to start out with determinants of finite matrices, rather than immediately grapple with functional determinants– we have presented here the spacetime deterministic field theory in its discretized, d-dimensional lattice form. We expect the periodic orbit formulation of continuum spacetime theory to be of essentially of the same form, with the spacetime periodicities (Bravais lattice primitive vectors) defined over the continuum, $\mathbf{a}_j \in \mathbb{R}^d$, the stability exponent Eq. (111) evaluated as functional integral over its Brillouin zone, generating function variable z replaced by a Laplace transform variable s, $z = e^{-s}$ (see ChaosBook Eq. (21.20)), and the deterministic partition sum Eq. (116) of form

$$Z[\beta, s] = \sum_c t_c\,, \quad t_c = \left(e^{\beta\cdot a_c - \lambda_c - s}\right)^{N_c}\,. \tag{151}$$

   We have not encountered such sums over Bravais lattices in solid state and mathematical physics literature. In field theory they play a key role,[60,61] so one could refer to them as field theorists do, as 'sums over geometries'.

   Show that our zeta-function Eq. (129) formulation of spatiotemporal chaos applies also to spacetime continuous systems, such as Kuramoto-Sivashinsky and Navier-Stokes PDEs.

3. Evaluate the stability exponents of a set of unstable Kuramoto-Sivashinsky (or another spatially 1-dimensional PDE) periodic states, test the quality of zeta function predictions.

4. Evaluate the stability exponents of a set of unstable Navier-Stokes periodic states.

5. In Sec. V we have assumed that the only symmetry of the theory is the translation group T. However, one needs to quotient all spacetime and internal symmetries. For a one-dimensional lattice field theory we have done this in companion paper I,[16] and derived the dihedral-space group $G = \mathrm{D}_\infty$ zeta function for time-reversal invariant field theories, drawing inspiration from Lind's topological (rather than our weighted, 'dynamical') zeta function,[143]

$$\zeta_{Lind}(z) = \exp\Big(\sum_H \frac{N_H}{|G/H|} z^{|G/H|}\Big)\,, \tag{152}$$

a generalization of Artin-Mazur zeta function. In present context, G is the crystallographic space group of a field theory over a hypercubic lattice $\mathbb{Z}^d$, H a finite-index $|G/H|$ subgroup of G, and N_H is the number of the periodic states that are invariant under actions of the subgroup H.

6. Describe the admissible mosaics of the spatiotemporal cat Eq. (48).

   For one-dimensional temporal cat the answer is given in terms of walks on the transition graph of ChaosBook Fig. 14.18 (d).

   In two dimensions Axenides *et al.* use Fibonacci polynomials, forward in time evolution of a fixed initial spatial interval to generate all admissible mosaics over $[L\times T]_0$ rectangular primitive cells.[38,40,202] A corresponding algorithm for general $[L\times T]_S$ Bravais lattices has not been implemented.

7. Describe the admissible mosaics of a nonlinear field theory with pruning, i.e., with couplings weaker than those topologically equivalent to the anti-integrable limit (see Sec. II C and companion paper III[17]).

ACKNOWLEDGMENTS

This paper has been profoundly influenced by anti-integrability viewpoint of Serge Aubry, whose 80th birthday it celebrates.

The work of H. L. was fully supported, and of P. C. was in part supported by the family of late G. Robinson, Jr.. This research was initiated during the KITP UC Santa Barbara 2017 *Recurrent Flows: The Clockwork Behind Turbulence* program, supported in part by the National Science Foundation under Grant No. NSF PHY-1748958.

We are grateful to S.D.V. Williams, M.N. Gudorf and X. Wang for many inspiring discussions. No actual cats, graduate or undergraduate, have shown interest in, or were harmed during this research.

Appendix A: Bravais sublattices

When is a two-dimensional Bravais lattice $\mathcal{L}_\mathbb{A}$ a sublattice of a finer Bravais lattice $\mathcal{L}_{\mathbb{A}_p}$? Define $\mathcal{L}_{\mathbb{A}_p}$ by a pair of primitive vectors in the Hermite normal form $[L_p\times T_p]_{S_p}$,

$$\mathbf{a}_1^p = \begin{pmatrix} L_p \\ 0 \end{pmatrix}\,, \qquad \mathbf{a}_2^p = \begin{pmatrix} S_p \\ T_p \end{pmatrix}\,. \tag{A1}$$

The sublattices $\mathcal{L}_\mathbb{A}$ of $\mathcal{L}_{\mathbb{A}_p}$ have primitive vectors that are linear combinations of $\mathbf{a}_1$ and $\mathbf{a}_2$:

$$\begin{aligned} \mathbf{a}_1 &= r_1\,\mathbf{a}_1^p + s_2\,\mathbf{a}_2^p \\ \mathbf{a}_2 &= s_1\,\mathbf{a}_1^p + r_2\,\mathbf{a}_2^p\,, \end{aligned} \tag{A2}$$

where r_1, r_2, s_1 and s_2 are integers, so that every lattice site of the sublattice $\mathcal{L}_\mathbb{A}$ belongs to the Bravais lattice $\mathcal{L}_{\mathbb{A}_p}$. If we also choose $\mathcal{L}_\mathbb{A}$ primitive vectors in the Hermite normal form $[L\times T]_S$, the relation Eq. (A2) can be rewritten as:

$$\mathbb{A} = \mathbb{A}_p\mathbb{R}\,, \tag{A3}$$

where

$$\mathbb{A} = \begin{bmatrix} L & S \\ 0 & T \end{bmatrix}\,,\ \mathbb{A}_p = \begin{bmatrix} L_p & S_p \\ 0 & T_p \end{bmatrix}\,,\ \mathbb{R} = \begin{bmatrix} r_1 & s_1 \\ s_2 & r_2 \end{bmatrix}\,.$$

Then the matrix $\mathbb{R}$ is:

$$\mathbb{R} = \mathbb{A}_p^{-1}\mathbb{A} = \begin{bmatrix} L/L_p & S/L_p - S_pT/L_pT_p \\ 0 & T/T_p \end{bmatrix}\,. \tag{A4}$$

Comparing Eq. (A4) with Eq. (A3), we note that $\mathcal{L}_\mathbb{A}$ is a sublattice of $\mathcal{L}_{\mathbb{A}_p}$ if L is a multiple of L_p, T is multiple of T_p and

$$\mathbf{a}_2 \times \mathbf{a}_2^p = ST_p - TS_p \tag{A5}$$

is a multiple of the prime tile area L_pT_p.

So, given Bravais lattice $\mathcal{L}_{\mathbb{A}_p}$ with primitive cell $\mathbb{A}_p$, one gets all of its sublattices by computing $\mathbb{A} = \mathbb{A}_p\mathbb{R}$, with the repeats matrix $\mathbb{R}$ in the Hermite normal form,

$$\mathbb{R} = \begin{bmatrix} r_1 & s \\ 0 & r_2 \end{bmatrix}\,, \tag{A6}$$

where $r_1, r_2 > 0$ and $0 \le s < r_1$ are integers.

1. Examples of prime orbits

The square lattice unit primitive cell,

$$\mathbb{A} = \begin{bmatrix} 1 & 0 \\ 0 & 1 \end{bmatrix}\,, \qquad N_\mathbb{A} = 1\,, \tag{A7}$$

$[1\times1]_0$-periodic field configuration, or the constant lattice field

$$\Phi = \begin{bmatrix} \phi_{00} \end{bmatrix}$$

is the unit cell of a square $\mathbb{Z}^2$ integer lattice.

$[2\times1]_0$-periodic field configuration

$$\Phi = \begin{bmatrix} \phi_{00} & \phi_{10} \end{bmatrix} ,$$

$[1\times2]_0$-periodic field configuration

$$\Phi = \begin{bmatrix} \phi_{01} \\ \phi_{00} \end{bmatrix}$$

have 'bricks' stacked atop each other, see mosaics of Fig. 6 (a) and (b). $[2\times1]_1$-periodic field configuration

$$\Phi = \begin{bmatrix} \phi_{00} & \phi_{10} \end{bmatrix}$$

has layers of 'bricks' stacked atop each other, but with a relative-periodic boundary condition, with layers shifted by $S = 1$, as in Fig. 3 (a).

The boundary conditions for the above three kinds of primitive cells can illustrated by repeats of the three 'bricks', on top, sideways, and on top and shifted:

$$[2\times1]_0 \ : \ \begin{bmatrix} \phi_{00} & \phi_{10} \\ \phi_{00} & \phi_{10} \end{bmatrix} , \quad [1\times2]_0 \ : \ \begin{bmatrix} \phi_{01} & \phi_{01} \\ \phi_{00} & \phi_{00} \end{bmatrix}$$

$$[2\times1]_1 \ : \ \begin{bmatrix} & \phi_{00} & \phi_{10} \\ \phi_{00} & \phi_{10} & \end{bmatrix} .$$

$[3\times2]_1$-periodic field configuration can be presented as a field over the *parallelepiped*-shaped tilted primitive cell of Fig. 2 (a),

$$[3\times2]_1 \ : \ \begin{bmatrix} & \phi_{11} & \phi_{21} & \phi_{01} \\ \phi_{00} & \phi_{10} & \phi_{20} & \end{bmatrix} ,$$

or as an $[3\times2]$ rectangular array

$$\Phi = \begin{bmatrix} \phi_{01} & \phi_{11} & \phi_{21} \\ \phi_{00} & \phi_{10} & \phi_{20} \end{bmatrix} , \tag{A8}$$

with the Bravais lattice relative-periodicity imposed by a shift boundary condition, as in Fig. 3 (b) and the mosaic of Fig. 6 (f).

As shown above, an $[L\times T]_S$ primitive cell field configuration is not prime if it is invariant under the translations of lattice $[L_p\times T_p]_{S_p}$, and $[L\times T]_S$ is a sublattice of $[L_p\times T_p]_{S_p}$.

For example, a field configuration over primitive cell $[2\times2]_0$,

$$\Phi = \begin{bmatrix} \phi_{10} & \phi_{00} \\ \phi_{00} & \phi_{10} \end{bmatrix} .$$

is a repeat and shift of the field configuration

$$\Phi_p = \begin{bmatrix} \phi_{00} & \phi_{10} \end{bmatrix}$$

over primitive cell $[2\times1]_1$. As shown in Fig. 3 (a), Bravais lattice $[2\times2]_0$ is a sublattice of $[2\times1]_1$. Over the infinite spacetime Φ and Φ_p are the same field configuration, as is clear by inspection of Fig. 6 (c).

For further examples of orbits and their symmetries, see companion papers I and III.[16,17]

Appendix B: Computation of spatiotemporal cat periodic states

Defining equations Eq. (49) are piecewise linear, and, given a primitive cell $\mathbb{A}$ and a mosaic M Eq. (37) over it, always has a unique solution Φ_{M}. We solve it by reciprocal lattice diagonalization (Sec. VIII B), by direct determinant evaluation (Appendix B 3), or by matrix inversion:

$$\phi_z = \sum_{z'\in\mathbb{Z}^d} g_{zz'} m_{z'} , \qquad g_{zz'} = \left[\frac{1}{-\Box + \mu^2} \right]_{zz'} , \tag{B1}$$

where $g_{zz'}$, the inverse of the orbit Jacobian operator, is the Klein-Gordon free-field Eq. (48) Green's function. In literature, $g_{zz'}$ is known as the Green's function for the d-dimensional discretized screened Poisson equation.

The solution Φ_{M} is a periodic state, and the mosaic M is said to be *admissible*, if and only if all lattice-site field values ϕ_z of Φ_{M} lie in the compact boson state space Eq. (48)

$$\mathcal{M} = \left\{ \Phi \mid \phi_z \in [0,1) \, , \ z \in \mathbb{Z}^d \right\} . \tag{B2}$$

So we need to define the range of permissible integers m_z ('covering' alphabet), and, if we are able, the grammar of admissible mosaics M.

1. Spatiotemporal cat mosaics

'Letter' m_z is the integer part of the LHS of defining equations Eq. (48) that enforces the circle (mod 1) condition for field ϕ_z on lattice site z. Its range depends on the Klein-Gordon mass-squared μ^2, and the lattice dimension d. If all nearest neighbor fields are as large as allowed, $\phi_{z'} = 1 - \epsilon$, in two spatiotemporal dimensions the integer part of the LHS of Eq. (51) can be as low as -3, for $\phi_z = 0$, or as high as μ^2+3, for $\phi_z = 1 - \epsilon$, hence the covering alphabet $\mathcal{A} = \{m_z\}$ is

$$\mathcal{A} = \{\underline{3}, \underline{2}, \underline{1} \, ; \, 0, \cdots, \mu^2 \, ; \, \mu^2+1, \mu^2+2, \mu^2+3\} , \tag{B3}$$

where symbol $\underline{m_z}$ denotes m_z with the negative sign, i.e., '$\underline{3}$' stands for symbol '-3'. All our numerical calculations are carried out for $\mu^2 = 1$, with alphabet

$$\mathcal{A} = \{\underline{3}, \underline{2}, \underline{1} \, ; \, 0, 1 \, ; \, 2, 3, 4\} . \tag{B4}$$

As each M corresponds to a unique periodic state Φ_{M}, the periodic state can be visualized by its color-coded mosaic M.

Given a two-dimensional spatiotemporal mosaic M, the corresponding periodic state can be computed using Eq. (B1),

$$\Phi_{i_1 j_1} = \sum_{i_2=0}^{2} \sum_{j_2=0}^{1} \mathsf{g}_{i_1 j_1, i_2 j_2} \mathsf{M}_{i_2 j_2} \,,$$

provided that the correct boundary conditions are imposed on $\mathsf{g}_{i_1 j_1, i_2 j_2}$.

If all nearest neighbor fields are as small as allowed, $\phi_{z'} = 0$, the Laplacian does not contribute, and the integer part of the LHS of Eq. (48) ranges from 0, for $\phi_z = 0$, to μ^2, for $\phi_z = 1$, hence the $\mu^2 + 7$ letter alphabet Eq. (B3) can be divided into two subsets, the interior and the exterior alphabets $\mathcal{A}_0$ and $\mathcal{A}_1$, respectively.

$$\begin{aligned} \mathcal{A}_0 &= \{0, \ldots, \mu^2\} \,, \\ \mathcal{A}_1 &= \{\underline{3}, \underline{2}, \underline{1}\} \cup \{\mu^2{+}1, \mu^2{+}2, \mu^2{+}3\} \,. \end{aligned} \tag{B5}$$

If all m_z of a mosaic M belong to the interior alphabet $\mathcal{A}_0$, the mosaic M is admissible.[37]

We have no algorithm that would generate admissible spatiotemporal cat mosaics (see question 6 of Sec. XII B *Open questions*). Instead, we solve the linear equation Eq. (B1) for each covering mosaic, and then -for mosaics containing exterior alphabets $\mathcal{A}_1$ letters- discard those for which Φ_{M} lies outside the unit hypercube Eq. (B2).

For example, for $\mu^2 = 1$ the mosaic

$$\mathsf{M} = \begin{bmatrix} -1 & 1 & 0 \\ 4 & -1 & -1 \end{bmatrix}$$

over primitive cell $[3\times 2]_1$ of Fig. 3 (b) corresponds to the periodic state:

$$\Phi_{\mathsf{M}} = \begin{bmatrix} \phi_{01} & \phi_{11} & \phi_{21} \\ \phi_{00} & \phi_{10} & \phi_{20} \end{bmatrix} = \frac{1}{35} \begin{bmatrix} 5 & 17 & 6 \\ 34 & 5 & 3 \end{bmatrix} .$$

One can check that defining equations are satisfied everywhere by substituting this solution into Eq. (51).

2. Spatiotemporal cat primitive cells' orbit Jacobians

(Continuation of calculations of Sec. VIII.) Developing some feel for the orbit Jacobian formulas for two-dimensional spatiotemporal cat examples is now in order. The simplest examples of periodic states, illustrated by spatiotemporal mosaic tilings of Fig. 6, are (i) space-time steady states over the unit cell $[1\times 1]_0$, (ii) spatial steady states over $[1\times T]_0$, (iii) temporal steady states over $[L\times 1]_0$, and (iv) time-relative steady states over $[L\times 1]_S$, $S \neq 0$, stationary patterns in a time-reference frame[203] moving with a constant velocity S/T.

For explicit values of orbit Jacobians, we take the lowest integer value of the Klein-Gordon mass, $\mu^2 = 1$, throughout the paper.

Consider first the family of primitive cells of temporal period one, $T = 1$ in Eq. (93),

$$\mathrm{Det}\, \mathcal{J}_{[L\times 1]_0} = \mu^2 \prod_{m_1=1}^{L-1} \left[p\Big(\frac{2\pi}{L} m_1\Big)^2 + \mu^2 \right] . \tag{B6}$$

This is the one-dimensional temporal cat orbit Jacobian, with calculations carried out as in Eq. (92). The steady state orbit Jacobian is

$$\mathrm{Det}\, \mathcal{J}_{[1\times 1]_0} = \mu^2 \Rightarrow 1 \,, \tag{B7}$$

the period-2 periodic state orbit Jacobian is

$$\mathrm{Det}\, \mathcal{J}_{[2\times 1]_0} = \mu^2(\mu^2 + 4) \Rightarrow 5 \,, \tag{B8}$$

and so on. However, for the simplest relative-periodic state, with tilt $S/T = 1$, the orbit Jacobian Eq. (96) is already more surprising, it is larger than $\mathrm{Det}\, \mathcal{J}_{[2\times 1]_0} \Rightarrow 5$:

$$\begin{aligned} \mathrm{Det}\, \mathcal{J}_{[2\times 1]_1} &= \mu^2 \left[p\,(\pi)^2 + p\,(-\pi)^2 + \mu^2 \right] \\ &= \mu^2(\mu^2 + 8) \Rightarrow 9 \,. \end{aligned} \tag{B9}$$

The spatiotemporal spatiotemporal cat calculations then proceed as in example Eq. (97),

$$\mathrm{Det}\, \mathcal{J}_{[2\times 2]_0} = \mu^2(\mu^2 + 4)^2(\mu^2 + 8) \Rightarrow 225 \,,$$

and so on.

For example, one can check that the orbit Jacobian formula Eq. (93) for the $[3\times 2]_0$ periodic states,

$$\begin{aligned} \mathrm{Det}\, \mathcal{J}_{[3\times 2]_0} &= \prod_{m_1=0}^{2} \prod_{m_2=0}^{1} \left[p\Big(\frac{2\pi}{3} m_1\Big)^2 + p\Big(\frac{2\pi}{2} m_2\Big)^2 + \mu^2 \right] \\ &\Rightarrow 5120 \,, \end{aligned} \tag{B10}$$

is in agreement with our alternative method of its evaluation, the fundamental fact count Eq. (B17) explained below.

Consider next the primitive cell $[3\times 2]_1$ of Fig. 2 (a), Fig. 3 (b) and Fig. 7 (a). We have computed the eigenvalues of its Laplacian in Eq. (97), so the corresponding orbit Jacobian Eq. (66) is

$$\mathrm{Det}\, \mathcal{J}_{[3\times 2]_1} = \mu^2(\mu^2 + 4)^3(\mu^2 + 6)^2 = 6125 \,. \tag{B11}$$

For a list of such two-dimensional spatiotemporal cat orbit Jacobians, see Table I, and the list of the spatiotemporal cat orbit Jacobians evaluated for $\mu^2 = 1$, see Table II.

3. Spatiotemporal cat: Fundamental fact

As shown in the companion paper I,[16] for one-dimensional lattice temporal cat orbit Jacobians count the numbers of period-n periodic states,

$$N_n = |\mathrm{Det}\, \mathcal{J}_n| \,. \tag{B12}$$

TABLE I. The numbers of spatiotemporal cat periodic states for primitive cells $\mathbb{A} = [L\times T]_S$ up to $[3\times 3]_2$. Here $N_{\mathbb{A}}(\mu^2)$ is the number of periodic states, and $M_{\mathbb{A}}(\mu^2)$ is the number of prime orbits. The Klein-Gordon mass μ^2 can take only integer values.

$\mathbb{A}$	$N_{\mathbb{A}}(\mu^2)$	$M_{\mathbb{A}}(\mu^2)$
$[1\times 1]_0$	μ^2	μ^2
$[2\times 1]_0$	$\mu^2(\mu^2+4)$	$\mu^2(\mu^2+3)/2$
$[2\times 1]_1$	$\mu^2(\mu^2+8)$	$\mu^2(\mu^2+7)/2$
$[3\times 1]_0$	$\mu^2(\mu^2+3)^2$	$\mu^2(\mu^2+2)(\mu^2+4)/3$
$[3\times 1]_1$	$\mu^2(\mu^2+6)^2$	$\mu^2(\mu^2+5)(\mu^2+7)/3$
$[4\times 1]_0$	$\mu^2(\mu^2+2)^2(\mu^2+4)$	$\mu^2(\mu^2+1)(\mu^2+3)(\mu^2+4)/4$
$[4\times 1]_1$	$\mu^2(\mu^2+4)^2(\mu^2+8)$	$\mu^2(\mu^2+3)(\mu^2+4)(\mu^2+5)/4$
$[4\times 1]_2$	$\mu^2(\mu^2+4)(\mu^2+6)^2$	$\mu^2(\mu^2+4)(\mu^2+5)(\mu^2+7)/4$
$[4\times 1]_3$	$\mu^2(\mu^2+4)^2(\mu^2+8)$	$\mu^2(\mu^2+3)(\mu^2+5)(\mu^2+8)/4$
$[5\times 1]_0$	$\mu^2(\mu^4+5\mu^2+5)^2$	$\mu^2(\mu^2+1)(\mu^2+2)(\mu^2+3)(\mu^2+4)/5$
$[5\times 1]_1$	$\mu^2(\mu^4+10\mu^2+23)^2$	$\mu^2(\mu^2+3)(\mu^2+7)(\mu^4+10\mu^2+19)/5$
$[2\times 2]_0$	$\mu^2(\mu^2+4)^2(\mu^2+8)$	$\mu^2(\mu^2+3)/2\times(\mu^4+13\mu^2+38)/2$
$[2\times 2]_1$	$\mu^2(\mu^2+4)(\mu^2+6)^2$	$\mu^2(\mu^2+7)/2\times(\mu^2+4)(\mu^2+5)/2$
$[3\times 2]_0$	$\mu^2(\mu^2+3)^2(\mu^2+4)(\mu^2+7)^2$	$\mu^2(\mu^2+3)(\mu^2+4)(\mu^6+17\mu^4+91\mu^2+146)/6$
$[3\times 2]_1$	$\mu^2(\mu^2+4)^3(\mu^2+6)^2$	$\mu^2(\mu^2+3)(\mu^2+5)(\mu^6+16\mu^4+85\mu^2+151)/6$
$[3\times 3]_0$	$\mu^2(\mu^2+3)^4(\mu^2+6)^4$	
$[3\times 3]_1$	$\mu^2(\mu^2+3)^2(\mu^6+15\mu^4+72\mu^2+111)^2$	
$[3\times 3]_2$	$\mu^2(\mu^2+3)^2(8s^3+3(\mu^2+4)^2-1)^2$	

TABLE II. The numbers of the $\mu^2=1$ spatiotemporal cat $[L\times T]_S$ periodic states: $N_{[L\times T]_S}$ is the number of periodic states, and $M_{[L\times T]_S}$ is the number of prime orbits.

$[L\times T]_S$	M	N
$[1\times 1]_0$	1	1
$[2\times 1]_0$	2	$5 = 2\,[2\times 1]_0 + 1\,[1\times 1]_0$
$[2\times 1]_1$	4	$9 = 4\,[2\times 1]_1 + 1\,[1\times 1]_0$
$[3\times 1]_0$	5	$16 = 5\,[3\times 1]_0 + 1\,[1\times 1]_0$
$[3\times 1]_1$	16	$49 = 16\,[3\times 1]_1 + 1\,[1\times 1]_0$
$[4\times 1]_0$	10	$45 = 10\,[4\times 1]_0 + 2\,[2\times 1]_0 + 1\,[1\times 1]_0$
$[4\times 1]_1$	54	$225 = 54\,[4\times 1]_1 + 4\,[2\times 1]_1 + 1\,[1\times 1]_0$
$[4\times 1]_2$	60	$245 = 60\,[4\times 1]_2 + 2\,[2\times 1]_0 + 1\,[1\times 1]_0$
$[2\times 2]_0$	52	$225 = 52\,[2\times 2]_0 + 2\,[2\times 1]_0 + 2\,[1\times 2]_0 + 4\,[2\times 1]_1 + 1\,[1\times 1]_0$
$[2\times 2]_1$	60	$245 = 60\,[2\times 2]_1 + 2\,[1\times 2]_0 + 1\,[1\times 1]_0$
$[3\times 2]_0$	850	$5\,120 = 850\,[3\times 2]_0 + 5\,[3\times 1]_0 + 2\,[1\times 2]_0 + 1\,[1\times 1]_0$
$[3\times 2]_1$	1 012	$6\,125 = 1\,012\,[3\times 2]_1 + 16\,[3\times 1]_2 + 2\,[1\times 2]_0 + 1\,[1\times 1]_0$
$[3\times 3]_0$	68 281	$614\,656 = 68\,281\,[3\times 3]_0 + 5\,[3\times 1]_0 + 16\,[3\times 1]_1 + 16\,[3\times 1]_2 + 5\,[1\times 3]_0 + 1\,[1\times 1]_0$
$[3\times 3]_1$	70 400	$633\,616 = 70\,400\,[3\times 3]_1 + 5\,[1\times 3]_0 + 1\,[1\times 1]_0$

We now show that for a spatiotemporal cat orbit Jacobian counts the number of periodic states in any spatiotemporal dimension d.

Spatiotemporal cat periodic state $\mathsf{\Phi_M}$ over primitive cell $\mathbb{A}$ is a point within the unit hypercube $[0,1)^{N_{\mathbb{A}}}$, where $N_{\mathbb{A}}$ is the primitive cell volume Eq. (11). Visualize now what spatiotemporal cat defining equation Eq. (49)

$$\mathcal{J}_{\mathbb{A}}\mathsf{\Phi_M} - \mathsf{M} = 0$$

means geometrically. The $[N_{\mathbb{A}}\times N_{\mathbb{A}}]$ orbit Jacobian matrix $\mathcal{J}_{\mathbb{A}}$ stretches the state space unit hypercube $\mathsf{\Phi}\in[0,1)^{N_{\mathbb{A}}}$ into an $N_{\mathbb{A}}$-dimensional *fundamental parallelepiped* (or parallelogram), and maps the periodic state $\mathsf{\Phi_M}$ into a point on integer lattice $\mathbb{Z}^{N_{\mathbb{A}}}$ within it, in the $N_{\mathbb{A}}$-dimensional configuration state space Eq. (12). This point is then translated by integer winding numbers M into the origin. What Baake *et al.*[204] call the *'fundamental fact'* follows:

$$N_{\mathbb{A}} = |\mathrm{Det}\,\mathcal{J}_{\mathbb{A}}|\,, \tag{B13}$$

the number of periodic states equals the number of integer lattice points within the fundamental parallelepiped.

For the history of 'fundamental fact' see *Appendix A. Historical context* of the companion paper I.[16] Reader might also want to check the figures of a few fundamental parallelepipeds there, but we know of no good way of presenting them visually for primitive cells of interest here, with $N_{\mathbb{A}} > 3$.

It is a peculiarity of the spatiotemporal cat that it involves two *distinct* integer lattices. (i) The spacetime *coordinates* Eq. (6) are discretized by integer lattice $\mathbb{Z}^d$. The primitive cell $\mathbb{A}$ Eq. (10) is an example of a fundamental parallelepiped, and we use the fundamental fact when we express the volume Eq. (11) of the primitive cell, i.e. the determinant of the matrix $\mathbb{A}$, as the number of lattice sites within the primitive cell. (ii) For a spatiotemporal cat the lattice site *field* ϕ_z Eq. (48) is compactified to the unit circle $[0,1)$, imparting integer lattice structure to the configuration *state space* Eq. (12): the orbit

Jacobian matrix $\mathcal{J}_{\mathbb{A}}$ maps a periodic state $\Phi_{\mathsf{M}} \in [0,1)^{N_{\mathbb{A}}}$ to a $\mathbb{Z}^{N_{\mathbb{A}}}$ integer lattice site M. Nothing like that, and no 'fundamental fact' applies to general nonlinear field theories of Sec. III.

Example: Fundamental parallelepiped evaluation of a orbit Jacobian. As a concrete example consider periodic states of two-dimensional spatiotemporal cat with periodicity $[3\times 2]_0$, i.e., space period $L=3$, time period $T=2$ and tilt $S=0$. Periodic states within the primitive cell and their corresponding mosaics can be written as two-dimensional $[3\times 2]$ arrays:

$$\Phi_{[3\times 2]_0} = \begin{bmatrix} \phi_{01} & \phi_{11} & \phi_{21} \\ \phi_{00} & \phi_{10} & \phi_{20} \end{bmatrix}, \qquad \mathsf{M}_{[3\times 2]_0} = \begin{bmatrix} m_{01} & m_{11} & m_{21} \\ m_{00} & m_{10} & m_{20} \end{bmatrix}. \tag{B14}$$

Reshape the periodic states and mosaics into vectors:

$$\Phi_{[3\times 2]_0} = \begin{pmatrix} \phi_{01} \\ \phi_{00} \\ \hline \phi_{11} \\ \phi_{10} \\ \hline \phi_{21} \\ \phi_{20} \end{pmatrix}, \quad \mathsf{M}_{[3\times 2]_0} = \begin{pmatrix} m_{01} \\ m_{00} \\ \hline m_{11} \\ m_{10} \\ \hline m_{21} \\ m_{20} \end{pmatrix}. \tag{B15}$$

The reshaped orbit Jacobian matrix acting on these periodic states is a block matrix:

$$\mathcal{J}_{[3\times 2]_0} = \left(\begin{array}{cc|cc|cc} 2s & -2 & -1 & 0 & -1 & 0 \\ -2 & 2s & 0 & -1 & 0 & -1 \\ \hline -1 & 0 & 2s & -2 & -1 & 0 \\ 0 & -1 & -2 & 2s & 0 & -1 \\ \hline -1 & 0 & -1 & 0 & 2s & -2 \\ 0 & -1 & 0 & -1 & -2 & 2s \end{array}\right). \tag{B16}$$

where the stretching factor $2s = 4+\mu^2$. The fundamental parallelepiped generated by the action of orbit Jacobian matrix $\mathcal{J}_{[3\times 2]_0}$ on the state space unit hypercube Eq. (48) is spanned by 6 primitive vectors, the columns of the orbit Jacobian matrix Eq. (B16). The 'fundamental fact' now expresses the orbit Jacobian, i.e., the number of periodic states within the fundamental parallelepiped, as a polynomial of order $N_{\mathbb{A}}$ in the Klein-Gordon mass μ^2 Eq. (60),

$$\begin{aligned} N_{[3\times 2]_0} &= |\mathrm{Det}\, \mathcal{J}_{[3\times 2]_0}| \\ &= \mu^2(\mu^2+3)^2(\mu^2+4)(\mu^2+7)^2\,, \end{aligned} \tag{B17}$$

without recourse to any explicit diagonalization, such as the reciprocal lattice diagonalization Eq. (93). For $\mu^2=1$ this agrees with the reciprocal lattice evaluation Eq. (B10). For a list of the numbers of spatiotemporal cat periodic states for primitive cells $[L\times T]_S$ up to $[3\times 3]_2$, see Table I.

For $\mu^2=1$ spatiotemporal cat the pruning turns out to be very severe. Only 52 of the prime $[2\times 2]_0$ mosaics are admissible. As for the repeats of smaller mosaics, there are 2 admissible $[1\times 2]_0$ mosaics repeating in time and 2 $[2\times 1]_0$ mosaics repeating in space. There are 4 admissible 1/2-shift periodic boundary $[1\times 2]_0$ mosaics. And there is 1 admissible mosaic which is a repeat of letter 0. The total number of $[2\times 2]_0$ of periodic states is obtained by all cyclic permutations of admissible prime mosaics,

$$\begin{aligned} N_{[2\times 2]_0} &= 52\,[2\times 2]_0 + 2\,[2\times 1]_0 + 2\,[1\times 2]_0 \\ &\quad +4\,[2\times 1]_1 + 1\,[1\times 1]_0 \;=\; 225\,, \end{aligned} \tag{B18}$$

summarized in Table II. This explicit list of admissible prime orbits verifies the orbit Jacobian formula Eq. (93).

4. Prime lattice field configurations

Here we show how to enumerate the total numbers of distinct periodic states in terms of prime orbits.

The enumeration of spatiotemporal cat doubly-periodic states proceeds in 3 steps:

1. Construct a hierarchy of two-dimensional Bravais lattices $\mathcal{L}_{\mathbb{A}}$, starting with the smallest primitive cells, list Bravais lattices by increasing $[L\times T]_S$, one per each set related by translation symmetries Eq. (70) (here we are ignoring discrete point group D_4).

2. For each $\mathcal{L}_{\mathbb{A}} = [L\times T]_S$ Bravais lattice, compute $N_{\mathbb{A}}$, the number of doubly-periodic spatiotemporal cat periodic states, using the 'fundamental fact' $N_{\mathbb{A}} = |\mathrm{Det}\, \mathcal{J}_{\mathbb{A}}|$.

3. We have defined the *prime orbit* in Sec. VI.

The total number of (doubly) periodic mosaics is the sum of all cyclic permutations of prime mosaics,

$$N_{\mathbb{A}} = \sum_{\mathbb{A}_p|\mathbb{A}} M_{\mathbb{A}_p}\, [L_p\times T_p]_{S_p}$$

where the sum goes over every lattice $\mathcal{L}_{\mathbb{A}_p} = [L_p\times T_p]_{S_p}$ which contains $[L\times T]_S$.

Given the number of periodic states, the number of $\mathbb{A} = [L\times T]_S$-periodic prime orbits is computed recursively:

$$M_{\mathbb{A}} = \frac{1}{LT}\left(N_{\mathbb{A}} - \sum_{\mathbb{A}_p|\mathbb{A}}^{L_pT_p<LT} L_pT_p\, M_{\mathbb{A}_p}\right). \tag{B19}$$

5. Example: 'Escape rate' of temporal cat

The topological zeta function of temporal cat is:[16,205]

$$1/\zeta_{AM}(z) = \exp\left(-\sum_{n=1}^{\infty}\frac{N_n}{n}z^n\right) = \frac{1-(\mu^2+2)z+z^2}{(1-z)^2}\,, \tag{B20}$$

where N_n is the number of periodic states with period n. Due to the uniform stretching factor μ^2+2, the deterministic zeta function of temporal cat has the same form, up to a rescaling:

$$1/\zeta[0,z] = \exp\left(-\sum_{n=1}^{\infty}\frac{N_n}{n}t^n\right) = 1/\zeta_{AM}(t)\,,$$
$$t = \frac{z}{\Lambda}\,, \tag{B21}$$

where Λ is the stability multiplier

$$\Lambda = e^{\lambda} = \frac{1}{2}\left(\mu^2+2+\mu\sqrt{\mu^2+4}\right)\,. \tag{B22}$$

Solving for the roots of $1/\zeta[0,z]=0$, we have:

$$t = \Lambda^{\pm 1} \to z = 1 \text{ or } \Lambda^2\,. \tag{B23}$$

The leading root is 1 so the 'escape rate' is 0. The Fredholm determinant[139] of temporal cat is:

$$F(0,z) = \exp\left(-\sum_{n=1}^{\infty}\frac{N_n z^n}{n\,|\mathrm{Det}\,\mathcal{J}_n|}\right) = \exp\left(-\sum_{n=1}^{\infty}\frac{z^n}{n}\right) = 1-z\,, \tag{B24}$$

where we have used the 'fundamental fact' Eq. (B12). The 'escape rate' is again 0, as it should be - cat map is by construction probability conserving.

6. Example: Expectation value of stability exponent of temporal cat.

To compute the expectation value of the stability exponent, take the logarithm of periodic state's primitive cell stability as the Birkhoff sum A, Eq. (19), stability exponent observable, and compute the corresponding deterministic zeta function:

$$1/\zeta[\beta,z] = \exp\left(-\sum_{n=1}^{\infty}\frac{N_n}{n}\frac{\exp(\beta\ln|\mathrm{Det}\,\mathcal{J}_n|)z^n}{\Lambda^n}\right)\,, \tag{B25}$$

where $|\mathrm{Det}\,\mathcal{J}_n|$ is the primitive cell stability of period-n periodic states, and Λ is the stability multiplier which is related to the stability exponent by Eq. (B22). Note that the number of n-periodic state is given by the primitive cell stability:[16,205]

$$N_n = |\mathrm{Det}\,\mathcal{J}_n| = \Lambda^n + \Lambda^{-n} - 2\,. \tag{B26}$$

Using Eq. (137) the expectation value of the stability exponent is:

$$\langle\lambda\rangle = \frac{\langle A\rangle_\zeta}{\langle N\rangle_\zeta} = \frac{\partial\zeta[\beta,z]}{\partial\beta}\Big/ z\frac{\partial\zeta[\beta,z]}{\partial z}\Big|_{\beta=0,z=z(0)} = \frac{\partial\ln\zeta[\beta,z]}{\partial\beta}\Big/ z\frac{\partial\ln\zeta[\beta,z]}{\partial z}\Big|_{\beta=0,z=1}\,. \tag{B27}$$

The numerator of Eq. (B27) is:

$$\sum_{n=1}^{\infty}\frac{(\Lambda^n+\Lambda^{-n}-2)\ln(\Lambda^n+\Lambda^{-n}-2)}{n\Lambda^n}\,, \tag{B28}$$

and the denominator is:

$$\sum_{n=1}^{\infty}\frac{\Lambda^n+\Lambda^{-n}-2}{\Lambda^n}\,. \tag{B29}$$

Both the numerator and the denominator of Eq. (B27) diverge to infinity. Using the Stolz-Cesàro theorem,[206] the ratio of Eq. (B28) and Eq. (B29) equals:

$$\langle\lambda\rangle = \lim_{n\to\infty}\frac{\ln(\Lambda^n+\Lambda^{-n}-2)}{n} = \ln\Lambda = \lambda\,, \tag{B30}$$

which agrees with the fact that every periodic state has a same stability exponent λ.

Appendix C: Spectra of orbit Jacobian operators for nonlinear field theories

The simplicity of the spatiotemporal cat orbit Jacobian operator band spectrum Eq. (106), plotted in Fig. 9 (a) and Fig. 11 (a), is a bit misleading. As explained in Sec. IV B, the uniform stretching factor describes only the stability of a steady state solution, for any field theory. To get a feeling for the general case, in section 10 of paper I[16] we compute the stability of a period-2 periodic state for two nonlinear field theories. Here we outline such calculations, to illustrate the essential difference between the very special spatiotemporal cat case, and the general, nonlinear case. For a detailed exposition, see companion paper III,[17] where we evaluate stabilities of large sets of nonlinear field theories' periodic states.

An analytic eigenvalue formula is feasible only for the period-2 periodic state; in general, periodic states and the associated orbit Jacobian operator spectra are evaluated numerically. The simplest non-constant solutions, a period-2 periodic states, suffice to illustrate the general case.

1. One-dimensional ϕ^3 field theory period-2 periodic state

Consider the ϕ^3 theory, Eq. (45),

$$-\Box\,\phi_z \;+\; \mu^2\,(1/4-\phi_z^2) = 0\,.$$

In one spatiotemporal dimension, this field theory is a temporal lattice reformulation of the forward-in-time Hénon map, where large numbers of periodic solutions can be easily computed[193]. The ϕ^3 theory, to which companion paper III[17] assigns binary alphabet $\mathcal{A} = \{0,1\}$, Eq. (36), has one period-2 prime orbit $\{\Phi_{01},\Phi_{10}\}$, with the 2-lattice site periodic state, mosaic

$$\Phi_{01} = \begin{bmatrix} \phi_0 \\ \phi_1 \end{bmatrix} = \begin{bmatrix} \overline{\phi} - \sqrt{\frac{1}{4}-\overline{\phi}^2} \\ \overline{\phi} + \sqrt{\frac{1}{4}-\overline{\phi}^2} \end{bmatrix}, \quad \mathsf{M} = \boxed{0}\boxed{1}, \quad \text{(C1)}$$

where $\overline{\phi} = (\phi_0+\phi_1)/2 = 2/\mu^2$ is the Birkhoff average Eq. (19) of the field ϕ_t. In the anti-integrable limit Eq. (63) the lattice site field values tend to parabola $1/4-\phi_z^2=0$ steady state values $[\phi_0,\phi_1] \to [-1/2,1/2]$.

The Bloch theorem Eq. (110) yields two eigenstate bands,

$$\Lambda_\pm(\mathsf{k}) = -2 \pm \sqrt{\mu^4 - 12 - p(2k)^2}\,, \quad \text{(C2)}$$

plotted in Fig. 9 (b), in the $k \in (-\pi/2,\pi/2]$ Brillouin zone for $\mu^2 = 3.5$. For a finite primitive cell of even period, tiled by rth repeat of the period-2 periodic state Φ_p, the eigenvalues of its orbit Jacobian matrix are $\Lambda_{01,\pm}(k)$ evaluated at k restricted to a discrete set of wave vectors k, multiples of π/r: an example is worked out in Sec. VIII C, with third and fourth repeats plotted in Fig. 9 (b).

2. Two-dimensional ϕ^4 field theory $[2\times1]_0$ periodic state

The ϕ^4 spatiotemporal lattice field theory, Eq. (46),

$$-\Box\,\phi_z \;+\; \mu^2(\phi_z - \phi_z^3) = 0\,,$$

to which companion paper III[17] assigns alphabet Eq. (36) $\mathcal{A} = \{-1,0,1\}$, has at most 3 steady states. The two spacetime dimensions ϕ^4 has has at most 3 period-2 prime orbits of periodicity $[2\times1]_0$, with mosaics $\boxed{-1}\boxed{0}$, $\boxed{-1}\boxed{1}$ and $\boxed{0}\boxed{1}$. For example, for Klein-Gordon mass-squared $\mu^2 = 5$, one of the period-2 prime orbits is

$$\Phi_{01} = \begin{bmatrix} \sqrt{\frac{7-\sqrt{33}}{10}} \\ \sqrt{\frac{7+\sqrt{33}}{10}} \end{bmatrix}, \quad \mathsf{M} = \boxed{0}\boxed{1}. \quad \text{(C3)}$$

The orbit Jacobian operator has two Bloch bands:

$$\Lambda_\pm(\mathsf{k}) = -\frac{7}{2} + p(k_2)^2 \pm \sqrt{\frac{313}{4} - p(2k_1)^2} \quad \text{(C4)}$$

plotted in Fig. 11 (b). While the period-2 periodic state $[2\times1]_0$ is the same in one and two spatiotemporal dimensions, it stability, Eq. (C4), is evaluated in two dimensions, with transverse k_2, temporal direction eigenstates included. For any finite primitive cell tiled by repeats of the prime orbit Φ_p, eigenstates of the orbit Jacobian matrix have a discrete set of wave vectors k. As an example, eigenvalues of a $[6\times4]_0$ periodic state tiled by 12 repeats of Φ_p have wave vectors k marked by black dots in Fig. 11 (b).

REFERENCES

[1] D. Ruelle, "Large volume limit of the distribution of characteristic exponents in turbulence," Commun. Math. Phys. **87**, 287–302 (1982).
[2] C. Foias, O. P. Manley, R. Témam, and Y. M. Treve, "Asymptotic analysis of the Navier-Stokes equations," Physica D **9**, 157–188 (1983).
[3] B. Nicolaenko, "Some mathematical aspects of flame chaos and flame multiplicity," Physica D **20**, 109–121 (1986).
[4] P. Grassberger, "Information content and predictability of lumped and distributed dynamical systems," Phys. Scr. **40**, 346 (1989).
[5] S. Lepri, A. Politi, and A. Torcini, "Chronotopic Lyapunov analysis. I. A detailed characterization of 1D systems," J. Stat. Phys. **82**, 1429–1452 (1996).
[6] S. Lepri, A. Politi, and A. Torcini, "Chronotopic Lyapunov analysis. II. Towards a unified approach," J. Stat. Phys. **88**, 31–45 (1997).
[7] S. Lepri, A. Politi, and A. Torcini, "Entropy potential and Lyapunov exponents," Chaos **7**, 701–709 (1997).
[8] F. Waleffe, "Exact coherent structures in channel flow," J. Fluid Mech. **435**, 93–102 (2001).
[9] H. Wedin and R. R. Kerswell, "Exact coherent structures in pipe flow," J. Fluid Mech. **508**, 333–371 (2004).
[10] G. Kawahara and S. Kida, "Periodic motion embedded in plane Couette turbulence: Regeneration cycle and burst," J. Fluid Mech. **449**, 291 (2001).
[11] B. Hof, C. W. H. van Doorne, J. Westerweel, F. T. M. Nieuwstadt, H. Faisst, B. Eckhardt, H. Wedin, R. R. Kerswell, and F. Waleffe, "Experimental observation of nonlinear traveling waves in turbulent pipe flow," Science **305**, 1594–1598 (2004).
[12] J. F. Gibson, J. Halcrow, and P. Cvitanović, "Visualizing the geometry of state-space in plane Couette flow," J. Fluid Mech. **611**, 107–130 (2008).
[13] N. B. Budanur, K. Y. Short, M. Farazmand, A. P. Willis, and P. Cvitanović, "Relative periodic orbits form the backbone of turbulent pipe flow," J. Fluid Mech. **833**, 274–301 (2017).
[14] C. J. Crowley, J. L. Pughe-Sanford, W. Toler, M. C. Krygier, R. O. Grigoriev, and M. F. Schatz, "Turbulence tracks recurrent solutions," Proc. Natl. Acad. Sci. **119**, 120665119 (2022).
[15] P. Cvitanović, "Recurrent flows: The clockwork behind turbulence," J. Fluid Mech. Focus Fluids **726**, 1–4 (2013).
[16] H. Liang and P. Cvitanović, "A chaotic lattice field theory in one dimension," J. Phys. A **55**, 304002 (2022).
[17] S. D. V. Williams, X. Wang, H. Liang, and P. Cvitanović, "Nonlinear chaotic lattice field theory," (2025), in preparation.
[18] M. C. Gutzwiller, *Chaos in Classical and Quantum Mechanics* (Springer, New York, 1990).
[19] D. Ruelle, *Thermodynamic Formalism: The Mathematical Structure of Equilibrium Statistical Mechanics*, 2nd ed. (Cambridge Univ. Press, Cambridge, 2004).
[20] P. Cvitanović, R. Artuso, R. Mainieri, G. Tanner, and G. Vattay, *Chaos: Classical and Quantum* (Niels Bohr Inst., Copenhagen, 2025).

[21] A. Politi, A. Torcini, and S. Lepri, "Lyapunov exponents from node-counting arguments," J. Phys. IV **8**, 263 (1998).
[22] G. Giacomelli, S. Lepri, and A. Politi, "Statistical properties of bidimensional patterns generated from delayed and extended maps," Phys. Rev. E **51**, 3939–3944 (1995).
[23] T. Bountis and R. H. G. Helleman, "On the stability of periodic orbits of two-dimensional mappings," J. Math. Phys. **22**, 1867–1877 (1981).
[24] R. S. MacKay and J. D. Meiss, "Linear stability of periodic orbits in Lagrangian systems," Phys. Lett. A **98**, 92–94 (1983).
[25] A. S. Pikovsky, "Spatial development of chaos in nonlinear media," Phys. Lett. A **137**, 121–127 (1989).
[26] S. H. Strogatz, *Nonlinear Dynamics and Chaos* (Westview Press, Boulder, CO, 2014).
[27] E. Ott, *Chaos and Dynamical Systems* (Cambridge Univ. Press, Cambridge, 2002).
[28] R. L. Devaney, *An Introduction to Chaotic Dynamical systems*, 2nd ed. (Westview Press, Cambridge, Mass, 2008).
[29] K. T. Alligood, T. D. Sauer, and J. A. Yorke, *Chaos, An Introduction to Dynamical Systems* (Springer, New York, 1996).
[30] A. Katok and B. Hasselblatt, *Introduction to the Modern Theory of Dynamical Systems* (Cambridge Univ. Press, Cambridge, 1995).
[31] R. C. Robinson, *An Introduction to Dynamical Systems: Continuous and Discrete* (Amer. Math. Soc., New York, 2012).
[32] T. Engl, J. D. Urbina, and K. Richter, "Periodic mean-field solutions and the spectra of discrete bosonic fields: Trace formula for Bose-Hubbard models," Phys. Rev. E **92**, 062907 (2015).
[33] M. Akila, D. Waltner, B. Gutkin, P. Braun, and T. Guhr, "Semiclassical identification of periodic orbits in a quantum many-body system," Phys. Rev. Lett. **118**, 164101 (2017).
[34] M. Akila, D. Waltner, B. Gutkin, and T. Guhr, "Particle-time duality in the kicked Ising spin chain," J. Phys. A **49**, 375101 (2016).
[35] K. Richter, J. D. Urbina, and S. Tomsovic, "Semiclassical roots of universality in many-body quantum chaos," J. Phys. A **55**, 453001 (2022).
[36] B. Gutkin and V. Osipov, "Classical foundations of many-particle quantum chaos," Nonlinearity **29**, 325–356 (2016).
[37] B. Gutkin, L. Han, R. Jafari, A. K. Saremi, and P. Cvitanović, "Linear encoding of the spatiotemporal cat map," Nonlinearity **34**, 2800–2836 (2021).
[38] W. Alderson, R. Dubertrand, and A. Shudo, "Classical transport in a maximally chaotic chain," J. Phys. A **58**, 165201 (2025).
[39] M. Axenides, E. Floratos, and S. Nicolis, "The quantum cat map on the modular discretization of extremal black hole horizons," Eur. Phys. J. C **78** (2018), 10.1140/epjc/s10052-018-5850-9.
[40] M. Axenides, E. Floratos, and S. Nicolis, "Arnol'd cat map lattices," Phys. Rev. E **107**, 064206 (2023).
[41] G. Vattay, "Noise and quantum corrections to trace formulas," in *Chaos: Classical and Quantum*, edited by P. Cvitanović, R. Artuso, R. Mainieri, G. Tanner, and G. Vattay (Niels Bohr Inst., Copenhagen, 1997).
[42] V. Subramanyan, S. S. Hegde, S. Vishveshwara, and B. Bradlyn, "Physics of the inverted harmonic oscillator: From the lowest Landau level to event horizons," Ann. Phys. **435**, 168470 (2021).
[43] E. Fermi, J. Pasta, and S. Ulam, "Studies of nonlinear problems," in *E. Fermi: Note e Memorie (Collected Papers)*, Vol. II (Accademia Nazionale dei Lincei, Roma, and The University of Chicago Press, Chicago, 1965) pp. 977–988.
[44] D. K. Campbell, S. Flach, and Y. S. Kivshar, "Localizing energy through nonlinearity and discreteness," Phys. Today **57**, 43–49 (2004).
[45] P. Gaspard, *Chaos, Scattering and Statistical Mechanics* (Cambridge Univ. Press, Cambridge, 1997).
[46] G. W. Hill, "On the part of the motion of the lunar perigee which is a function of the mean motions of the sun and moon," Acta Math. **8**, 1–36 (1886).
[47] H. Poincaré, "Sur les déterminants d'ordre infini," Bull. Soc. Math. France **14**, 77–90 (1886).
[48] H. Liang and P. Cvitanović, "A derivation of Hill's formulas," (2025), in preparation.
[49] R. Artuso, E. Aurell, and P. Cvitanović, "Recycling of strange sets: I. Cycle expansions," Nonlinearity **3**, 325–359 (1990).
[50] P. Cvitanović and H. Liang, "A chaotic lattice field theory in two dimensions," (2025).
[51] I. Montvay and G. Münster, *Quantum Fields on a Lattice* (Cambridge Univ. Press, Cambridge, 1994).
[52] G. Münster and M. Walzl, "Lattice gauge theory - A short primer," (2000).
[53] N. W. Ashcroft and N. D. Mermin, *Solid State Physics* (Holt, Rinehart and Winston, 1976).
[54] M. M. P. Couchman, D. J. Evans, and J. W. M. Bush, "The stability of a hydrodynamic Bravais lattice," Symmetry **14**, 1524 (2022).
[55] P. Cvitanović and H. Liang, "Appendix WKB quantization," in *Chaos: Classical and Quantum*, edited by P. Cvitanović, R. Artuso, R. Mainieri, G. Tanner, and G. Vattay (Niels Bohr Inst., Copenhagen, 2025).
[56] J. H. Van Vleck, "The correspondence principle in the statistical interpretation of quantum mechanics," Proc. Natl. Acad. Sci. **14**, 178–188 (1928).
[57] Y. Colin de Verdière, "Spectrum of the Laplace operator and periodic geodesics: thirty years after," Ann. Inst. Fourier **57**, 2429–2463 (2007).
[58] S. Levit and U. Smilansky, "A theorem on infinite products of eigenvalues of Sturm-Liouville type operators," Proc. Amer. Math. Soc. **65**, 299–299 (1977).
[59] S. Levit and U. Smilansky, "A new approach to Gaussian path integrals and the evaluation of the semiclassical propagator," Ann. Phys. **103**, 198–207 (1977).
[60] A. Maloney and E. Witten, "Quantum gravity partition functions in three dimensions," J. High Energy Phys. **2010**, 029 (2010).
[61] A. Castro, M. R. Gaberdiel, T. Hartman, A. Maloney, and R. Volpato, "Gravity dual of the Ising model," Phys. Rev. D **85**, 024032 (2012).
[62] E. V. Ivashkevich, N. S. Izmailian, and C.-K. Hu, "Kronecker's double series and exact asymptotic expansions for free models of statistical mechanics on torus," J. Phys. A **35**, 5543–5561 (2002).
[63] M. Campos, G. Sierra, and E. López, "Tensor renormalization group in bosonic field theory," Phys. Rev. B **100**, 195106 (2019).
[64] B. Simon, "Almost periodic Schrödinger operators: A review," Adv. Appl. Math. **3**, 463–490 (1982).
[65] S. Simons, "Analytical inversion of a particular type of banded matrix," J. Phys. A **30**, 755 (1997).
[66] M. Toda, *Theory of Nonlinear Lattices* (Springer, Berlin, 1989).
[67] L. A. Bunimovich and Y. G. Sinai, "Spacetime chaos in coupled map lattices," Nonlinearity **1**, 491 (1988).
[68] A. Politi and A. Torcini, "Towards a statistical mechanics of spatiotemporal chaos," Phys. Rev. Lett. **69**, 3421–3424 (1992).
[69] S. D. Pethel, N. J. Corron, and E. Bollt, "Symbolic dynamics of coupled map lattices," Phys. Rev. Lett. **96**, 034105 (2006).
[70] S. D. Pethel, N. J. Corron, and E. Bollt, "Deconstructing spatiotemporal chaos using local symbolic dynamics," Phys. Rev. Lett. **99**, 214101 (2007).
[71] S.-N. Chow, J. Mallet-Paret, and E. S. Van Vleck, "Pattern formation and spatial chaos in spatially discrete evolution equations," Random Comput. Dynam. **4**, 109–178 (1996).
[72] S.-N. Chow, J. Mallet-Paret, and W. Shen, "Traveling waves in lattice dynamical systems," J. Diff. Equ. **149**, 248–291 (1998).
[73] J. Mallet-Paret and S.-N. Chow, "Pattern formation and spatial chaos in lattice dynamical systems. I," IEEE Trans. Circuits Systems I Fund. Theory Appl. **42**, 746–751 (1995).
[74] J. Mallet-Paret and S.-N. Chow, "Pattern formation and spatial chaos in lattice dynamical systems. II," IEEE Trans. Circuits Systems I Fund. Theory Appl. **42**, 752–756 (1995).
[75] R. Coutinho and B. Fernandez, "Extended symbolic dynamics

in bistable CML: Existence and stability of fronts," Physica D **108**, 60–80 (1997).
[76]D. G. Sterling, *Anti-integrable Continuation and the Destruction of Chaos*, Ph.D. thesis, Univ. Colorado, Boulder, CO (1999).
[77]W. Just, "On symbolic dynamics of space-time chaotic models," in *Collective Dynamics of Nonlinear and Disordered Systems* (Springer, 2005) pp. 339–357.
[78]R. S. MacKay, "Indecomposable coupled map lattices with non-unique phase," in *Dynamics of Coupled Map Lattices and of Related Spatially Extended Systems*, edited by J.-R. Chazottes and B. Fernandez (Springer, 2005) pp. 65–94.
[79]S. Aubry and G. Abramovici, "Chaotic trajectories in the standard map. The concept of anti-integrability," Physica D **43**, 199–219 (1990).
[80]S. Aubry, "Anti-integrability in dynamical and variational problems," Physica D **86**, 284–296 (1995).
[81]D. Sterling and J. D. Meiss, "Computing periodic orbits using the anti-integrable limit," Phys. Lett. A **241**, 46–52 (1998).
[82]C. Beck, *Spatio-Temporal Chaos and Vacuum Fluctuations of Quantized Fields* (World Scientific, Singapore, 2002).
[83]S. Friedland and J. Milnor, "Dynamical properties of plane polynomial automorphisms," Ergodic Theory Dynam. Systems **9**, 67–99 (1989).
[84]H. R. Dullin and J. D. Meiss, "Generalized Hénon maps: the cubic diffeomorphisms of the plane," Physica D **143**, 262–289 (2000).
[85]M.-C. Li and M. Malkin, "Bounded nonwandering sets for polynomial mappings," J. Dynam. Control Systems **10**, 377–389 (2004).
[86]G. Münster, "Lattice quantum field theory," Scholarpedia **5**, 8613 (2010).
[87]S. Anastassiou, A. Bountis, and A. Bäcker, "Homoclinic points of 2D and 4D maps via the parametrization method," Nonlinearity **30**, 3799–3820 (2017).
[88]S. Anastassiou, A. Bountis, and A. Bäcker, "Recent results on the dynamics of higher-dimensional Hénon maps," Regul. Chaotic Dyn. **23**, 161–177 (2018).
[89]S. Anastassiou, "Complicated behavior in cubic Hénon maps," Theoret. Math. Phys. **207**, 572–578 (2021).
[90]D. A. Lind and B. Marcus, *An Introduction to Symbolic Dynamics and Coding* (Cambridge Univ. Press, Cambridge, 1995).
[91]M. Pollicott, "Dynamical zeta functions," in *Smooth Ergodic Theory and Its Applications*, Vol. 69, edited by A. Katok, R. de la Llave, Y. Pesin, and H. Weiss (Amer. Math. Soc., Providence RI, 2001) pp. 409–428.
[92]D. Cimasoni, "The critical Ising model via Kac-Ward matrices," Commun. Math. Phys. **316**, 99–126 (2012).
[93]C. Godsil and G. F. Royle, *Algebraic Graph Theory* (Springer, New York, 2013).
[94]F. W. Dorr, "The direct solution of the discrete Poisson equation on a rectangle," SIAM Rev. **12**, 248–263 (1970).
[95]A. L. Fetter and J. D. Walecka, *Theoretical Mechanics of Particles and Continua* (Dover, New York, 2003).
[96]L. P. Kadanoff, *Statistical Physics: Statics, Dynamics and Renormalization* (World Scientific, Singapore, 2000).
[97]E. Fradkin, *Field Theories of Condensed Matter Physics* (Cambridge Univ. Press, Cambridge UK, 2013).
[98]R. Shankar, *Quantum Field Theory and Condensed Matter* (Cambridge Univ. Press, Cambridge UK, 2017).
[99]E. C. Marino, *Quantum Field Theory Approach to Condensed Matter Physics* (Cambridge Univ. Press, Cambridge UK, 2017).
[100]Y. Shimizu, "Tensor renormalization group approach to a lattice boson model," Mod. Phys. Lett. A **27**, 1250035 (2012).
[101]M. Campos, E. López, and G. Sierra, "Integrability and scattering of the boson field theory on a lattice," J. Phys. A **54**, 055001 (2021).
[102]J. P. Keating, "The cat maps: quantum mechanics and classical motion," Nonlinearity **4**, 309–341 (1991).
[103]I. Percival and F. Vivaldi, "A linear code for the sawtooth and cat maps," Physica D **27**, 373–386 (1987).
[104]M. Cheng and N. Seiberg, "Lieb-Schultz-Mattis, Luttinger, and 't Hooft – anomaly matching in lattice systems," (2022).
[105]L. Fazza and T. Sulejmanpasic, "Lattice quantum Villain Hamiltonians: compact scalars, U(1) gauge theories, fracton models and quantum Ising model dualities," J. High Energy Phys. **2023**, 17 (2023).
[106]V. I. Arnol'd and A. Avez, *Ergodic Problems of Classical Mechanics* (Addison-Wesley, Redwood City, 1989).
[107]R. Sturman, J. M. Ottino, and S. Wiggins, *The Mathematical Foundations of Mixing* (Cambridge Univ. Press, 2006).
[108]A. Zee, *Quantum Field Theory in a Nutshell*, 2nd ed. (Princeton Univ. Press, Princeton NJ, 2010).
[109]I. S. Gradshteyn and I. M. Ryzhik, *Tables of Integrals, Series and Products*, 8th ed. (Elsevier LTD, Oxford, New York, 2014).
[110]N. Karve, N. Rose, and D. Campbell, "Periodic orbits in Fermi-Pasta-Ulam-Tsingou systems," Chaos: An Interdisciplinary Journal of Nonlinear Science **34**, 093117 (2024).
[111]C. Kittel, *Introduction to Solid State Physics*, 8th ed. (Wiley, 2004).
[112]M. S. Dresselhaus, G. Dresselhaus, and A. Jorio, *Group Theory: Application to the Physics of Condensed Matter* (Springer, New York, 2007).
[113]J. W. S. Cassels, *An Introduction to the Geometry of Numbers* (Springer, Berlin, 1959).
[114]C. L. Siegel and K. Chandrasekharan, *Lectures on the Geometry of Numbers* (Springer Berlin Heidelberg, Berlin, Heidelberg, 1989).
[115]S. Lang, *Linear Algebra* (Addison-Wesley, Reading, MA, 1987).
[116]J. L. Cardy, "Operator content of two-dimensional conformally invariant theories," Nucl. Phys. B **270**, 186–204 (1986).
[117]R. M. Ziff, C. D. Lorenz, and P. Kleban, "Shape-dependent universality in percolation," Physica A **266**, 17–26 (1999).
[118]E. M. Stein and R. Shakarchi, *Complex Analysis* (Princeton Univ. Press, Princeton, 2003).
[119]H. Cohen, *A Course in Computational Algebraic Number Theory* (Springer, Berlin, 1993).
[120]Y. Okabe, K. Kaneda, M. Kikuchi, and C.-K. Hu, "Universal finite-size scaling functions for critical systems with tilted boundary conditions," Phys. Rev. E **59**, 1585–1588 (1999).
[121]T. M. Liaw, M. C. Huang, Y. L. Chou, S. C. Lin, and F. Y. Li, "Partition functions and finite-size scalings of Ising model on helical tori," Phys. Rev. E **73**, 041118 (2006).
[122]N. S. Izmailian, K. B. Oganesyan, and C.-K. Hu, "Exact finite-size corrections for the square-lattice Ising model with Brascamp-Kunz boundary conditions," Phys. Rev. E **65**, 056132 (2002).
[123]V. Baladi, *Positive transfer operators and decay of correlations* (World Scientific, Singapore, 2000).
[124]Wikipedia contributors, "Chord (geometry) — Wikipedia, The Free Encyclopedia," (2023).
[125]E. H. Berger, *Die geographischen Fragmente des Hipparch* (Teubner, 1869).
[126]A. Pikovsky and A. Politi, *Lyapunov Exponents: A Tool to Explore Complex Dynamics* (Cambridge Univ. Press, Cambridge, 2016).
[127]A. J. Guttmann, "Lattice Green's functions in all dimensions," J. Phys. A **43**, 305205 (2010).
[128]P. A. Martin, "Discrete scattering theory: Green's function for a square lattice," Wave Motion **43**, 619–629 (2006).
[129]E. N. Economou, *Green's Functions in Quantum Physics* (Springer, Berlin, 2006).
[130]G. Floquet, "Sur les équations différentielles linéaires à coefficients périodiques," Ann. Sci. Ec. Norm. Sér **12**, 47–88 (1883).
[131]L. Brillouin, "Les électrons libres dans les métaux et le role des réflexions de Bragg," J. Phys. Radium **1**, 377–400 (1930).
[132]J. Mathews and R. L. Walker, *Mathematical Methods of Physics* (Addison-Wesley, Reading, MA, 1973).
[133]P. Cvitanović, "Counting," in *Chaos: Classical and Quantum*, edited by P. Cvitanović, R. Artuso, R. Mainieri, G. Tanner, and

G. Vattay (Niels Bohr Inst., Copenhagen, 2025).
[134]P. Cvitanović, *Field Theory* (Nordita, Copenhagen, 1983) notes prepared by E. Gyldenkerne.
[135]Y. Pomeau and P. Manneville, "Intermittent transition to turbulence in dissipative dynamical systems," Commun. Math. Phys. **74**, 189 (1980).
[136]D. Ruelle, "Generalized zeta-functions for Axiom A basic sets," Bull. Amer. Math. Soc **82**, 153–157 (1976).
[137]D. Ruelle, "Zeta-functions for expanding maps and Anosov flows," Inv. Math. **34**, 231–242 (1976).
[138]P. Cvitanović, "Trace formulas," in *Chaos: Classical and Quantum*, edited by P. Cvitanović, R. Artuso, R. Mainieri, G. Tanner, and G. Vattay (Niels Bohr Inst., Copenhagen, 2025).
[139]P. Cvitanović, "Spectral determinants," in *Chaos: Classical and Quantum*, edited by P. Cvitanović, R. Artuso, R. Mainieri, G. Tanner, and G. Vattay (Niels Bohr Inst., Copenhagen, 2025).
[140]P. Cvitanović, R. Artuso, L. Rondoni, and E. A. Spiegel, "Cycle expansions," in *Chaos: Classical and Quantum*, edited by P. Cvitanović, R. Artuso, R. Mainieri, G. Tanner, and G. Vattay (Niels Bohr Inst., Copenhagen, 2025).
[141]L. Kadanoff and C. Tang, "Escape rate from strange repellers," Proc. Natl. Acad. Sci. **81**, 1276–1279 (1984).
[142]J. Bell, "Euler and the pentagonal number theorem," (2005).
[143]D. A. Lind, "A zeta function for Z^d-actions," in *Ergodic Theory of Z^d Actions*, edited by M. Pollicott and K. Schmidt (Cambridge Univ. Press, 1996) pp. 433–450.
[144]I. M. Gel'fand and A. M. Yaglom, "Integration in functional spaces and its applications in quantum physics," J. Math. Phys. **1**, 48–69 (1960).
[145]M. Ludewig, "Heat kernel asymptotics, path integrals and infinite-dimensional determinants," J. Geom. Phys. **131**, 66–88 (2018).
[146]E. Barreto, "Shadowing," Scholarpedia **3**, 2243 (2008).
[147]K. Palmer, "Shadowing lemma for flows," Scholarpedia **4**, 7918 (2009).
[148]Wikipedia contributors, "Lyapunov time — Wikipedia, The Free Encyclopedia," (2023).
[149]X. Ding and P. Cvitanović, "Periodic eigendecomposition and its application in Kuramoto-Sivashinsky system," SIAM J. Appl. Dyn. Syst. **15**, 1434–1454 (2016).
[150]B. D. Mestel and I. Percival, "Newton method for highly unstable orbits," Physica D **24**, 172 (1987).
[151]J. I. Glaser, "Numerical solution of waveguide scattering problems by finite-difference Green's functions," IEEE Trans. Microwave Theory Tech. **18**, 436–443 (1970).
[152]B. L. Buzbee, G. H. Golub, and C. W. Nielson, "On direct methods for solving Poisson's equations," SIAM J. Numer. Anal. **7**, 627–656 (1970).
[153]W. L. Wood, "Periodicity effects on the iterative solution of elliptic difference equations," SIAM J. Numer. Anal. **8**, 439–464 (1971).
[154]S. Katsura, T. Morita, S. Inawashiro, T. Horiguchi, and Y. Abe, "Lattice Green's function. Introduction," J. Math. Phys. **12**, 892–895 (1971).
[155]S. Katsura and S. Inawashiro, "Lattice Green's functions for the rectangular and the square lattices at arbitrary points," J. Math. Phys. **12**, 1622–1630 (1971).
[156]S. Katsura, S. Inawashiro, and Y. Abe, "Lattice Green's function for the simple cubic lattice in terms of a Mellin-Barnes type integral," J. Math. Phys. **12**, 895–899 (1971).
[157]T. Morita, "Useful procedure for computing the lattice Green's function - square, tetragonal, and bcc lattices," J. Math. Phys. **12**, 1744–1747 (1971).
[158]T. Morita and T. Horiguchi, "Calculation of the lattice Green's function for the bcc, fcc, and rectangular lattices," J. Math. Phys. **12**, 986–992 (1971).
[159]T. Horiguchi, "Lattice Green's function for the simple cubic lattice," J. Phys. Soc. Jpn. **30**, 1261–1272 (1971).
[160]M. Fiedler, "Algebraic connectivity of graphs," Czech. Math. J **23**, 298–305 (1973).
[161]T. Horiguchi and T. Morita, "Note on the lattice Green's function for the simple cubic lattice," J. Phys. C **8**, L232 (1975).
[162]W. N. Anderson and T. D. Morley, "Eigenvalues of the Laplacian of a graph," Lin. Multilin. Algebra **18**, 141–145 (1985).
[163]M. Chen, "On the solution of circulant linear systems," SIAM J. Numer. Anal. **24**, 668–683 (1987).
[164]F. Chung and S.-T. Yau, "Discrete Green's functions," J. Combin. Theory A **91**, 19–214 (2000).
[165]R. de la Llave, "Variational methods for quasiperiodic solutions of partial differential equations," in *Hamiltonian Systems and Celestial Mechanics (HAMSYS-98)*, edited by J. Delgado, E. A. Lacomba, E. Pérez-Chavela, and J. Llibre (World Scientific, Singapore, 2000).
[166]J. H. Asad, "Differential equation approach for one- and two-dimensional lattice Green's function," Mod. Phys. Lett. B **21**, 139–154 (2007).
[167]H. S. Bhat and B. Osting, "Diffraction on the two-dimensional square lattice," SIAM J. Appl. Math. **70**, 1389–1406 (2010).
[168]I. Stewart and D. Gökaydin, "Symmetries of quotient networks for doubly periodic patterns on the square lattice," Int. J. Bifurcat. Chaos **29**, 1930026 (2019).
[169]R. Artuso, E. Aurell, and P. Cvitanović, "Recycling of strange sets: II. Applications," Nonlinearity **3**, 361–386 (1990).
[170]R. Artuso, H. H. Rugh, and P. Cvitanović, "Why does it work?" in *Chaos: Classical and Quantum*, edited by P. Cvitanović, R. Artuso, R. Mainieri, G. Tanner, and G. Vattay (Niels Bohr Inst., Copenhagen, 2025).
[171]M. C. Gutzwiller, "Periodic orbits and classical quantization conditions," J. Math. Phys. **12**, 343–358 (1971).
[172]G. J. Chandler and R. R. Kerswell, "Invariant recurrent solutions embedded in a turbulent two-dimensional Kolmogorov flow," J. Fluid Mech. **722**, 554–595 (2013).
[173]F. Christiansen, P. Cvitanović, and V. Putkaradze, "Spatiotemporal chaos in terms of unstable recurrent patterns," Nonlinearity **10**, 55–70 (1997).
[174]P. Cvitanović, R. L. Davidchack, and E. Siminos, "On the state space geometry of the Kuramoto-Sivashinsky flow in a periodic domain," SIAM J. Appl. Dyn. Syst. **9**, 1–33 (2010).
[175]P. Cvitanović and J. F. Gibson, "Geometry of turbulence in wall-bounded shear flows: Periodic orbits," Phys. Scr. T **142**, 014007 (2010).
[176]A. P. Willis, P. Cvitanović, and M. Avila, "Revealing the state space of turbulent pipe flow by symmetry reduction," J. Fluid Mech. **721**, 514–540 (2013).
[177]T. Kreilos and B. Eckhardt, "Periodic orbits near onset of chaos in plane Couette flow," Chaos **22**, 047505 (2012).
[178]B. Suri, L. Kageorge, R. O. Grigoriev, and M. F. Schatz, "Capturing turbulent dynamics and statistics in experiments with unstable periodic orbits," Phys. Rev. Lett. **125**, 064501 (2020).
[179]C. J. Crowley, J. L. Pughe-Sanford, W. Toler, R. O. Grigoriev, and M. F. Schatz, "Observing a dynamical skeleton of turbulence in Taylor-Couette flow experiments," (2022).
[180]J. F. Gibson and P. Cvitanović, "Movies of plane Couette," Tech. Rep. (Georgia Inst. of Technology, 2015).
[181]M. N. Gudorf, *Spatiotemporal Tiling of the Kuramoto-Sivashinsky Equation*, Ph.D. thesis, School of Physics, Georgia Inst. of Technology, Atlanta (2020).
[182]J. F. Gibson, "Channelflow: A spectral Navier-Stokes simulator in C++," Tech. Rep. (U. New Hampshire, 2019) `Channelflow.org`.
[183]A. P. Willis, "Openpipeflow: Pipe flow code for incompressible flow," Tech. Rep. (U. Sheffield, 2014) `Openpipeflow.org`.
[184]D. Ruelle, "Statistical mechanics on a compact set with Z^ν action satisfying expansiveness and specification," Bull. Amer. Math. Soc. **78**, 988–991 (1972).
[185]P. Cvitanović, P. Gaspard, and T. Schreiber, "Investigation of the Lorentz gas in terms of periodic orbits," Chaos **2**, 85–90 (1992).
[186]P. Cvitanović, "Dynamical averaging in terms of periodic orbits," Physica D **83**, 109–123 (1995).

[187]P. Cvitanović, "Averaging," in *Chaos: Classical and Quantum*, edited by P. Cvitanović, R. Artuso, R. Mainieri, G. Tanner, and G. Vattay (Niels Bohr Inst., Copenhagen, 2025).
[188]H. H. Rugh, "Un interview de David Ruelle," Gaz. Math. **161**, 55–59 (2019).
[189]H. H. Rugh, "An interview with David Ruelle," EMS Newsletter **2020-3**, 21–24 (2020).
[190]P. Dahlqvist, "Least action method," in *Chaos: Classical and Quantum*, edited by P. Cvitanović, R. Artuso, R. Mainieri, G. Tanner, and G. Vattay (Niels Bohr Institute, 2023) 14th ed.
[191]P. Cvitanović and Y. Lan, "Turbulent fields and their recurrences," in *Correlations and Fluctuations in QCD : Proceedings of 10. International Workshop on Multiparticle Production*, edited by N. Antoniou (World Scientific, Singapore, 2003) pp. 313–325.
[192]Y. Lan and P. Cvitanović, "Variational method for finding periodic orbits in a general flow," Phys. Rev. E **69**, 016217 (2004).
[193]M. N. Gudorf, "Orbithunter: Framework for Nonlinear Dynamics and Chaos," Tech. Rep. (School of Physics, Georgia Inst. of Technology, 2021).
[194]M. V. Lakshmi, G. Fantuzzi, S. I. Chernyshenko, and D. Lasagna, "Finding unstable periodic orbits: A hybrid approach with polynomial optimization," Physica D **427**, 133009 (2021).
[195]S. Azimi, O. Ashtari, and T. M. Schneider, "Constructing periodic orbits of high-dimensional chaotic systems by an adjoint-based variational method," Phys. Rev. E **105**, 014217 (2022).
[196]J. P. Parker and T. M. Schneider, "Variational methods for finding periodic orbits in the incompressible Navier-Stokes equations," J. Fluid. Mech. **941**, A17 (2022).
[197]D. Wang and Y. Lan, "A reduced variational approach for searching cycles in high-dimensional systems," (2022).
[198]J. Page, P. Norgaard, M. P. Brenner, and R. R. Kerswell, "Recurrent flow patterns as a basis for two-dimensional turbulence: Predicting statistics from structures," Proc. Natl. Acad. Sci. **121**, 23 (2024).
[199]F. Christiansen, P. Cvitanović, and V. Putkaradze, "Hopf's last hope: Spatiotemporal chaos in terms of unstable recurrent patterns," Nonlinearity **10**, 55–70 (1997).
[200]D. Viswanath, "Recurrent motions within plane Couette turbulence," J. Fluid Mech. **580**, 339–358 (2007).
[201]X. Ding, H. Chaté, P. Cvitanović, E. Siminos, and K. A. Takeuchi, "Estimating the dimension of the inertial manifold from unstable periodic orbits," Phys. Rev. Lett. **117**, 024101 (2016).
[202]M. Axenides, E. Floratos, and S. Nicolis, "Exponential mixing of all orders for Arnol'd cat map lattices," (2024).
[203]A. Politi and A. Torcini, "Periodic orbits in coupled Hénon maps: Lyapunov and multifractal analysis," Chaos **2**, 293–300 (1992).
[204]M. Baake, J. Hermisson, and A. B. Pleasants, "The torus parametrization of quasiperiodic LI-classes," J. Phys. A **30**, 3029–3056 (1997).
[205]S. Isola, "ζ-functions and distribution of periodic orbits of toral automorphisms," Europhys. Lett. **11**, 517–522 (1990).
[206]M. Muresan, *A Concrete Approach to Classical Analysis* (Springer, New York, 2009).